ADDIS ABABA UNIVERSITY

ADDIS ABABA INSTITUTE OF TECHNOLOGY

SCHOOL OF CIVIL AND ENVIRONMENTAL ENGINEERING

Analysis and Parametric Study of Load-displacement Behavior of Large Group Pile Under Lateral Loading

A Thesis in Geotechnical Engineering

By Bayissa Waltaji

10/4/2019

Addis Ababa

A Thesis

Submitted in Partial Fulfillment of the Requirements for the Degree of Master of Science

The undersigned have examined the thesis entitled '**Analysis and Parametric Study of Load-displacement Behavior of Large Group Pile Under Lateral Loading** ' presented by **Bayissa Waltaji**, a candidate for the degree of **Master of Science** and hereby certify that it is worthy of acceptance.

Dr. Ing Henok Fikre		
Advisor	Signature	Date
Internal Examiner	Signature	Date
External Examiner	Signature	Date
Chair person	Signature	Date

UNDERTAKING

I certify that research work titled "**Analysis and Parametric Study of Load-displacement Behavior of Large Group Pile under Lateral Loading**" is my own work. The work has not been presented elsewhere for assessment. Where material has been used from other sources it has been properly acknowledged / referred.

Bayissa Waltaji

ACKNOWLEDGEMENT

Primarily, I would like to express my sincere thanks to my Advisor, Dr.Ing Henok Fikre for contributing and supporting in all aspects of this research. He was providing me a continuous source of ideas relating to numerical modelling, and the practical applications of the research. I gratefully acknowledge his help and guidance in preparing this thesis. I also appreciate his caring and encouragement during the period of the research study.

Secondly, thanks for the financial support for this research that was provided by Ethiopian Road Authority (ERA) for its Full sponsorship of this study, I wish to thank the School of Civil and Environmental Engineering of AAiT to support in every direction.

Finally, I wish to thank my wife, and my all families and friends love and support throughout this thesis.

ABSTRACT

Investigating the effects of lateral loads in design of foundation is important as compared to axial loads, although it gets normally less consideration in the usual practice. This study investigates the behavior of group piles in terms of load - displacement curves for trailing, intermediate and leading rows when it is laterally loaded by using FEM analysis employing Plaxis 3-D FOUNDATION. Mohr-Coulomb model has been used to model the soil material. A 15-noded triangular element is executed while 3-D meshing for soil material. The soil parameters were taken from previously done thesis, which has been calibrated from local soil property. Structural materials were modeled by using linear-elastic model, since steel and concrete behaves elastically under loading. Parameters which has been considered were pile geometry such as pile length/depth, spacing and pile number (number of rows) with different loading step. In addition, the pile is fixed head system, but the effects of pile cap have not been considered, only used for distributing lateral loads equally. It has been found out that pile group lateral deformations are small when the pile spacing is large enough, while the number of piles in the group increases, lateral movement of leading rows are decreasing. This is due to the overlapping shearing zones of the intermediate rows. When depth of piles increases there is increment of lateral confinement because of the increment of over burden pressures. It is concluded for the laterally loaded group of piles; the leading rows can resist more reaction loads from the soil than the trail rows and deformed less than the trail and intermediate rows. Finally based on the parameter analysis the difference of row displacement of leading, intermediate and trailing row were from 4% up to 8%, 9% up to 14%, 15 up to 20% respectively of total pile movements.

TABLE OF CONTENTS

CONTENTS

LIST OF TABLES

LIST OF FIGURES

SYMBOLS AND NOTATIONS

A	area [m^2]
B	width of pile [m]
β_m	base angle []
C_u	Undrained shear strength [kN/m^2]
D	Pile diameter [m]
D_r	Relative density [%]
E	Modulus of elasticity, Young's modulus [kN/m^2]
E_0	Elastic modulus at the ground surface [kN/m^2]
EI	Bending stiffness [kN/m^2]
EI_i	Beam element's bending stiffness [kNm^2]
E_{py}	Modulus of a parameter that relates p and y [kN/m^2]
E_{pymax}	Initial slope of a p-y curve [kN/m^2]
E_{50}^{ref}	Secant stiffness in drained triaxial test [kN/m^2]
E_{oed}^{ref}	Tangent/loading oedometric stiffness [kN/m^2]
E_{ur}^{ref}	Unloading/reloading stiffness [kN/m^2]
F	Force [KN]
K_0	Coefficient of soil at rest [-]
K_a	Coefficient of active soil [-]
K_i	Stiffness matrix of a pile element i [kN/m]
$k_{i,j}$	Single pile head's stiffness matrix's element i,j [kN/m]

K_{py}	Initial slope of p-y curve [kN/m^3]
K_q	Single pile head's stiffness matrix [kN/m]
ks	Lateral spring constant [kN/m]
L	Length [m]
LLGP	laterally loaded group pile
Np	ultimate lateral soil resistance coefficient
P_u	Ultimate soil resistance [kN/m]
P_x, P_y	Lateral soil resistances at directions x and y [kN/m]
R_{inter}	Interface strength reduction factor
S_u	Undrained shear strength of a geomaterial [kN/m^2]
SWM	strain wedge model
S	Pile spacing [m]
γ'	Effective unit weight [kN/m^3]
γ	Unit weight [kN/m^3]
δi	Displacement vector of a single pile element [m]
δtot	Displacement vector of a single pile [m]
ε	Strain corresponding to compressive stress [-]
ε50	Strain at which 50 percent mobilization in triaxial test [-]
θ	Batter angle of a pile [°]
λ	Time effect multiplier [-]
ν	Poisson's ratio [-]
αy	Yield stress [KPa]
ϖ_	Angular displacement [°]
ϖi,j	Angular displacement of a pile element i,j [°]

CHAPTER 1 INTRODUCTION

1.1 Back ground

Pile foundations are frequently used for structures when the soil immediately below the base will not provide adequate bearing capacity. The purpose of the piles is to transfer the load from the structure to soil strata which can sustain the applied loads. If all loads from the structure and all piles are vertical, then the loads transmitted to the piles will all be principally axial. If some horizontal component of load is present, a lateral force will also be transmitted to the piles. If some of the piles are battered, an axial and lateral force will be transmitted to the piles regardless of the direction of the applied load.

For most structures both horizontal and vertical components of loads are present. In some instances, the horizontal component may be small and can be neglected. However, for many structures, such as offshore drilling platforms or tall bridge bents, wind and wave action will produce significant horizontal forces. Therefore, for a complete analysis of a pile foundation, the behavior of the piles must be analyzed for both lateral and axial loads. Examples of structures where piles are commonly used as foundations are tall buildings, bridges, offshore platforms, defense structures dams and lock structures, transmission towers, retaining structures, wharfs and jetties. However, in all these structures, it is not only the axial force that the piles carry; often the piles are subjected to lateral forces. In fact, there are some structures (e.g., oil production platforms, earth retaining structures, wharfs and jetties) where the primary function of piles is to transfer lateral loads to the ground.

Wind gusts are the most common cause of lateral force that a pile has to support. The other major cause of lateral force is seismic activity. The horizontal shaking of the ground during earthquakes generates lateral forces that the piles have to withstand. Certain buildings are also acted upon by lateral earth pressures, which transmit lateral forces to the foundations. Depending on the type of structures a pile supports, there can be different causes of lateral forces. For tall buildings and transmission towers, wind action is the primary cause. For offshore oil production platforms, quays, harbors, wharfs and jetties, wave action gives rise to lateral forces. In the case of bridge abutments and piers,

horizontal forces are caused due to traffic and wind movement. Dams and lock structures have to withstand water pressures which transfer as horizontal forces on the supporting piles. Defense structures often have to withstand blasts that cause lateral forces.

In the case of earth retaining structures, the primary role of piles is to resist lateral forces caused due to the lateral pressures exerted by the soil mass behind the retaining wall. Sometimes, piles are installed into slopes, where slow ground movements are taking place, in order to arrest the movement. In such cases, the piles are subjected only to lateral forces. Piles are used to support open excavations; here also, there is no axial force and the only role of the piles is to resist lateral forces.

In the above examples, there are some cases in which the external horizontal loads act at the pile head. Such loading is active loading. Common examples are lateral loads (and moments) transmitted to the pile from superstructures like buildings, bridges and offshore platforms. Sometimes the applied horizontal load acts in a distributed way over a part of the pile shaft; such a loading is passive loading. Examples of passive loading are loads acting on piles due to movement of slopes or on piles supporting open excavations. There are cases in which external horizontal loads are minimal or absent; even then external moments often exist because of load eccentricities caused by construction defects, e.g., out-of-plumb constructions. Thus, piles in most cases are subjected to lateral loads. Consequently, proper analysis of laterally loaded piles is very important to the geotechnical engineering profession.

Major problems associated with pile groups subjected to lateral masses represent final load capacity, Resistance to overturning moments, and Lateral Movement. The pile analysis technique unremarkably employed in follow is the p-y approach. p-y curves represent the relationships between the lateral load (p) and also the displacement (y) at some extent within the pile.

1.2 Laterally Loaded Large group piles

Piled foundations are most often designed in a group configuration, and piled foundations that support long span bridges are no exception. Such a foundation configuration typically

contains a large number of closely spaced piles cast into a substantial pile cap, referred to here as a "large pile group."

Large group pile is a pile which contain more rows especially four rows and above, it is called large group piles (Michael McVay, 1998**).** Field data is lacking given that full-scale load testing is obviously not feasible, and instrumentation of constructed large pile groups are rare. Experimental tests on large group pile was very expensive therefore scholar is modeled large group piles by constant p- multiplier from single piles. It is found value of lateral deformation for large group piles**.**

Pile group will be divided into two classes depending on the spacing: (1) groups of large spaced piles; and (2) groups of closely spaced piles. The primary class consists of piles that measure spaced way enough apart so the deflection of one pile within the group doesn't have an effect on the opposite piles, which the piles act individually through the pile cap. Group of large spaced piles will be analyzed by distributing the lateral loads equally among all piles within the group, and considering the behavior of anyone pile in isolation. In group of closely spaced piles, the response of one pile affects the close piles by influencing deflection of the soil between them.

Moss et al. (1998) wanted to further investigate pile group response in clay. Using model tests and cyclic loading conditions he found an interesting phenomenon. As cycling progressed the clay compressed and gapping formed in front of the pile. This caused the resistance to become more dependent on the pile stiffness instead of the p-y curve, and maximum moments occurred at greater depths. This phenomenon was not as significant in pile groups tested in sand. Rao et al. (1998) also did model tests in clay, with the intent to investigate the influence of pile rigidity on pile group response. He found that pile strength was only significant in long flexible piles, and with short rigid piles the response depended more on soil resistance.

Finite component analysis is that the most vital tools for modeling load interaction and capable of modeling non-linearity and additionally for large group piles and for various non-standard geometries.

Nowadays, installation-induced changes to the effective stress around single piles can't be modelled properly exploitation routine finite component analysis, understanding of the

method has been increased by instrumented single pile tests (i.e. Jardine et al., 2005). McCabe and Lehane (2006a) examined resistive stresses on the center pile of a 5-pile group in capital of Northern Ireland soft clay/silt thanks to near pile installations and all over that their effect was transient.

The behavior of pile group beneath lateral loads will be analyzed exploitation the p-y technique.

Poulos (1971) best owed elastic behavior for load – deflection relationships in each free-headed and fixed-headed single piles and he makes the solutions for group of piles by exploitation the principal of superposition. An increase in spacing between the piles magnified the resistance to lateral loads in an exceedingly groups of laterally loaded piles underneath vertical and batter piles (Brungraber (1976).

1.3 Statement of the problem

There is a gap of understanding about the group of piles which are laterally loaded, especially the deformation of piles along their rows. Limited knowledge on the behavior of large pile groups exists due to lacking of field data because of full-scale load testing is obviously not feasible. There are no specific design procedures for large pile groups, current practice is therefore forced to use numerical predictions to assess large pile group behavior ,Therefore this study want to show deformation of leading, intermediate and trailing rows while laterally loaded.

1.4 Research objectives

This paper help to address a quantitative information on laterally loaded large group piles, and to clarify issues of laterally loaded large group pile parameters. The ultimate objective is to quantify behavior of large pile group response based on different pile geometry.

The specific objectives of this paper are

- Modeling and developing *load-displacement* curves for Laterally Loaded large group piles under layered soil. The soil profile is divided into a number of layers.

- Determining displacement (deformation) of the leading, trailing and the intermediate piles in respect to pile depth, spacing and pile number.
- Comparing the deflections of (trailing rows with the leading rows and intermediate rows too).

1.5 Scope of the Study

This paper focuses on local soil parameters and laterally loaded group piles which equally spaced in each orthogonal direction. Factors considered include pile number, loading step and depth of pile and spacing center to center.

- **Loading type:** static lateral loads (only translational load), no existence of axial load;
- **Number of piles**: 6×6, 4 × 4 and 7×*3* pile group configurations are considered as large pile groups.
- **Soil parameters**: Soil is simulated using Mohr coulomb model which states elasto-plastic non- linear characteristic.
- **Pile head fixity**: fixed head condition, is only distributing loads equally for all piles in group
- **Center to center pile spacing**: For each pile group configuration spacing of 3*D* and *5D*, are considered.
- **Pile depth**: the pile length is 10m, 20m and 30m is used in the parameter.

1.6 Structure of the Study

Chapter 1 deals with introduction about deep foundation specifically pile foundation and sources of lateral loads, statement of the problem, scope and structure of the study and objectives were discussed. Chapter 2 reviews of the literature comprehensively. This chapter starts with different methods for analysis group of pile under lateral loading. Previous numerical and experimental studies on the lateral loading of pile groups are also reviewed in this chapter.

Chapter 3 presents the tools and methodologies used in this research to fulfill the objectives listed in above section. Chapter 4 result and discussion of different parameters on the overall response of the pile groups through the calculation for different pile group

configurations. Chapter 5 provides conclusion and recommendations of load displacement curves of large group piles, and directions for some future research and the gap of knowledge.

CHAPTER 2 LITERATURE RIVIEWE

2.1 Laterally Loaded Group of piles

The behavior of pile groups under lateral loads can be analyzed using the p-y method. Recently, extensive research has been carried out on the p-multiplier concept originally suggested by (Brown et al. (1988). This method accounts for the loss of soil resistance due to the ‘‘shadowing’’ effect (that is, overlapping of shearing zones), and different values of p-multipliers are assigned to each row within the group. The p-y curves of individual piles in the groups are then obtained by multiplying the soil resistance values of p-y curves for a single pile by the assigned values of p-multipliers.

A horizontal load test on piles can be conducted by either pulling toward each other or by pushing apart the neighboring piles. A load-displacement curve obtained from a test by (Briaud (1997) for single piles is presented below.

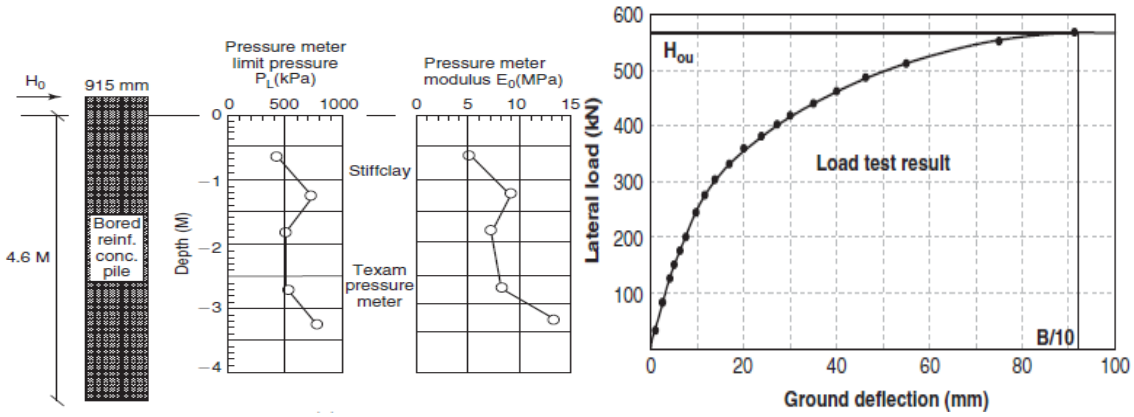

Figure 2-1 Load displacement curve for single piles (Briaud, 1997)

The ultimate load is defined as the one resulting in a displacement of 0.1B. The ultimate load can be obtained from horizontal force equilibrium of the portion above the point of zero shear (or max. moment). Thus,

$$H_{OU} = P_h B z_{\max} \qquad \textbf{(2-1)}$$

Based on analysis of database from pile load tests and associated pressure -meter data, Briaud (1997) proposed for the mean pressure p_h with in z_{max}

$$p_h = 0.75 p_L \qquad \textbf{(2-2)}$$

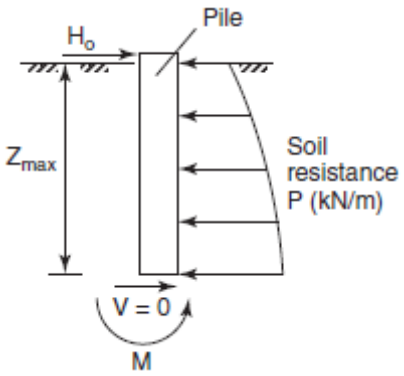

Figure 2-2 the depth at where the shear force is zero and M max and Zmax for single piles of laterally loaded.

When it came back to the group piles under lateral loadings the major issues include Ultimate load Capacity, Resistance to overturning moments, and Lateral Movement. The horizontal ultimate load capacity may be expressed as follow.

$$y_o = \frac{H_O}{l_o k} \qquad \textbf{(2-3)}$$

Where $H_{ou,g}$ = ultimate horizontal load of group piles, *e = group efficiency, n = number of piles,* $H_{ou,s}$ = ultimate horizontal load of single piles

However, load distribution is uneven, piles in the front row (leading piles) resist more than those in the back rows (trailing piles). This is because the soil around the trailing piles loosen up partially when the front piles are pushed forward.

The figure 2.3 below shows that how the leading piles and trailing piles are reacted under lateral loading. Estimation of lateral movement of a pile group is not an easy task. The simplest option is to assume that the pile cap prevents rotation of the pile heads as shown in the sketch. In this case, the horizontal displacement of the single pile was obtained above as

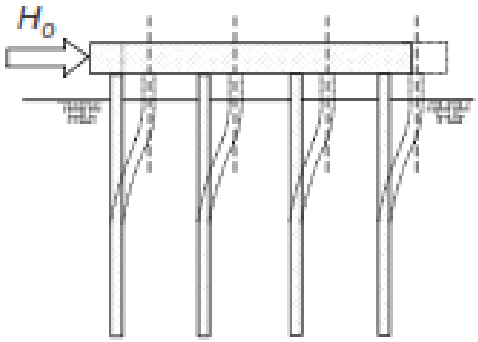

Figure 2-3 The reaction of leading piles and trialing piles under lateral loading

Fixed head flexible piles, $$y_o = \frac{H_O}{l_o k} \quad \textbf{(2-4)}$$

Fixed head rigid pile $$y_o = \frac{H_O}{LK} \quad \textbf{(2-5)}$$

$$l_0 = \sqrt[4]{4E_p I / K} \quad \textbf{(2-6)}$$

The soil stiffness, K, is given by

$$K = 2.3E_0 \quad \textbf{(2-7)}$$

Where E_0 is the pressure meter first load modulus of the soil, for pile group, a reduced value of E_0 is used to account for the group interaction, y_o lateral deffelection ,H_O horizal load, l_o is tranfer length and L is length of pile.

Piles are very rarely isolated but are usually put into pile-groups in order to strengthen load resistance. Although a pile-group strengthens overall lateral load resistance can weaken the individual pile response of the piles in the group. The overall lateral load is divided among each of the piles in the group. Each pile pushes against the soil behind it creating a shear zone in the soil. These shear zones begin to enlarge and overlap as the lateral load increases. More overlapping occurs if the piles are spaced very closely together. When overlapping occurs between two piles in the same row it is called “edge effects” and when overlapping occurs between piles in different rows it is known as “shadowing effects.” All of these “group interaction effects” result in less lateral resistance per pile.

Piles installed in groups at close spacing takes less load than a single pile subjected to the same lateral deflection because of the group effect. The group effect is caused by the overlap of the resistance zones of piles and the consequential reduction of lateral soil resistance. Many researchers (e.g. Prakash and Saran 1967, Brown and Reese 1985, McVay et al. 1998) have performed the pile group load tests and presented different approaches to consider the group effect. The widely used approach in current practices is to use the concept of p-multipliers described by Brown et al. (1988).

Numerous groups of piles must support loadings that are both axial and lateral; however, for the purpose of this study only group of piles subjected a lateral loading will be taken in account. Reese and Van Impe (2001) had mention that the behavior o f a group of piles may be influenced by two forms of interaction:

1. Interaction between piles in close proximity where efficiency is involved: -Here the relevant forces are transmitted through the soil.

2. Interaction by distribution of loading to individual piles from the pile cap: - In this case the forces are transmitted by the superstructure.

In practice, piles are sometimes used as single piles to transmit a column load to a deeper and stronger soil layer, but they are generally used in groups. The response of a single pile can be drastically different from the response of a similar pile in a pile group. When piles act in a group, pile–soil–pile interaction reduces the lateral resistance of the individual piles so that the group will generally exhibit less lateral resistance than the sum of the lateral resistances of the individual piles.

Approach used for analysis of a single pile, except that the p-value are reduced using a p-multiplier to account for the group effect. The value of the p-multiplier is related to the pile spacing and the pile location within the group. Leading row in a pile group has a higher value of p-multiplier than that of trailing row because the overlap of the resistance zone for trailing row is more significant. The average value of p-multipliers of all piles is used to represent the group efficiency of pile group in the design practice. Mokwa and Duncan (2001) provided a design chart for estimating the value of p-multipliers as functions of pile group arrangement and pile spacing.

In the pile group, every pile pushes against the soil before of it, creating a shear zone within the soil. These shear zones begin to enlarge and overlap because the lateral load will increase. Additional overlapping happens if the piles are spaced near one another. In this context the term edge impact is employed to explain the impact of overlapping zones of influence between piles within the same row. The term shadowing impact is used to explain the impact of overlapping zones of influence between piles in different rows (Larkela, 2008).

Figure 2.4 describes the sting impact and shadowing effect in a very laterally loaded pile group. Leading row and trailing rows are outlined based on the direction of loading as shown in Figure below Group impact reduces the lateral resistance of every individual pile within the pile group compared to single pile. Test measurements indicate that the leading row of the piles in the group will carry higher loads than the piles in the trailing rows at the same deflection. Group effect is expected to become less significant as the spacing between piles increases because there is less overlap between adjacent zones of influence.

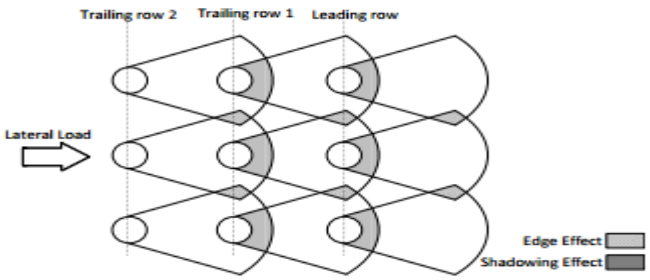

Figure 2-4 Illustration of shadowing effect and edge effect

2.2 Load Transfer Mechanism

2.2.1 Static load

A proper means of the load transfer mechanisms for piles is very important for analysis. Piles will transfer axial loads and lateral loads through totally different mechanisms. Within the case of lateral loads, apart or whole of the pile tries to shift horizontally within the direction of applied load, as a result it causes bending, rotation or translation of the pile (Fleming et al. 1992, Salgado 2008). The soil mass presence within the direction of

applied load develops compressive stresses and strains within the soil that gives resistance of the pile movement. The soil resistance acting over the complete pile shaft behaves the external horizontal load. Typically, within the case of laterally loaded pile, piles behave as transversely loaded beams. In case of this research a large group pile subjected to translational Load at the ground line with fixed head were considered.

The figure below shows that they transfer lateral load to the surrounding soil mass by using the lateral resistance of soil.

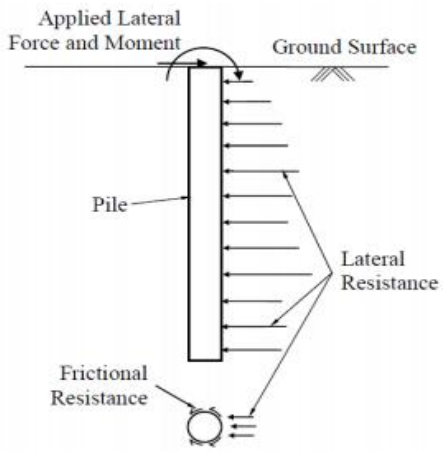

Figure 2-5 Load transfer mechanism of laterally loaded piles (Basu, 2006)

Interaction between piles happens within the case of laterally loaded pile groups furthermore. Furtherly laterally loaded pile group, every pile pushes the soil before of it (i.e., within the direction of the applied force). Movement of the piles placed within the leading row force is resisted by the soil before of it. In distinction, the piles within the rows behind the primary row (i.e., the piles within the trailing rows) go on the soil that successively pushed on the piles within the rows before of them (Figure 1-4). The resistive forces applied on the trailing-row piles groups' measure generally but the resistive forces working on the leading row (Prakash and Sharma, 1990)

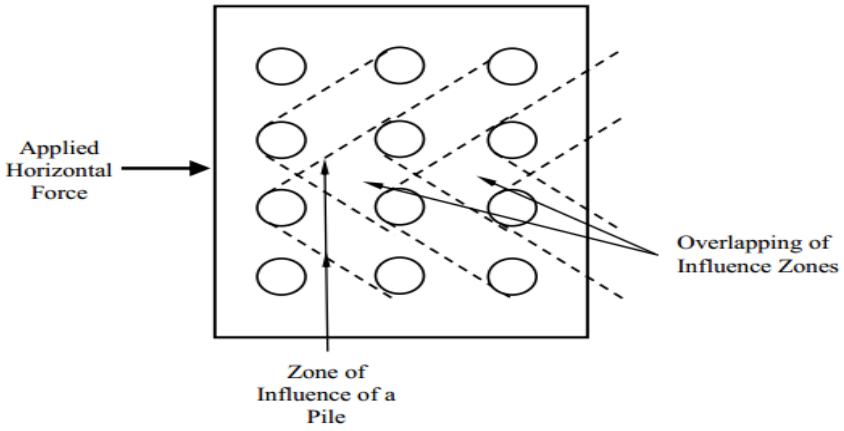

Figure 2-6 Illustration of over-lapping zones creating additional load on piles within a group

2.2.2 Kinematic Load

The mechanics of axially loaded piles is simple: the pile moves vertically downward below the acting load and, if the resistive forces (i.e., shaft and base resistances) exceed the limiting values, then the pile suffers excessive plunging, resulting in failure. The mechanics of laterally loaded piles is a lot of advanced and varies betting on the pile types. Since laterally loaded piles are transversally loaded, the pile might rotate, bend and/or translate. Because the pile moves within the direction of the applied force, a spot may additionally open up between the rear of the pile and therefore the close soil over the highest few meters. If the pile is rigid and short, not bend abundant however will rotate or perhaps translate, such piles are known as rigid piles. If the pile is long and slender, then it bends. These piles are known as flexible piles. In most sensible things, piles are long enough to behave as flexible piles. For flexible piles, the laterally loaded pile problem could be a common soil-structure interaction (SSI); i.e., the lateral deflection of the pile depends on the soil resistance, and therefore the resistance of the soil, in turn, depends on the pile deflection.

2.3 Soil -Pile-Soil- Interactions

In structures founded on non-rigid formations, the soil flexibility influences structural response and the structure flexibility itself influences the soil responses. This phenomenon is called soil structure interaction. Soil structure interaction involves the

interaction of three inter-linked systems: The structure, the foundation and the geological medium (Paulson, 1985).

In practice, when a pile group is subjected to the lateral load, the induced interaction between the piles and the surrounding soil can be very complicated. The non-linear nature of soil response is an obvious source of complexity and the interaction of pile behavior on the surrounding soil increases this complexity. Presence of other piles in the vicinity of each pile provides further complexity through pile–soil–pile interaction. Understanding the behavior of group pile under lateral loading helps to comprehend general soil–pile interaction issues as well as providing a basis for assessing the lateral response (McVay et al. 1996b).

2.4 Response of Soil from a Pile under Lateral Loading

Soil response to a given lateral load is modeled by developing a relationship between the pile's lateral deflection and the resistance of the soil. This relationship is represented graphically in a p-y curve, where y represents the lateral displacement of the pile and p represents the soil resistance per unit length of the pile. Each layer of soil that the pile passes through will have a different amount of resistance depending on the strength of the soil, and therefore a different p-y curve

There are some strategies like those advised by Brinch-Hansen (1961) and Broms (1964a, b) for estimating the ultimate lateral resistance of single piles directly. However, they're not wide used as a result of these strategies don't offer the corresponding data concerning the lateral deflections (Tehrani, 2009). The most approaches for analyzing soil–pile interaction is the strain wedge (SW) methodology, p–y method, and continuum methodology. All of those approaches are delineating in short within the following sections.

2.4.1 Strain Wedge Method

The strain wedge (SW) technique has been developed to predict the lateral response of a flexible pile (Ashour and author, 2000,). The SW model parameters are associated with the passive wedge of soil developing before of the pile. The SW model relates stress strain-strength behavior of the bedded soil within the wedge to pile parameters.

Therefore, the strain wedge model is in a position to supply a theoretical link between the additional advanced 3D soil–pile interaction and also the less complicated one-dimensional BEF characterization. Figure 2.7 shows the concept of SW model. The geometry of the passive failure wedge is characterized by the mobilized effective friction angle of the soil (φ_m), the depth of pile deflection under lateral load (h), and mobilized base angle (β_m= 90-θm), where θ_m= 45◦ -φ_m. For the calculation of soil reaction at each stress level (SL) in the soil, the initial pile deflection pattern is assumed to be linear (being zero at depth h and reaching to a nominal value at the surface) and an iterative procedure is used to determine φm and h for a given head load. Iteration terminates when equilibrium between mobilized geometry of the passive wedge and the deflected pattern of the pile is satisfied (Ashour et al. 1998).

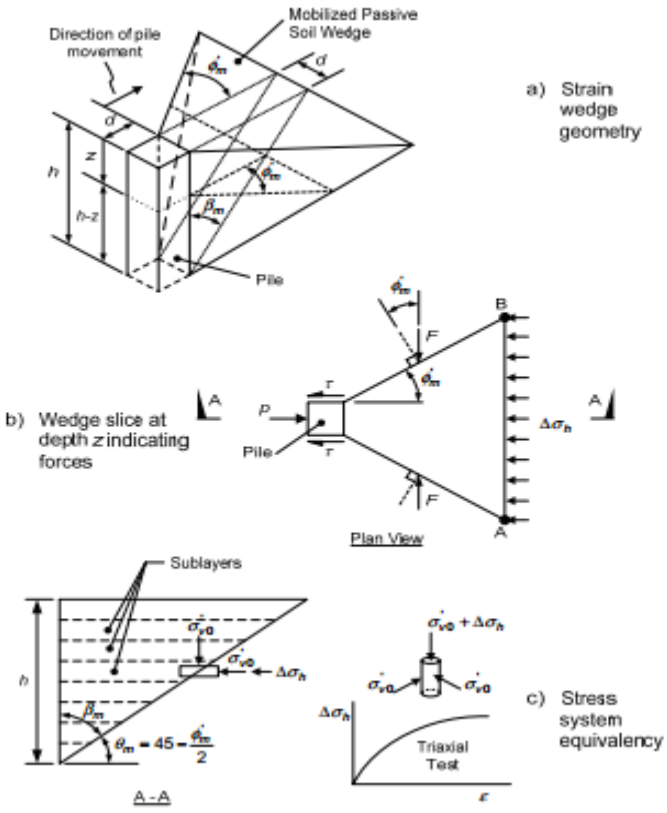

Figure 2-7 Strain Wedge model concept (after Dodd's and Martin, 2007)

2.4.2 P− y method

The p–y technique is the most typical analysis tool for pile foundations in practice. During this approach resistance of the surrounding soil is drawn by a series of non-linear springs that are connected to the pile as shown in Figure 2.8. The properties of those non-

linear springs are outlined by the thus referred to as p–y curves. Figure 2.8 additionally shows that p–y curves get stiffer increasingly with depth. The pile during this technique is modeled with beam elements.

$$p = \frac{d^2 M_p}{dz^2} = \frac{E_P I_p d^4 y}{dz^4} \qquad \textbf{(2-8)}$$

Where $\boldsymbol{M_P}$ = $\boldsymbol{E_p I_p}$ is moment in pile at the depth of z,

y = is lateral deflection of the pile at depth of z,

$\boldsymbol{E_p I_p}$ =is flexural rigidity of pile and

P= is soil reaction at depth of z.

The prediction of the soil resistance at any point along the pile as a function of pile deflection is perhaps one of the most critical factors in solving the problem of a laterally loaded pile. The distribution of stresses against a cylindrical pile before installation is shown in figure 2.8 (a) at a given depth, the stresses will be uniform and normal to the pile wall (Reese and Van Impe 2001). After the pile is subjected to lateral loading, the pile will deflect and the soil stresses acting on the pile would have a distribution similar to that shown in figure 2.8 (b). It is important to point out that some of the stresses will not be perpendicular to the pile wall due to development of shear stresses at the interface between the pile and the soil. The net soil reaction, p(x), is obtained by integrating the stresses around the pile cross section.

McClelland and Focht (1958) introduced the procedure for getting p and y for laterally loaded piles. Matlock (1970) and Reese et al. (1974) have developed the thought of p–y curves for finding laterally loaded pile issues. Since the initial work of McClelland and Focht (1958) various studies have been undertaken to calibrate the p–y curves for various depths, soil varieties or pile geometries.

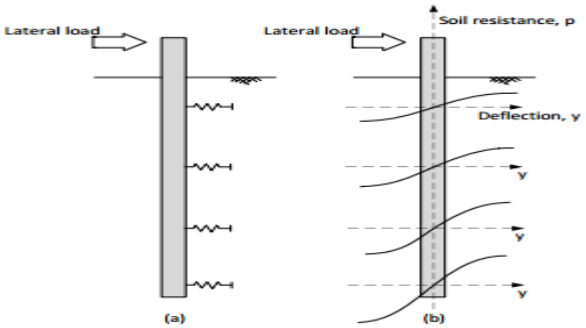

Figure 2-8 Representation of (a) pile and non-linear springs in *p–y* method, (b) corresponding *p–y* curves

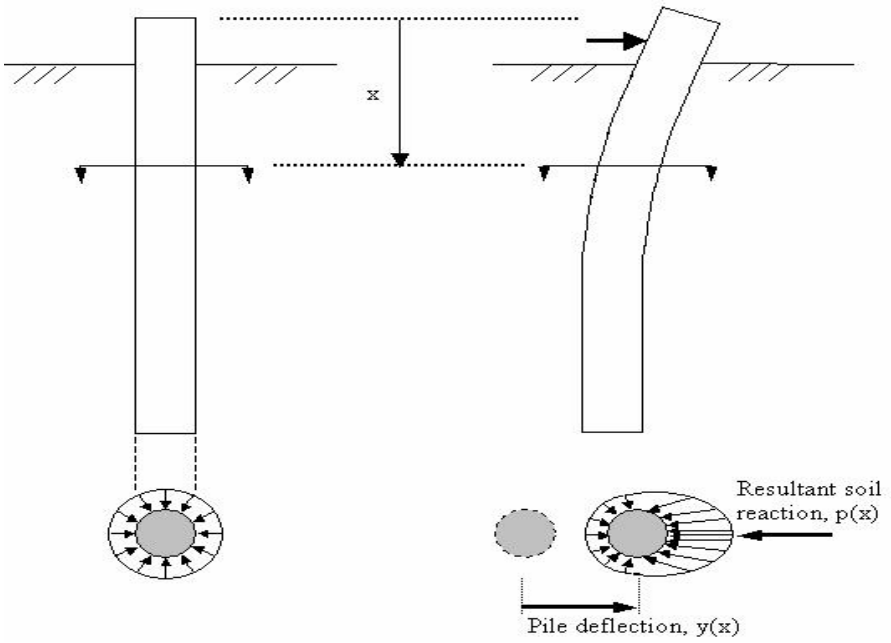

Figure 2-9 distribution of stresses against a pile before and after lateral loading (adapted from Reese and Van Impe 2001).

In general, p-y curves are non-linear and they are a function of depth, soil type, and pile dimensions and properties. A typical p-y curve is shown in figure. Important elements of the p-y curve include the initial slope, E_{py}-max, and the ultimate soil resistance value, P_{ult}. At any point of the p-y curve the soil reaction, p, is related to the pile deflection, y, through the p-y modulus, E_{py} (Reese and Van Impe 2001). The p-y modulus is also known as the reaction modulus and it has units of force/length^2. Reese and Van Impe (2001) propose using the nomenclature given above instead of the modulus of subgrade reaction, which was originally developed to describe settlement of footings and relates the footing pressure (units of force/length^2) to the footing settlement (units of length). These

authors also point out that, although the subgrade modulus and E_{py} are related to the values of the Young modulus of the soil, E_s, they are not only a function of the soil, but rather a result of the soil-structure interaction process between the soil and the footing and pile, respectively.

2.4.3 American Petroleum institute (API) (2007) *p–y*-curves

The most commonly used p–y curves in engineering practice are those provided by American petroleum Institute (API, 2007). These recommendations are supported the works of Murchison (1983) and Matlock (1970). The API suggests totally different p–y curves for sand, soft clay and stiff clay that are referred as standard p–y curves.

Clay: The *p–y* curves derived from a full-scale test by Matlock (1970) are used in API (2007) for soft clays. To determine *p–y* curves for laterally loaded piles in soft clays the following relation is recommended in API:

$$P = \begin{cases} 0.5 p_u \left(\frac{y}{y_c}\right)^{1/3}, & \left(\frac{y}{y_c}\right) < 8 \\ p_u, & \left(\frac{y}{y_c}\right) \geq 8 \end{cases} \quad \textbf{(2-9)}$$

Where *y*: lateral deflection, in (m)

$y_c = 2.5\varepsilon_c D$, in (m),

ε_c: strain which occurs at one-half the maximum stress on laboratory unconsolidated undrained compression tests of undisturbed soil samples, p_u: ultimate resistance, psi (kPa) (for obtaining p_u please refer to API (2007)) API (2007) does not have any relationship for stiff clays but it refers to the work of Reese et al. (1975) for stiff clays.

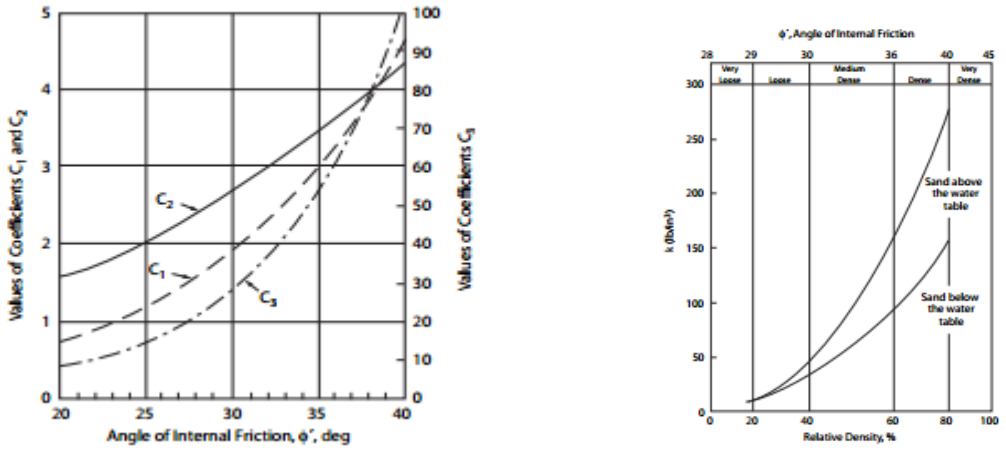

a) b)

Figure 2-10 a) Graph presented in API (2007) for coefficients *C*1, *C*2, and *C*3 b) Graph presented in API (2007) for initial modulus of subgrade reaction.

2.4.4 Continuum Method

The major weakness of the *p–y* method is the independence of each spring from others. However, in reality soil should be considered as continuum media. Finite Difference (FD) and Finite Element (FE) methods are two numerical approaches for discretization and solution of the problem which consider the soil as continuum media.

Continuum approaches, as defined here, comprise an assortment of solution techniques utilizing either the theory of elasticity alone or both the theory of elasticity and plasticity. These include fully three-dimensional analyses and simplifications using two-dimensional analyses (plane strain or plane -stress). Three-dimensional analyses offer the most realistic approach to assessing pile-soil interaction, and are divided into integral equation (or boundary element) method and differential method analysis categories.

The main advantage of the continuum approach compared to other approaches is that less simplifications need to be made in simulation of a real problem. Other features include the ability to apply any combination of axial, torsion, and lateral loads, the capability of considering the non-linear behavior of structure and soil, and the capability to model soil–pile-structure interactions. The continuum approach potentially provides the most powerful means for performing Soil–Structure Interaction (SSI) analyses, but it has not yet been fully realized as a practical tool. Challenges to successful implementation of

numerical technique lie in the selection of appropriate constitutive models for materials for the soil and the pile, and the accurate assignment of the parameter values for these models. The selection or development of constitutive models and quantification of their parameters are still open areas of research. The degree of uncertainty associated with the specification of model parameters as well as laborious mesh generation and interpretation of results, often renders the continuum approach a secondary option (to the *p–y* approach) in engineering practice (Tehrani, 2009). Also, performing three-dimensional continuum analysis requires considerable time for generating input and interpreting results. Therefore, continuum approach has been mostly used for research on pile group behavior, rarely for design

2.4.5 Boundary Element for laterally loaded piles

An advantage of the boundary element method over other methods is its use of surface discretization that provides for the greatest numerical efficiency when dealing with three-dimensional problems possessing low surface area to volume ratios, as is the case with pile foundation problems (Banerjee, 1976). This enables a three-dimensional solution with the least computational effort and is certainly a redeeming feature of the method. Boundary element methods use the Mindlin (1936) solution for lateral displacement induced by a horizontal point load (refer Figure: 2.10) as the mechanism responsible for interdependency. Through numerical integration of this solution over a discretized pile surface, equating lateral displacements from the elastic soil (Mindlin's solution) and elastic pile (Bernoulli-Euler beam theory), and imposing equilibrium conditions, a simultaneous equation solution ensues to solve for unknown forces that then allows determination of pile actions.

Introducing this type of approach to assess lateral response of piles, Spillers and Stoll (1964) noted that the purely elastic solution generated very high lateral pressures against the pile near the surface that would result in yielding of real soil. Non-linear behavior of the soil model was therefore introduced by specifying maximum permissible pressures mobilized against the pile based on plastic yield criteria, considered a "first modifying effect" towards reconciling results with observed behavior. This reiterated the need for attention to surficial soils when assessing lateral load behavior, and the need of non-linearity in the pile- soil system. Subsequent work developed the boundary element principle put forward by Spillers and Stoll to produce useful design information for

various pile-soil configurations, albeit from a mostly linear-elastic perspective. Notable was the work of Poulos (1971a), Banerjee and Davies (1978), Davies and Budhu (1986), and Budhu and Davies (1987, 1988).

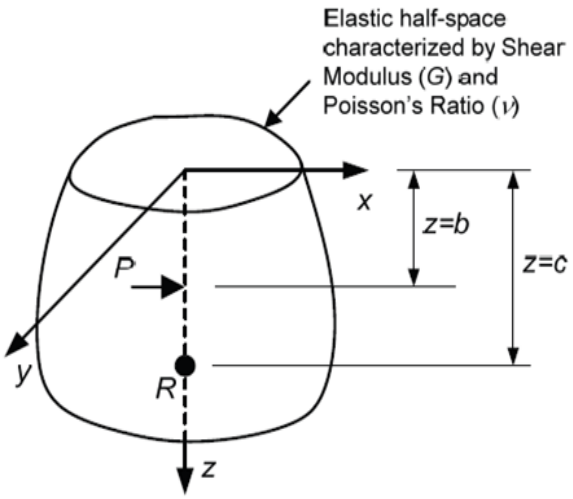

Figure 2-11 Mindlin (1936) solution

U_R = Lateral displacement at point R due to point load P

$$U_R = \frac{P}{16\pi G(1-v)}\left[\frac{3-4v}{|b-c|} + \frac{1+(1-v)(1-2v)}{b+c} + \frac{2bc}{(b+c)^3}\right] \quad \textbf{(2-10)}$$

Poulos (1971a) choose a somewhat crude approach, starting with the depiction of a pile as a thin rectangular strip of width equal to the pile diameter (d), and possessing a length (L) and flexibility (E_pI_p) corresponding to that of the pile. A linear-elastic continuum with Young's modulus (E_s) constant with depth was used to represent the surrounding soil, and no separation between the pile and soil allowed. Any shear stresses at the pile edges were neglected, pile-soil interaction derived solely from uniform distribution of normal stress assumed across each pile-segment width, where pile lengths were discretized into standard 21 equal-length segments. Although a very crude approximation of actual behavior, the approach provided a consistent framework in which to assess the behavior of both rigid and flexible piles.

Such behavior was presented using the concept of pile head influence factors of the form given by the following equation below, where rotational influence factors were similarly defined to obtain rotation at the pile head.

$$\delta_h = I_{\delta p}\frac{P}{E_s L} + I_{\delta M}\frac{M}{E_s L^2} \quad \textbf{(2-11)}$$

Where

δ_h = lateral deflection at pile head,

$I_{\delta p}$ =displacement influence factor for horizontal load only,

P =horizontal load (applied at pile head),

$I_{\delta M}$ =displacement influence factor for moment only, and

M =moment (applied at pile head).

Typical trends observed are shown in Figure-2.12, where the parameter *KR* represents a relative pile-soil stiffness measure, and the length-to-diameter (or slenderness) ratio, *L*/*d*, an appropriate parameter for distinguishing between rigid and flexible piles. In effect, *KR* accounts for non-rigidity of the pile foundation and *L*/*d* accounts for embedment (Kuhlemeyer, 1979). Poulos (1972) noted that displacement and rotation at the pile head are virtually unaffected by the boundary condition at the pile tip when *KR* values are less than about 0.01. Kuhlemeyer (1979) noted that this translates to an effective slenderness ratio at which flexible pile behavior can be assumed to apply, and such effective slenderness ratio values are plotted in Figure-2.13 against the ratio of the pile to soil modulus, E_p E_s. Shown are slenderness ratios corresponding to K_R-values of 0.01 and 0.05. Kuhlemeyer considered that K_R= 0.01 was appropriate for displacement behavior at the pile head, but K_R= 0.05 more appropriate for rotation behavior.

The work of Banerjee and Davies (1978) mainly served to provide a more rigorous boundary element technique whereby both normal and shear stresses around a cylindrical pile-soil interface were incorporated into the solution scheme using an a priori numerical procedure. Results for the soil modulus linearly increasing at the ground surface from both zero and half the pile tip modulus (i.e., triangular and trapezoidal distributions respectively) were also obtained, although these required an approximate solution scheme given that the Mindlin (1936) solution is strictly only valid for a constant modulus distribution with depth. These non-homogenous modulus cases exhibited a relative

increase in the values of influence factors and transfer of pile actions to greater depths compared with the homogeneous modulus case. Relatively higher bending moments in the pile were also noted in the non-homogeneous cases.

Davies and Budhu (1986) and Budhu and Davies (1987, 1988) advanced on Banerjee and Davies (1978) by acknowledging different soil resistance patterns around a pile. Assuming a solid cylindrical elastic beam for the pile (as used by Banerjee and Davies), limiting soil stresses were assigned at the front, sides and back of the pile. These were based on conventional bearing capacity values for the normal stresses acting against the front face of the pile, empirical adhesion values for shear stresses acting along the sides of the pile and limiting the decrease in normal stresses at the back of the pile to be no greater than in situ horizontal stresses derived from assumed lateral earth pressure coefficients. The latter served to prevent tensile stresses and thus convey a pile-soil separation effect. While only an approximate account of soil non-linearity, this approach emphasized the significant increase in pile displacements, rotations and bending moments as a result of soil yielding. This effect was shown to increase as the level of loading increased and was most apparent with flexible piles.

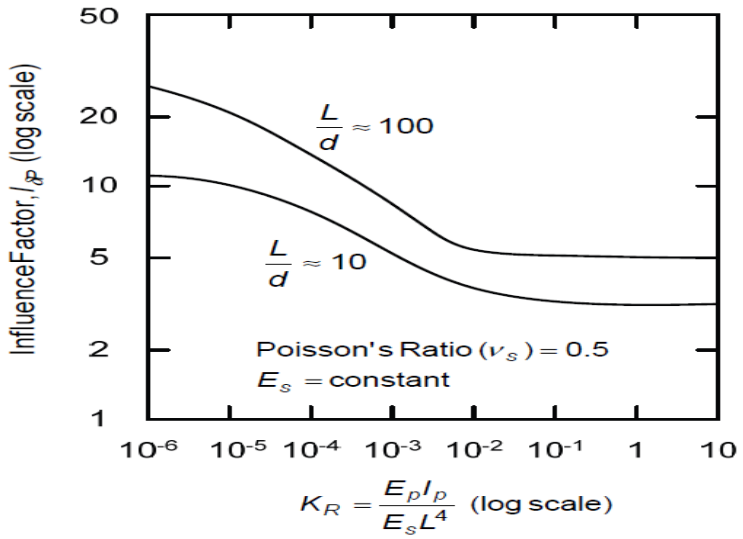

Figure 2-12 Influence factor for free headed pile

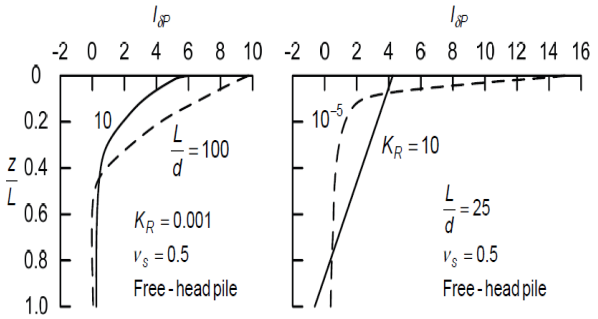

Figure 2-13 Typical displacement profiles showing effect of L/d and K_R

Typical trends for rigid and flexible piles (after Poulos and Davis, 1980)

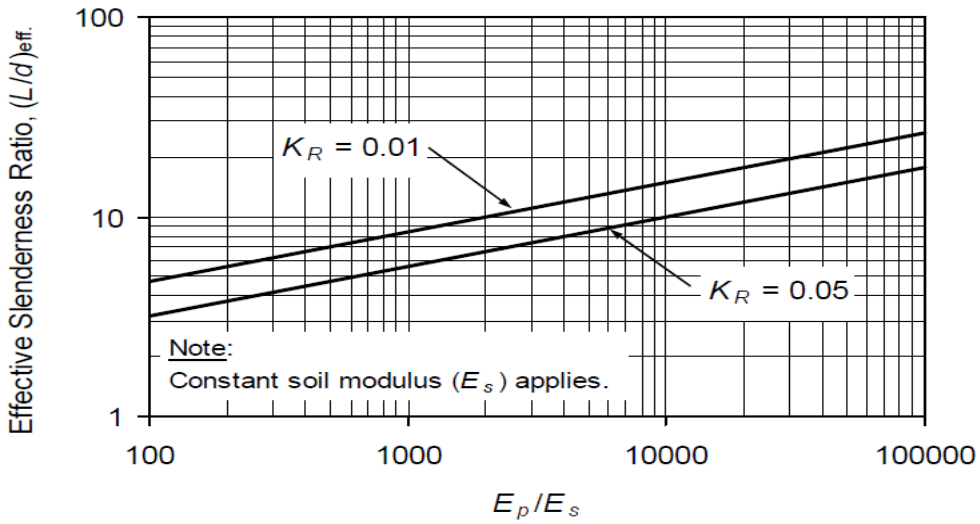

Figure 2-14 Apparent effective slenderness ratios for flexible pile behavior

Besides emphasizing the importance of nonlinear soil effects, the work of Davies and Budhu (1986) and Budhu and Davies (1987, 1988) also improved on prior elastic boundary element solutions by providing algebraic expressions to directly calculate pile head behavior for flexible piles. This approach was initiated by Kuhlemeyer (1979), who showed that, given flexible pile and elastic conditions, the independence of pile head displacement and rotation to pile length leads to behavior that is only a function of the pile-soil stiffness ratio. The algebraic expressions together with appropriate critical pile lengths for constant and linearly increasing distributions of Young's modulus with depth, as determined by Davies and Budhu and Budhu and Davies, are indicated in Table. Also given are expressions for a parabolic distribution of Young's modulus with depth, as determined by Pender (1993) using the work reported by Gazetas (1991). Such information can be used as a means of back-calculating equivalent elastic soil moduli at

small deflections using real load-deflection behavior. This is an important consideration when modeling pile load tests because the initial stiffness assigned to a soil model, particularly an elastic-plastic soil model, is one of the key parameters that control the nonlinear response of a modeled pile.

Although useful from a general design standpoint, the boundary element technique suffers in that its underlying elastic nature limits its applicability and allows for soil non-linearity in only an approximate manner (i.e., introduction of limiting pressures that are strictly out of place in an elastic system). Idealization of the pile as a line element, necessary to avoid otherwise prohibitively expensive numerical computations, is also restrictive. This is because the governing integral equations can be satisfied only at the centerline of the pile, which in turn enforces limitations on the nature of surface tractions (i.e., normal and shear stresses) acting around the mathematical pile circumference (Banerjee and Driscoll, 1976). To this end recourse to differential methods in the form of finite elements, and use of elastic-plastic soil models, affording a more rational representation of soil non-linearity, has provided a powerful alternative for modeling pile-soil interaction.

2.4.6 Group Reduction Factor (p-multiplier)

One of the most common strategies of accounting for the group effects in Winkler approach is to change the single pile p–y curves employing a p-multiplier, as recommended by Brown et al. (1988). During this approach, the soil resistance, p, is reduced by a constant issue, P_m, as shown in Figure 2.15 P_m cannot be larger than one. Supported accessible recommendations like AASHTO (2012) and FEMA P-751 (2012), process p-multipliers for pile group design depends on the row spacing with in the loading direction. The p-multiplier for a leading row is more than the p-multiplier for a trailing row due to the shadowing result. Given the relative prevalence of p-y curves, stress on determination of applicable p-multipliers for a given pile spacing is taken into account because the most applicable suggests that to research pile group response under lateral loading.

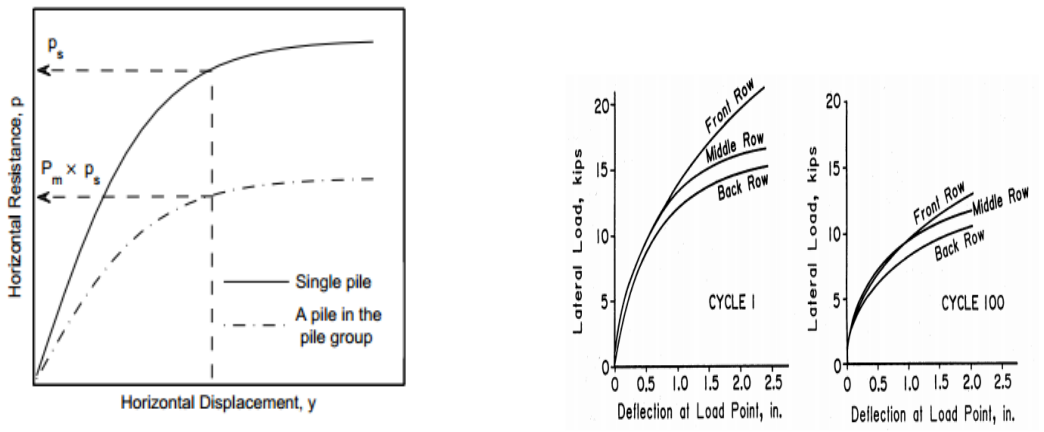

a) b)

Figure 2-15 a) definition of P multiplier b) Distribution of load in a pile group for different cycles of loading (after Brown et al., 1998)

Leading row has higher *p*-multiplier than trailing rows. In an alternative approach, rather than defining *p*-multipliers row by row, an average *p*-multiplier is used for all piles in the group which gives the same pile cap load–deflection curve (Brown et al., 2001). This average *p*-multiplier is called the group reduction factor. Use of a group reduction factor is convenient for seismic and cyclic loading because the direction of loading changes repeatedly and often unpredictably during the loading event, and each load reversal converts a leading row, with high *p*-multiplier, to a trailing row, with low *p*-multiplier, instantaneously.

2.5 Theoretical Studies

As De Beer (1977) indicated, the theoretical studies can be classified as (1) modulus of subgrade reaction method considering the pile as an elastic beam on a foundation, (2) elastic continuum methods assuming the soil to be a linear elastic or elastic-plastic material, (3) finite element methods simulating the stress-strain behavior of soil with multilinear or hyperbolic approximations and some other empirical methods.

2.5.1 Modulus of Subgrade Reaction Method

Hetenyi (1946) assumed piles as beams on an elastic foundation and soil reaction represented by Winkler springs. Equation (2-5) was proposed by Hetenyi (1946) for the

solution of loaded piles in soils as long as both pile and soil stay in elastic limits (Oztürk 2009).

$$\frac{d^2M}{dz^2} + Q\frac{d^2y}{dz^2} - p = 0 \qquad \textbf{(2-12)}$$

Where;

M: Bending moment

Q: Axial load on the pile

z: Depth along the pile

y: Lateral deflection of pile at point z

p: Lateral resistance of soil per unit length of pile

In case of slope stabilizing laterally loaded passive piles, axial loading on pile (Q), can be ignored and Equation (2.5) can be transformed into the following equation with some modifications as:

$$E_p I\frac{d^4y_p}{dz^4} = K_s(y_p - y_s) \qquad \textbf{(2-13)}$$

Where;

E_p: Deformation modulus of pile

I: Moment of inertia of pile

y_p: Lateral displacement of the pile at depth z

y_s: Lateral displacement of the soil at depth z if no pile was placed in the slope

K_s: Subgrade reaction modulus of soil

In Equation above, subgrade reaction modulus, (K_s) is variable with depth and relative displacement (y_p-y_s). De Beer (1977) indicated that there may be uncertainties of the solution of Equation above because of the difficulties of determining lateral displacement of the soil if no pile exists in the slope, (y_s).

2.5.2 Elastic Continuum Theory

The modeling of the soil as a homogeneous elastic continuum has been suggested for the analysis of the soil-pile interaction. For the analysis of limit pile capacity, Plane Strain Models were developed with some authors like Davis and Booker (1971). For modeling the 3D system as a series of parallel horizontal planes in plane strain, the Plane Strain Models are used which are related to the case of shallow-embedded sheet piling.

Douglas and Davis (1964); Poulos (1971, 1972), and other authors developed Three Dimensional Elastic models. These models were established on Mindlin's method for the horizontal displacement due to a horizontal point load within the interior of a semi-infinite elastic-isotropic homogeneous mass which can be found in various Elasticity handbooks, such as Poulos and Davis (1974).

Douglas and Davis (1964); Spillers and Stoll (1964) and Basile (2002) recommended integral solutions over a predefined area, representing a fraction of the pile surface, since Mindlin's solutions become singular when evaluating the displacement corresponding to the point where the load is located. These solutions which define the displacement field due to an assumed loading system (pattern) associated with the pile-soil interaction, are generally known as Green Functions.

Utilization of the model suggested by Poulos (1971, 1972), was presented by Poulos and Davis (1980). The pile is assumed to be a thin rectangular vertical strip divided in elements in this model, and it is observed that each element is acted upon by uniform horizontal stresses as it shown in Figure 2.10 which are related to the element displacements through the integral solution of Mindlin's problem.

At last, in which soil pressures over each element are unknown variables, they realized the differential equation of equilibrium of a beam element on an infinite soil with the Finite Difference Method (FDM). The displacements are found after achieving the pressures.

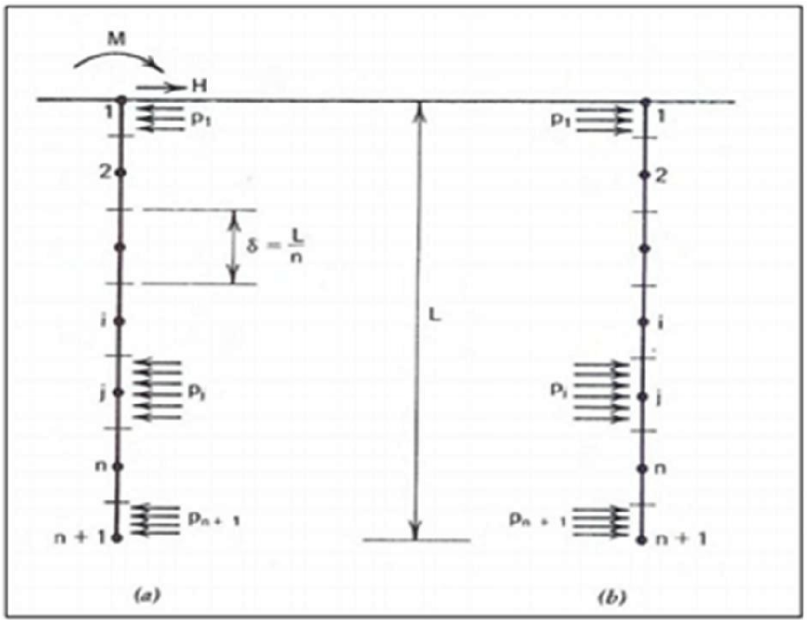

Figure 2-16 Continuous Analysis Model of Soil-Pile Stress reacting on (a) Pile, (b) Soil around the Pile (Poulos& Davis, 1980)

The ability to take into consideration the homogeneous nature of soil, the semi-infinite dimension of the half-space, and the boundary conditions along the unloaded ground surface is the advantage of this model. Although yielding of soil may be presented by varying the soil elastic modulus, this method does not allow to consider local yielding and layered soil conditions.

In this way, Spillers and Stoll (1964) suggested the calculation of the maximum allowable load by any appropriate yielding condition (e.g. a wedge model for the top part of the soil, where the yielding of soil happens and displacements are larger), together with the elastic solution and a repetitive procedure to control that the maximum load is not exceeded at any point.

Two of the disadvantages of the discretization by cooperating with means of the FDM is that the difficulty to present general boundary conditions at pile top and bottom, and the needed uniform size of the elements. This soil model was used for the BEM (Boundary Element Method) analysis of piled foundations, as Basile (2002) informed.

2.6 Constitutive Models

Soil is a complicated material that behaves non-linearly and often shows anisotropic and time dependent behavior when subjected to stresses. Generally, soil behaves differently in primary loading, unloading and reloading. It exhibits non-linear behavior well below the failure condition with stress dependent stiffness. Soil undergoes plastic deformation and is inconsistent in dilatancy and also experiences small strain stiffness at very low strains and upon stress reversal. In addition to soil behavior, its failure in three-dimensional state of stress is extremely complicated. Numerous criteria have been devised to explain the condition for failure of a material under such loading state.

Currently, various constitutive models for the soil have been developed. These models cover a wide range of soil features such as anisotropy, cyclic loading, creep etc. The selection of a constitutive model for a geotechnical application depends on the mechanical properties of the soil. (i.e. permeability, stiffness and strength), previous history on the mechanical properties of the soil and the stress changes that will occur in feature.

In the finite element analysis, reliable predictions can be achieved by using an appropriate constitutive model for a particular geotechnical problem. In general, the criterion for the soil model evaluation should always be a balance between the requirements from the continuum mechanics aspect, the requirements of realistic representation of soil behavior from the laboratory testing aspect, convenience of parameter derivation and simplicity in computational application. The application of some constitutive models in Plaxis finite element model and some parameters are listed below:

Linear Elastic Model (LE), Mohr Coulomb Model (MC), Hardening Soil Model with small stiffness (HSS), Soft Soil Model (SS), Soft Soil Creep Model (SSC), Modified Cam Clay Model (MCC), Linear Elastic Model (LE)

2.6.1 Linear elastic model

The linear Elastic Model (LE) is based on the Hook's law of isotropic elasticity. It only involves two basic parameters Young's modulus (E) and Poisson ratio (ν) . The LE Model is not suitable to model soil because soil behavior is highly non-linear and irreversible. Hooke's law is on the other hand a good idealization for material in

structural elements, such as steel, which often behaves linear elastic and isotropic, at least in its lower stress states

$$\begin{bmatrix} \dot{\sigma}'_{xx} \\ \dot{\sigma}'_{yy} \\ \dot{\sigma}'_{zz} \\ \dot{\sigma}'_{xy} \\ \dot{\sigma}'_{yz} \\ \dot{\sigma}'_{zx} \end{bmatrix} = \frac{E'}{(1-2\nu')(1+\nu')} \begin{bmatrix} 1-\nu' & \nu' & \nu' & 0 & 0 & 0 \\ \nu' & 1-\nu' & \nu' & 0 & 0 & 0 \\ \nu' & \nu' & 1-\nu' & 0 & 0 & 0 \\ 0 & 0 & 0 & \frac{1}{2}-\nu' & 0 & 0 \\ 0 & 0 & 0 & 0 & \frac{1}{2}-\nu' & 0 \\ 0 & 0 & 0 & 0 & 0 & \frac{1}{2}-\nu' \end{bmatrix} \begin{bmatrix} \dot{\varepsilon}_{xx} \\ \dot{\varepsilon}_{yy} \\ \dot{\varepsilon}_{zz} \\ \dot{\gamma}_{xy} \\ \dot{\gamma}_{yz} \\ \dot{\gamma}_{zx} \end{bmatrix} \quad \textbf{(2-14)}$$

Where ν is poison ratio, E young modulus, ε axial strain, ɤ shear strain and σ stress

According to Hook's law the relationship between *E, young* modulus, *G* shear modulus and K of bulk modulus is as the following equations.

$$G = \frac{E}{2(1+\nu)} \quad \textbf{(2-15)}$$

$$K = \frac{E}{3(1-2\nu)} \quad \textbf{(2-16)}$$

2.6.2 Mohr Coulomb Model (MC)

The Mohr-Coulombs model (MC-model) is an elastic perfectly-plastic model. The general behavior of an elastic perfectly plastic material is illustrated in Figure 2.17.The most widely used constitutive model for soils is the Mohr-Coulomb model, which has the advantage of requiring only the classical geotechnical parameters (unit weight, void ratio, deformation modulus and shear strength parameters). However, it has been noted that the Mohr-Coulomb model frequently overestimates soil deformations for small strains (Truty, 2008).

The Mohr Coulomb Model (MC) is a linear elastic and perfectly plastic model. It involves five parameters, both elastic and plastic behavior parameters i.e. Young's modulus (E) and Poisson's ratio (ν) for soil elasticity, friction angle (ϕ) and cohesion (c), for soil plasticity and the dilatancy angle (ψ).

Although the increase of stiffness with depth can be taken in to account. The stiffness behavior below the failure line is assumed to be linear elastic according to Hook's law. Hence, the model does not accurately predict deformation behavior before failure, especially in situation where the stress levels are changing or multiple different stresses paths are allowed. For tunnel construction, the MC model predicts too wide settlement trough. As far as its strength behavior is concerned, this model is suitable to analyze the stability of dams, slopes and embankments. However, the model does not show softening behavior after peak strength. Soft soils like normally consolidated clays, generally show a decreasing mean effective stress during undrained shearing, whereas the Mohr-Coulomb model would predict a constant mean effective stress in this case, which results in an over prediction of the shear strength.

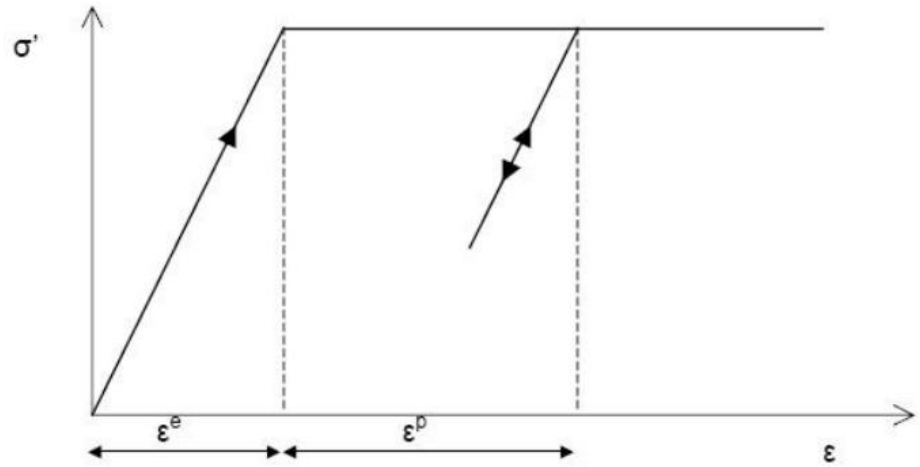

Figure 2-17 Basic idea of an elastic perfectly plastic model

2.6.3 Mohr coulomb's failure criteria and strength

Strength is the maximum stress a soil can withstand without failing. Failure in soil is, in general, caused by shear stress, i.e. shear failure. Shear failure occurs when particles slide or roll past each other. Failure due to compression would be particles crushing, but, since the particles start sliding and rolling, when exposed to compression, they fail in shear and not compression (Coduto C.P. (1999).

$$\boldsymbol{\tau = c' + \delta' tan\, \varphi'} \qquad \textbf{(2-17)}$$

Where $\boldsymbol{\tau}$ shear strength of soil, ***c' c***ohesive property of soil, δ' effective stress and φ' is frictional angle.

When modelling plasticity Plaxis introduces functions called yield functions, which are equal to zero when the material behaves plastic. The Mohr-Coulomb yield condition consists of six yield functions, all expressed with principal stresses, the friction angle and the cohesion. The Mohr-Coulomb yield condition is an extension of the Coulomb friction law and obeys this law in any plane within the material. When the six functions are set to zero (i.e. acting plastic) they create a surface in the principal stress space called the yield surface, illustrated in Figure 2.18.When the material is exposed to stress states within this surface it acts elastic and Hooke's law obey.

$$f_{1a} = \tfrac{1}{2}(\sigma'_2 - \sigma'_3) + \tfrac{1}{2}(\sigma'_2 + \sigma'_3)\sin\varphi - c\cos\varphi \le 0$$

$$f_{1b} = \tfrac{1}{2}(\sigma'_3 - \sigma'_2) + \tfrac{1}{2}(\sigma'_3 + \sigma'_2)\sin\varphi - c\cos\varphi \le 0$$

$$f_{2a} = \tfrac{1}{2}(\sigma'_3 - \sigma'_1) + \tfrac{1}{2}(\sigma'_3 + \sigma'_1)\sin\varphi - c\cos\varphi \le 0$$

$$f_{2b} = \tfrac{1}{2}(\sigma'_1 - \sigma'_3) + \tfrac{1}{2}(\sigma'_1 + \sigma'_3)\sin\varphi - c\cos\varphi \le 0$$

$$f_{3a} = \tfrac{1}{2}(\sigma'_1 - \sigma'_2) + \tfrac{1}{2}(\sigma'_1 + \sigma'_2)\sin\varphi - c\cos\varphi \le 0$$

$$f_{3b} = \tfrac{1}{2}(\sigma'_2 - \sigma'_1) + \tfrac{1}{2}(\sigma'_2 + \sigma'_1)\sin\varphi - c\cos\varphi \le 0 \qquad \textbf{(2-18)}$$

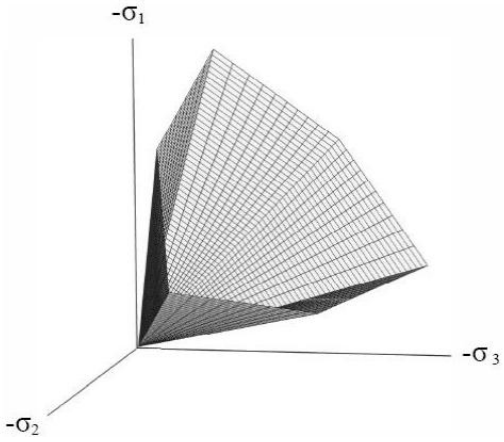

Figure 2-18 Mohr-Coulombs yield surface in principal stress space (Brinkgreve R.B.J 2008)

2.7 Analytical Studies

Reese (1975) presented two simple expressions for the determination of the ultimate lateral soil pressure P_{us}^{c} at any depth z below the surface:

For shallow depth

$$P_{us}^{\ c} = \frac{P_u}{d} = \left(3 + \frac{\gamma z}{S_u} + \frac{0.5z}{d}\right) S_u \qquad \textbf{(2-19)}$$

and for greater depth

$$P_{us}^{\ c} = 9S_u \qquad \textbf{(2-20)}$$

Where:

P_u = the ultimate lateral soil resistance

D = diameter of the pile and γ = soil unit weight (bulk).

The expression given above seems to suggest that the ultimate lateral load resistance, $P_{u,}$ in a purely cohesive soil increase a value of $3S_ud$ at the ground surface to $9S_ud$ down to a depth of about 3d and remain constant for greater depth.

Later, Randolph and Houlsby (1984) showed that the ultimate lateral soil resistance is very much depend up on the pile-soil interface. Using the method of characteristics, they produced the exact analytical solutions for the ultimate lateral load resistance which develops in front of the laterally loaded rigid circular pile $-11.94S_ud$ for a completely rough pile-soil interface, and $9.14S_ud$ for a smooth interface.

Similarly, for sand Broms (1964b) suggest a triangular distribution of a passive pressure along the front of a laterally loaded pile ignoring the active pressure at the back of the pile. The passive pressure being equal to 3 times the Rankine passive pressure:

$$P_{us}^{\ \phi} = 3\gamma' z K_p \qquad \textbf{(2-21)}$$

Where

γ' = effective soil unit weight

$$K_p = \frac{1+\sin\phi'}{1-\sin\phi'} \qquad \textbf{(2-22)}$$

ϕ' = angle of internal friction (effective stress)

For the more general case, Hansen (1961a) suggested that the following simplified expression for the determination of ultimate soil pressure $P_{us}^{c-\phi}$ at any depth z below the surface:

$$P_{us}^{c-\phi} = \gamma z K_{\phi} + S_u K_c \qquad \textbf{(2-23)}$$

Where

K_c, K_{ϕ} = factors that are function of ϕ and $\frac{z}{d}$

ϕ = friction angle

For purely cohesive soil, the factor K_{ϕ} is zero and the overburden pressure has no effect on P_u.

2.8 Experimental Tests

In addition to theoretical ways, matters of the pile subjected to lateral soil displacements has been investigated with laboratory tests by totally different researchers. It ought to be noted that this thesis concentrates on supportive the PLAXIS 3D foundation a group of piles by comparison with measurements from laboratory tests for validating the software. The results of those previous tests become terribly useful for the analysis of this analysis. A laboratory check of laterally loaded pile relating to the analysis of the influence of pile stiffness was allotted by city (1977).

The model pile was put in in Associate in Nursing iron box stuffed with soils. The pile was instrumented with strain gauges on the pile shaft to live the deformations. The uniform distribution of soil movements was incrementally applied to the pile. The pile model is varied with totally different materials (steel pile, wood pile) to research the influence of pile stiffness on its deformations. As a result of take a look at, it can be over that the misshapen form of the pile depends a lot of on the flexural rigidity of the pile. Moreover, variations of pile diameters were dole out by Matsui (1982) to research their influences. He conducted a series of experimental tests on the model piles loaded laterally by soil movements to predict lateral pressures performing on the piles. The model piles were inserted through clay layer and sand layer stuffed within a steel box. The soils were emotional towards the piles by the loading plates. Masses on the piles were recorded mistreatment the load cells.

It was found that they will increase of pile diameters lead to increasing pressure performing on the piles. Stewart (1992) used a geotechnical centrifuge to hold out a series of model tests on the pile adjacent to the development of Associate in nursing hill. The tests were conducted on each single piles and pile teams. The model piles were plane-strain gauged in order that the bending moments induced in piles can be measured.

The piles were put in through a soft clay layer and a dense sand layer. The development of Associate in nursing hill was dole out consecutive and therefore the bending moments within the piles were measured at every stage of hill construction. From the results, it can be thought-about that the utmost bending moment's area unit found at the pile heads and therefore the interface between the soft layer and therefore the stiff layer. As compared with the results from the sector take a look at, this technique was typically in smart agreement. The centrifuge tests offer insight within the pile behavior and therefore the results area unit thought-about to be of significant practical values.

2.9 In-situ tests

The in-site tests on the piles loaded laterally by soil movements are thought of because the best practical strategies that mirror the important pile behaviors. Several instrumented field tests are reportable by totally different researchers, as an example, Heyman & Boersma (1962), Heyman (1965), Leussink & Wenz (1969), and NICU (1971). Most of them concerned the piles supporting the bridge abutments wherever lateral soil movements were caused by the development of hill, whereas the others concerned the piles for slope stabilization and also the piles for retentive structures. But in term of this half, solely two reports created by Esu & D'Elia (1974) and Ingold (1977) square measure mentioned so as to achieve the summary of the pile behaviors.

Esu and D'Elia (1974) delineated a field trial referring to a landslide. A concrete pile with dimensions of 30m long and 0.79m in diameter was instrumented with pressure cells on the pile shaft Associate in nursing an inclinometer within. It may well be seen from the measurements that, the pile head malformed considerably and therefore the pressures engaged on the pile step by step hyperbolic.

Ingold (1977) bestowed a field trial wherever the steel pile was put in or so four months when the development of mound. The pile was set at the mound toe and inserted through the soft clay layer & the stiff sand layer. The bending moments and therefore the pile deflections were recorded by vibrating-wire strain-gauges and inclinometer severally. In short, the measurements showed that the utmost bending moments engaged on the pile may well be typically found at the pile high, the center of the soft layer and therefore the interface between totally different layers.

2.9.1 p-y curve criteria for clays

a) Soft clay criteria (Matlock, 1970)

Matlock (1970) planned a procedure for the event of p-y curves for piles in soft, saturated clays. The strain hardening criteria are supported the results of 4 lateral load test performed on a completely instrumented twelve.75 in. diameter pile driven into soft to medium loose clays at two completely different sites (Stevens & Audibert, 1979).

$$y_c = 2.5 \times \in 50 \times d \qquad \textbf{(2-24)}$$

Where, ε50= strain at one half the maximum deviator stress in undrained test

d = pile diameter.

The ultimate soil resistance, P_u, is calculated a**s**

$$P_u = N_p \times Su \times d \qquad \textbf{(2-25)}$$

Where, Su = undrained shear strength of soil

Np = ultimate lateral soil resistance coefficient

P_u =ultimate lateral soil resistance

P = lateral soil resistance

Matlock suggested that Np =9 for the great depths where sufficient confinement exists that corresponds to horizontal flow of the soil around the cylindrical pile. But near the surface the soil in front of pile is not well confined and as the pile deflects the soil is pushed up and away from the pile Np = 3 at the surface and increases with depth with the following relationship.

$$Np = 3 + \frac{\sigma' z}{Su} + J \times \frac{z}{d} \quad \textbf{(2-26)}$$

Where, σ'z = effective overburden stress at depth z.

Su =undrained soil shear strength at depth z

J = an empirical constant with an approximate value of 0.5 for the soft offshore clays and a value of 0.25 for somewhat stiffer clays.

2.9.1.1 Above water table stiff clay criteria (Reese & Welch, 1975)

Reese and Welch (1975) developed p-y curve criteria for piles embedded in stiff clays higher than the groundwater level on the premise of one full scale field lateral load take a look at. The load was performed on a 30-inches diameter trained shaft within which a 0.75-inches diameter instrumented pipe was embedded.

$$\frac{P}{P_u} = 0.5 \times (\frac{y}{y_c})^{1/4} \quad \textbf{(2-27)}$$

p-y curve for short term static load

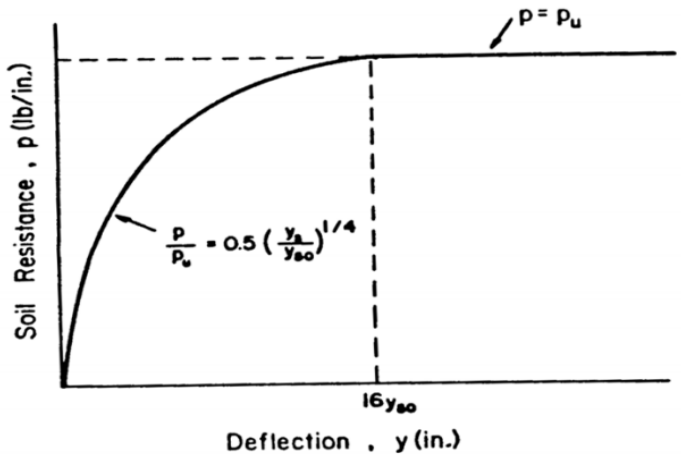

Figure 2-19**.** A graph of soil resistance p versus soil deflection y of clay above water table (Reese et al., 1975).

2.9.1.2 Below water table stiff clay criteria (Reese et al, 1975)

Reese, et al. (1975), projected a procedure for the event of p-y curve for piles embedded in stiff clays below the water level. Reese developed separate expressions for the ultimate soil resistance for two distinct mechanisms by that the pile was assumed to maneuver through the soil. supported the failure of wedge of soil ahead of pile and on the plastic

flow of soil round the pile in a very horizontal plane, the ultimate lateral soil resistance, Pu, per unit length of the pile is set because the lesser of the subsequent equations.

$$P_u = 2 \times Su \times d + \sigma' z \times d + 2.83 \times Su \times z \quad \textbf{(2-28)}$$

or $$P_u = 11 \times Su \times d \quad \textbf{(2-29)}$$

Where, σ'z = effective overburden stress at depth Z, Su = undrained soil shear strength at depth Where d= pile diameter,

The deflection at one half the ultimate soil resistance is given by:

$$y_c = \in 50 \times d \quad \textbf{(2-30)}$$

ε_{50}= strain at one half the maximum deviator stress in undrained test

d = pile diameter

The shape of the p-y curve for static loading condition generated by below water table stiff clay criteria is shown in Figure below.

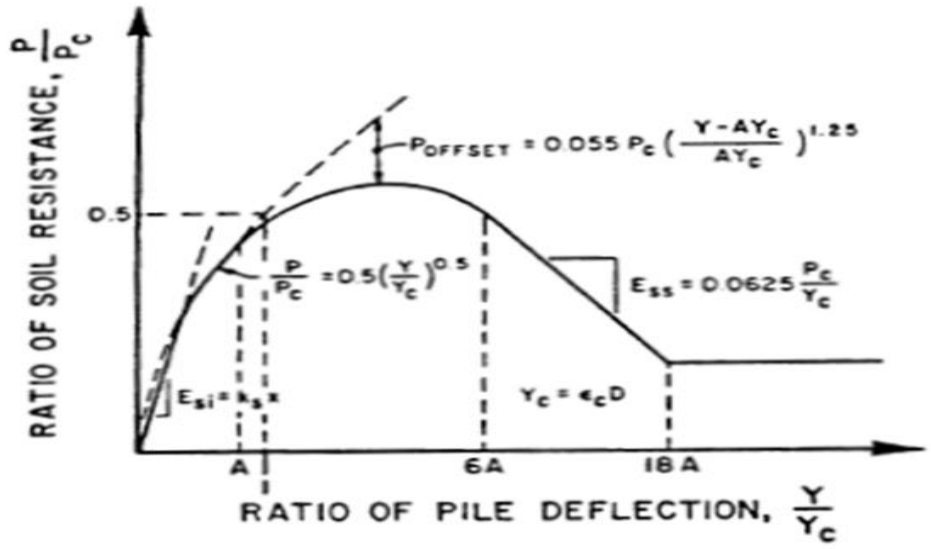

Figure 2-20 p-y curve for below water table for stiff clay criteria (Mac Vay, et.al, 1995)

2.10 Design Codes Recommendations for p-y Curve (API, 1993)

American Petroleum Institute (API, 1987, 1993) and Det Norske Veritas (DNV 2007) have recommendations for design of piles in offshore industries. The design regulations

for pile in soft and stiff clay are based on the work of (Matlock, 1970) and (Reese, Cox, & Koop, 1974). The only difference is variation of Np with depth. The API introduces a new term ZR to relate the variation of Np depending upon the depth. The Np values near the mud line are presumed to vary linearly from zero at mud line to nine at depths equal or greater than ZR. The relation for ZR given as:

$$Z_R = \frac{6d}{(\zeta d / Su + j)} \quad \textbf{(2-31)}$$

For static lateral loads the ultimate unit lateral bearing capacity of soft clay p_u has been found to vary between 8Su and 12Su except at shallow depths where failure occurs in a different mode due to minimum overburden pressure. Cyclic loads cause deterioration of lateral bearing capacity below that for static loads. In the absence of more definitive criteria, the following is recommended:

Pu increases from 3Su to 9Su as Z increases from 0 to Z_R according to:

$$Pu = 9 \times Su for Z > ZR \quad \textbf{(2-32)}$$

$$P_u = 3 \times Su + \gamma' + Z + J \times Su \times \frac{Z}{d} \quad \textbf{(2-33)}$$

Where, Pu=ultimate resistance, (KPa)

Su = undrained shear strength for undisturbed clay soil samples, (KPa)

d=pile diameter (m)

s"=effective unit weight of soil, kN/m^2

J = dimensionless empirical constant with values ranging from 0.25 to 0.5 having been determined by field testing.

Z = depth below soil surface, (m)

Z_R = depth below soil surface to bottom of reduced resistance zone in (m). For a condition of constant strength with depth,

2.11 Discrete Load-Transfer Approach

The Discrete Load-Transfer (DLT) approach maintains the subgrade reaction idea of replacing the soil with discrete soil reaction mechanisms, but enables a far more realistic

depiction of lateral pile-soil interaction through specification of soil reaction behavior of a form that mimics the reaction behavior that has been observed in full-scale field tests. A basis for obtaining soil reaction behavior in the field is evident from the beam theory relations given in Table below.

Table 2-1 A basis for obtaining soil reaction behavior in the field is evident from the beam theory

Displacement (2^{nd} Integral)		Slope (1^{st} Integral)		Moment		Shear (1^{st} Derivative)		Loading (2^{nd} Derivative)
y	$\leftarrow$	$\frac{dy}{dz}$	$\leftarrow$	$E_p I_p \frac{d^2 y}{dz^2}$	$\rightarrow$	$E_p I_p \frac{d^3 y}{dz^3}$	$\rightarrow$	$E_p I_p \frac{d^4 y}{dz^4}$

2.12 3 -Dimensional Finite Element group model

Continuum approaches utilizing a three-dimensional finite element framework have circumvented this problem to some extent, being able to provide a well-defined group pile-soil system from which observations of pile-soil-pile interaction can be inferred. Of course, and as was the case with isolated single pile behavior, the degree of realism afforded by a finite element approach relies on the ability to model the soil, pile and pile-soil components appropriately. Modeling pile groups is computationally intensive, a frequent approach has been to examine elements of the group in isolation using appropriate boundary conditions.

An example of this type of approach is shown in Figure below, used by Tamura, Ozawa, Sunami and Murakami (1982) to examine group effects for 3 x 3 and 5 x 5 configurations. Tamura et al. utilized a nonlinear (hyperbolic) stress-strain soil model in conjunction with a three-dimensional finite element framework, but no account of pile-soil separation is evident from the study. Nevertheless, the analyses confirmed the observation that the leading row attracts a disproportionately greater portion of the total applied lateral load, allowing some confidence in the ability of such an approach to provide insight into group effects. The analyses suggested that group effects increase at a decreasing rate with increasing number of rows, and that the effect is more pronounced with inner piles than with outer piles.

Trochanis et al. (1988, 1991a, 1991b) utilized an in-line pair of piles as a means of assessing the main features of group action. This extended on the single pile axisymmetric model adopting the same pile-soil-interface properties and loading as used for the single pile analysis, and performing the same series of three analyses (i.e. bonded/elastic soil, separation/elastic soil, separation/inelastic soil). Imposing equal loads to the pair of piles spaced at two and three pile diameters (i.e. $s = 2d$ and $3d$), a shadowing effect was clearly demonstrated by much larger deflections experienced by the trailing pile.

Brown and Shie (1990b, 1991a) also utilized an in-line pair of piles to assess group effects, but adopted a rectangular model configuration with symmetry boundaries following the modeling approach. This represented two rows of piles loaded in-line and extending to infinity in the direction perpendicular to loading. Group spacing of $3d$ and $5d$ were investigated, and a single row of piles with $10d$ spacing was used to simulate isolated single pile behavior. Two soil model cases were analyzed to depict "clay" (constant strength) and "sand" (frictional) conditions.

The work by Brown and Shie (1990b, 1991a) reaffirmed general observations from field testing, such as reduced shears for trailing piles leading to higher moment to shear ratios, and the occurrence of maximum bending moments in trailing piles at greater depths compared with the leading piles. Comparison of both cases also indicated more significant shadowing effects in the sand case, attributed to its stress-dependent shear strength. The latter was thought to have also affected leading pile behavior, in that increased shear strength near the sides of the pile, induced by increased confining stress imposed by load transfer from the trailing pile, served to "hold back" the pile and partially offset any additional displacement from strain superposition effects.

Leading pile behavior was therefore considered as being comparable with an isolated single pile in both the sand and clay cases.

A most significant aspect of the Brown and Shie (1990b, 1991a) work was the additional step taken for extracting *p*-*y* curves from each analysis and deriving *p*-multipliers and *y*-multipliers to represent group effects. This was undertaken by fitting discrete bending moment values along the pile (obtained via stress values at the pile element centroids) to a fifth-degree polynomial and then twice differentiating to obtain *p* values (*y* values being

extracted directly). A practice-orientated assessment in the form of *p-y* multipliers was thus achieved, providing a more rational basis for comparison with full-scale tests. In this way good correlation with field test results was demonstrated using numerical experiments.

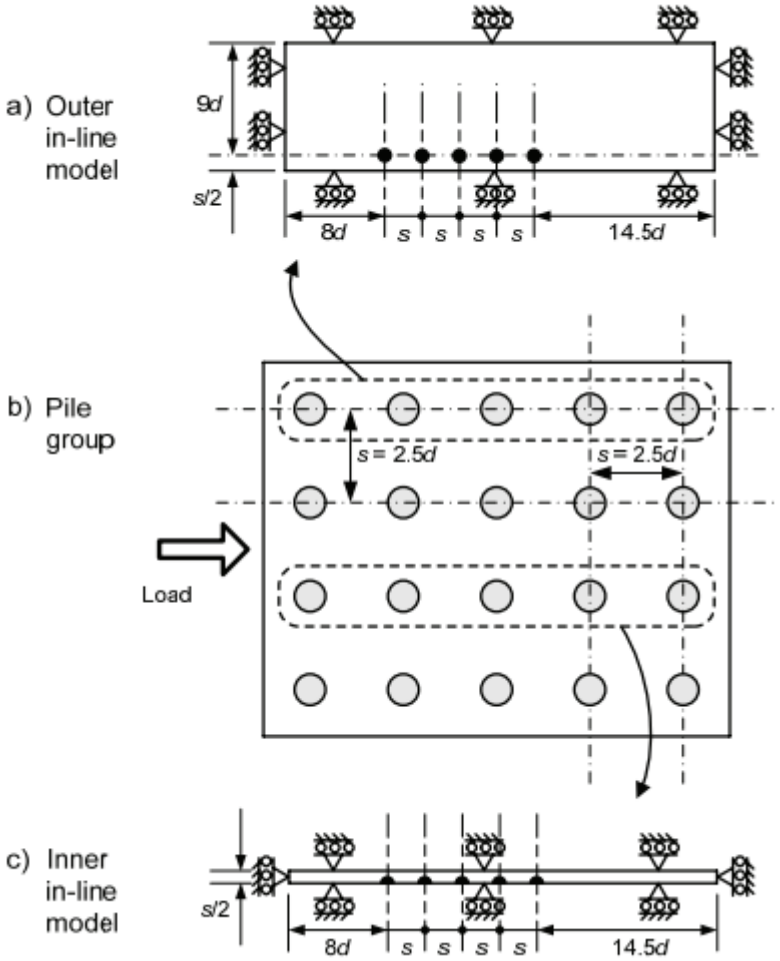

Figure 2-21: **Plan views of in-line analysis models used by Tamura et al. (1982)**

2.12.1 3-Dimentional finite element for large group piles

Three-dimensional efforts to the same extent and level of numerical sophistication as Wakia et al. (1999) are not apparent from the existing literature, indicating such an approach is relatively rare. In terms of very large pile groups, being the topic of the current study, three-dimensional approaches are necessarily restricted given the substantial number of piles typically involved, and a three-dimensional large group analysis to the totality of Wakia et al. is certainly beyond current computational standards. A partial three-dimensional finite element analysis undertaken by Ono,

Shimamura, Kasai and Omoto (1991) is likely to represent one of the largest problems investigated numerically, consisting of a circular tank 44 m in diameter, supported on 421 steel pipe piles (d = 700 mm; L/d = 43) spaced at 2.9 pile diameters.

By symmetry to reduce the problem by half for modeling purposes, three-dimensional soil elements were governed by the hyperbolic Duncan and Chang (1970) constitutive formulation, and piles modeled using one-dimensional beam ("stick") elastic elements (fixed-head conditions applying at the pile heads). Modeling up to 23 rows of piles at the center of the group, analysis results indicated piles in the leading third portion of the group attracted a greater share of the lateral load imposed (up to 4.9 times the average load of all the piles for the leading piles), while the remaining piles attracted a fairly uniform share of between 60% to 80% of the average load of all the piles. Bending moments in piles were similarly distributed, and deepening of the zone of significant pile-soil interaction apparent with trailing piles. In the case of the 23 piles located along the center of the group in the line of loading, an increasing depth of interaction was apparent to the seventh trailing pile, reaching a maximum depth at this point and then maintaining the same depth over the remaining trailing piles.

While the analysis by Ono et al. (1991) is obviously limited by the simplistic portrayal of piles as line elements, and furthermore provision for separation does not appear to have been made, the results nevertheless reflect a somewhat intuitive sense that uniform behavior should prevail for a large portion of 81 the piles in a large pile group. Such a notion has been adopted by Law and Lam (2001) in the form of a three-dimensional modeling economy employing periodic boundary conditions. The so-called periodic boundary concept, which results from viewing a large pile group as recurring rows of infinite number of piles, is illustrated in Figure below. The notion of infinite bounds is a fair approximation, at least for piles located in the interior region of a large pile group. As depicted in Figure below, this is seen to enforce periodic displacement conditions between piles, necessary in order to satisfy displacement compatibility between each tributary region.

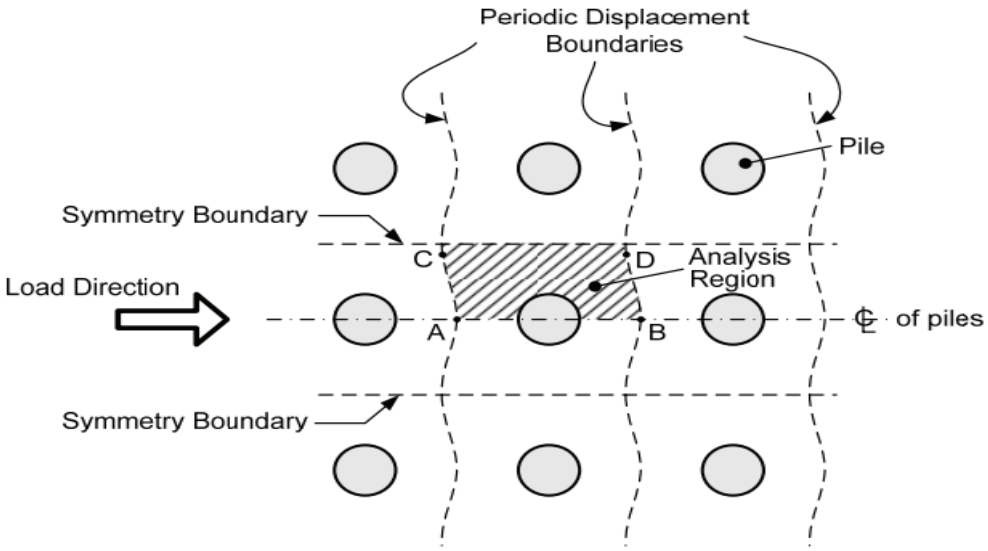

Figure 2-22 Periodic boundary analysis approach for large pile groups (after Law and Lam, 2001)

Deformations at adjacent points along periodic boundaries are therefore identical. For example, deformations at points A and B on Figure above are identical, likewise for points C and D. Further simplification arises by making use of symmetry boundaries through the centerline of the piles and through the midpoint between piles, also shown on Figure above. The resultant analysis model can therefore be reduced to the analysis region indicated in Figure above, with adjacent nodes along each periodic boundary slaved together to enforce the periodic displacement condition. Law and Lam (2001) utilized such a three-dimensional finite element model to assess the lateral behavior of 0.75 m diameter fixed-head cast-in-steel-shell piles (L/d = 30) forming a large pile group (380 piles) in soft clay soil conditions. By comparing the pile-head load-deflection behavior of the finite element model with an isolated single pile DLT model employing Matlock (1970) soft clay p-y curves, Law and Lam established appropriate p-multiplier and y-multiplier values. These results indicated the periodic boundary analysis approach was successful in portraying group effects, with increasingly lower lateral resistances mobilized at greater deflections for reduced pile spacing.

2.13 Previous studies on laterally loaded pile groups

The first theories on the subject of the ultimate load design for horizontally loaded foundations were developed in the 1960's. These theories are:

- Broms's (1964a) theory for cohesive soils (soils with cohesion > 0, friction = 0)
- Broms's (1964b) theory for cohesion less soils (soils with cohesion = 0, friction >0)
- Brinch-Hansen's (1961) theory for soils having both cohesion and friction (soils with cohesion > 0 and friction >0)

The first analysis conducted on laterally loaded piles is finished by Feagin (1937). Full scale tests were conducted on timber and concrete single piles in addition as numerous pile group. Configurations, just with the intent to get information on lateral load movements. Feagin ascertained that the common soil resistance per pile bated as additional piles were further to the group. Feagin additionally finished that group effects were solely important at massive deflections which at deflections of (0.25 in) group effects failed to occur. Additional all-out testing was done by Kim and Brungraber (1976) on numerous pile group in clay.

During this era piles were designed by using elasticity theory. This theory used nonlinear techniques in analyzing single isolated piles then used elastic interaction factors to work out more group responses.

This theory was challenged by Barton (1984). Barton conducted centrifuge check on different pile group at totally different spacing in sand. These tests over that soil nonlinearity should be accounted for in pile group arrangement which the elastic theory didn't account for this non-linearity.

Elastic strategies underestimated the interactions inside closely spaced pile group whereas overestimating the interaction with pile groups at larger spacing. Barton additionally determined that the number of total loads carried by every pile inside the group wasn't equally distributed (as calculable by the elastic theory) and trusted spacing. Separate model tests were worn out the identical year by Cox et al. (1984) in soft clay. These tests were performed on piles in an exceedingly line with lateral loads each parallel and perpendicular to the line of piles. Cox found that once load was placed perpendicular to the road of piles, group effects didn't occur in spacing bigger than three times diameters. once the load was parallel with the road of piles, group effects were enlarged and potency ablated with the amount of piles within the line.in the figure below it shows these results

comparison the efficiencies of the piles organized parallel (in-line) with the lateral loading to the piles organized perpendicular (side-by-side) to the lateral loading.

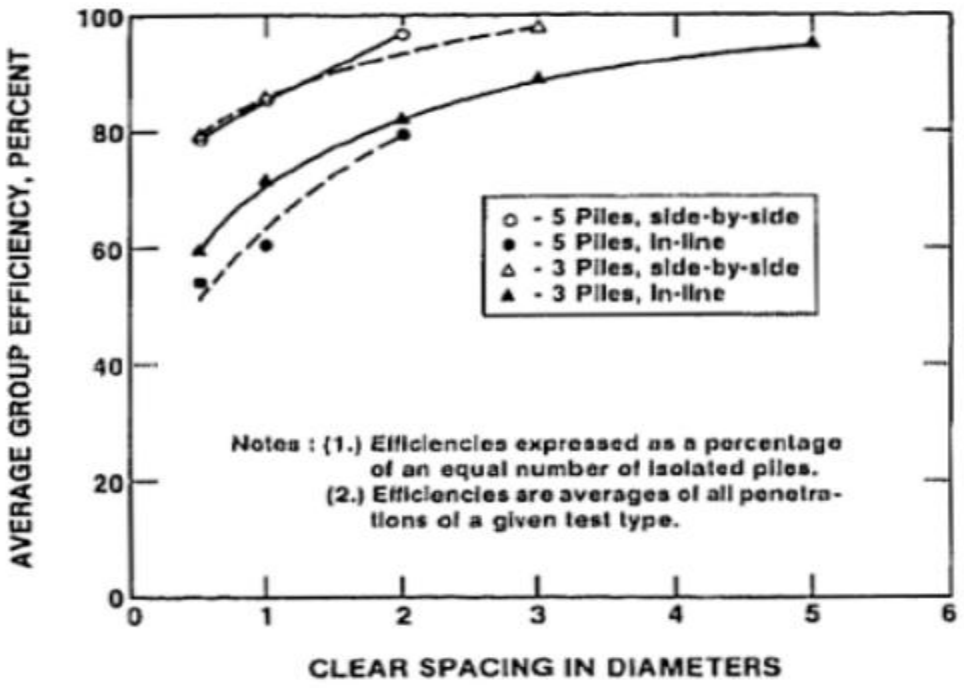

Figure 2-23 group efficiency vs clear spacing for both in-line and side –by side configurations (Cox et al., 1984).

Both of these tests made further insights into the influence of spacing on pile group response to lateral loads.

Several complete tests were additionally conducted throughout this point amount. Meimon et al. (1986) did full scale tests on steel piles and confirmed what had been discovered by Feagin (1937) therein group effects raised with larger deflections. Meimon additionally noted what Kim and Brungraber (1976) had discovered therein front row piles had bigger resistance and additionally developed bigger moments for a given pile group deflection. Neither Feagin (1937) nor Kim and Brungraber (1976) directly measured load on every pile group

Brown et al. (1987) conducted complete tests in stiff clay and in agreement with Barton (1984) that the elastic theory failed to address what he saw to be the key consider predicting pile group response; final soil resistance. Brown began to plot a brand-new

technique to predict soil resistance and also the planning of pile group with the idea of p-multipliers (Brown et al, 1988).

Brown et al (1988) prompt *p*-multipliers to account for the reduction in resistance in every row. These p-multipliers act as reduction factors that scale down the particular p-y curves of the isolated single pile model, so accounting for all non-linearity within the profile. These back-calculated p-multipliers, together with different p-multipliers prompt from different tests,

Previous numerical and experimental research performed by different researchers are reviewed in this section. Several field and laboratory tests have been performed by different researchers to evaluate the group effect, obtain parameters like *p*-multipliers or validate analytical methods. The existing research that has been done on laterally-loaded pile groups can be divided into three general categories:

a• **Full scale tests:** These tests are conducted in the field. They have advantages of real piles, real soil and realistic soil–pile condition. It is, however, very difficult and expensive to perform a full-scale test on a pile group. The capacity of the loading equipment also limits the size of the pile group that can be tested. Therefore, full scale tests are usually carried out on small pile groups with close spacing.

b• **Centrifuge tests:** These tests are conducted in the laboratory and we call it small scale tests. Centrifuge tests are more economical and easier to modify and repeat for parametric studies in comparison with full scale tests. The main advantage of centrifuge testing is that the gravitational stress field in the model can replicate the prototype. This consideration is crucial when testing materials such as sand for which the stress–strain behavior is a function of confining pressure (Meymand, 1998).

c. **Numerical studies:** This type of testing uses computer algorithms and equations to solve lateral-load problems. This is the least expensive type of testing but also the most difficult to represent actual conditions

Some analytical models like the ones by Poulos and Randolph (1983) have utilized elasticity-based relationships for modelling pile–soil–pile interaction and also modification of *p-y* curves (O'Neill et al., 1977). However, experimental research by Brown et al. (1987), Brown et al. (1988), Holloway et al. (1982), and Meimon et al.

(1986)) has indicated that the elasticity-based analytical models do not reproduce the degree of non-linearity observed in pile–soil–pile interaction.

Brown and Shie (1990) performed a series of numerical experiments on one row of piles subjected to lateral loading. To model clay soils, an elastic- perfectly plastic (Von Mises) model was used which provides a constant yield strength envelope. Sand was modeled using a modified Drucker-Prager model with no associated flow. They observed that group effects are most significantly influenced by row position and also center to center pile spacing. Brown and Shie (1991) used the same simulation to evaluate the group effects using *p-y* curves derived from pile stresses. Pile spacing effects were determined in terms of *p*-multipliers and related *y*-multiplier that were applied to *p-y* curves of single pile. First, *p*-multipliers were determined, and then appropriate *y*-multipliers were selected to best fit the sloped portion at the beginning of the *p-y* curve.

Trochanis et al. (1991) conducted numerical analysis on in-line pairs of piles to assess the main features of axial and lateral response of piles to monotonic and cyclic loading. They concluded that the assumption of purely elastic behavior for soil can substantially overestimate the degree of interaction in realistic situations. Finn and Wu (1994) showed that by relaxing some of the boundary conditions associated with a full 3D continuum analysis, it is possible to get reliable solutions for non-linear response of pile foundations including both kinematic and inertial interaction with reduced computational effort.

Yang and Jeremic (2003) also simulated centrifuge tests on 3 × 3 to 4 × 3 pile groups which were conducted by McVay et al. (1998). Yang and Jeremic (2003) showed their FE simulations can predict the behavior of pile groups with good accuracy. Finn (2004) explored the reliability of approximate methods for estimating the rotational and translational stiffness's of pile foundations in the 3D non-linear analyses of a superstructure. Como dromos and Pitilakis (2005) carried out parametric three-dimensional non-linear numerical analysis for different arrangements of pile groups. They used Finite Difference (FD) simulations to evaluate the influence of the interaction between piles on the lateral resistance of pile groups. They also proposed a relationship to predict the response of fixed-head pile groups using response of a single pile. Dodds and Martin (2007) examined large pile groups under lateral loading using a three-dimensional FD approach. They focused on local soil–pile interaction using *p-y* curves as the primary

assessment tool and *p*-multipliers to characterize group effects. In their research, two piles with in-line configuration and a single pile with periodic boundaries represented typical leading and immediately trailing piles, and internal piles, respectively. Ultimately, they provided *p*-multipliers to be applied to *p-y* curves for large pile groups in clay and sand conditions.

Ideally p-y curves should be generated from full-scale lateral load tests on instrumented test piles. In the absence of experimentally derived p-y curves, it is possible to use empirical p-y formulations that have been proposed in the literature for different types of soils. Table below lists the sources for some of the p-y expressions commonly used in practice.

Table 2-2 Sources of some scholars listed for p-y

Soil Type and Condition	Reference
Soft clay below the water table	Matlock (1970)
Stiff clay below the water table	Reese, et al. (1975)
Stiff clay above the water table	Welch and Reese (1972), Reese and Welch (1975)
Sands	Reese, et al. (1974)
Sands	API (1993)
Soils with cohesion and friction	Evans and Duncan (1982)
Weak rock	Reese (1997)
Strong rock	Nyman (1980)

2.14 Recent studies on laterally loaded pile groups

(Gouw and Hidayat, 2015), presented the research on Effects of pile lateral movement, pile spacing and pile numbers on laterally loaded group pile by employing PLAXIS 3D geotechnical finite element software with the circular bored piles of 1000mm diameter. The sub soil was assumed to be in undrained condition Su, of 50kPa and has stiffness of 500 times undrained shear strength, E=2500kPa. For material modeling, Mohr-coulomb model were used. The lateral load carrying capacity of single piles is determined at 6mm, 9mm, 12mm, 25mm, 40mm and 100mm lateral movement of the pile head .these selected lateral movement of pile heads are based on the following criteria's

- 6 mm is normally adopted as allowable lateral movement under static condition.

- 9 mm is allowable lateral movement under small earthquake shaking.
- 12 mm is allowable lateral movement under medium earthquake shaking
- 25 mm is allowable lateral movement under strong earthquake shaking.
- 40 mm is based on the local practice (Jakarta, Indonesia) that the pile ultimate Load is determined at pile head movement of 4% pile diameter, i.e. 4% x 1000mm = 40mm
- 7100mm is the original Terzaghi's 10% pile diameter failure criteria for lateral movement, i.e.10%x1000mm=100mm**.**

(1) The piles were modelled as embedded beam with unit weight of 24 kN/m^3 and structural stiffness of 3x10^7 kN/m^2**.**

(2) Model 3x3, 5x5 and 9x9 piles group subjected to lateral load.

(3) Lateral load is applied at the side the of the pile cap. Magnitude of the load is adjusted until all piles in the group move laterally by 100mm or more.

(4) The center to center pile spacing is varied from 3D, 4D, 5D, 6D, 8D to 10D (D=pile diameter).

(5) Since it has been found that the effect of pile cap thickness is marginal, on this further study the pile cap thickness for all pile groups are taken as 2D. The pile caps are modelled as soil cluster with non-porous, linear elastic material model, with the unit weight of 24 kN/m^3, stiffness of 3x10^7 kN/m^2, and Poisson's ratio of 0.15.

(6) To eliminate the effect of soil friction between the base of the piles cap and the underlying soil, a 10-cm thin layer of dummy soil with nearly zero strength and zero stiffness is placed under the pile cap.

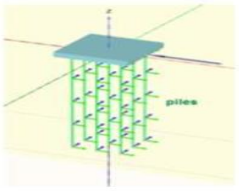

Figure 2-24 Typical Finite Element Model of the Pile Group (Gouw and Hidayat, 2015)

(7) To eliminate the effect of soil passive resistance acting on the pile cap, the pile cap is placed on the ground surface.

(8) The lateral movement of each pile in the group is then generated by Plaxis 3D. Then, load carrying capacity of each pile is derived at the corresponding pile head lateral movement of 6mm, 9mm, 12mm, 25mm, 40mm and 100mm. Generally, the results of the above models were summarized as figure below.

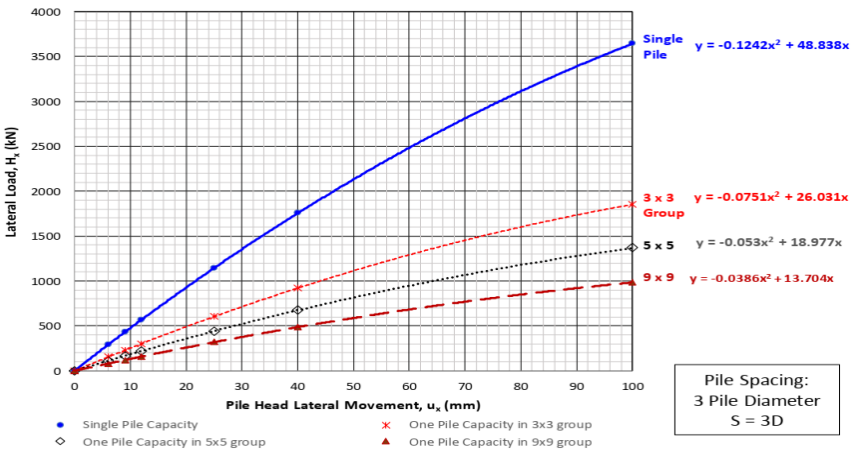

Figure 2-25 Pile Head Lateral Movement for Pile Spacing of 3 Pile Diameter

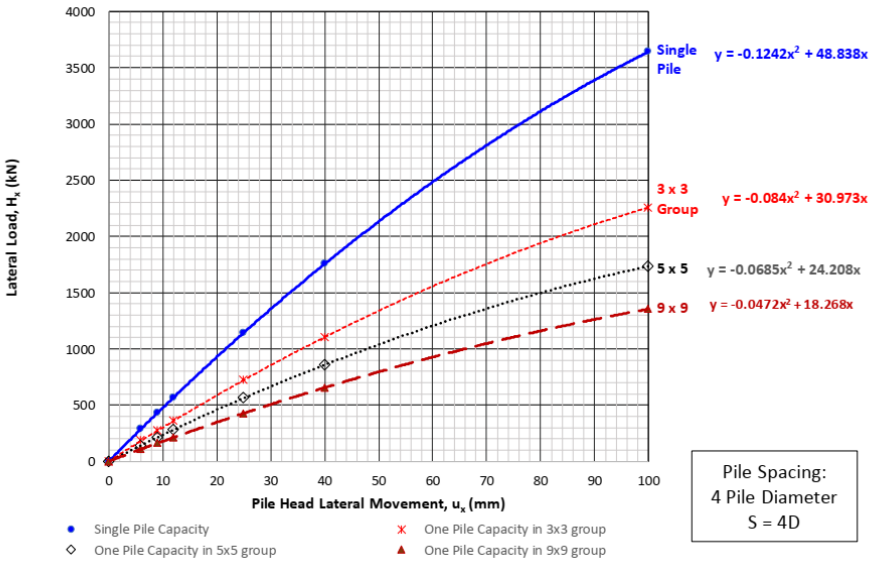

Figure 2-26 Pile Head Lateral Movement for Pile Spacing of 4 Pile Diameter

CHAPTER 3 MODELING PARAMETERS

3.1 Modeling in Plaxis 3- Dimensional foundation

Plaxis 3D Foundation is a three-dimensional program, developed for the analysis of three-dimensional Foundation and geotechnical problems. It is part of the Plaxis suite finite element software used world-wide for geotechnical engineering design. The software allows the complex finite element model to be solved quickly. In the finite element method, a continuum is divided into a number of elements. Each element consists of a number of nodes. Each node has a number of degrees of freedom that correspond to discrete values of the unknown variables to be solved. The various available output facilities can be used to display the detail computational results.

Piles are modeled using beams which are structural objects used to model slender structures in the ground with a significant flexure rigidity (bending) and a normal stiffness. A three-dimensional mesh is automatically generated taking into account the soil stratigraphy and structure levels as defined by the user.

Soil material is modeled by using Mohr–Coulomb constitutive model built in PLAXIS. In general stress state, the model's stress strain behaves linearly in the elastic range, with two defining parameters from Hooke's law (Young's modulus, E and Poisson's ratio, ν). Where the plasticity range were defined by the angle of shearing resistance (φ') and cohesion (*C*').

3.2 Steps involved in the finite element method

Step 1: Element Discretization

In this process, the geometry of the problem is modelled by an assembly of small regions termed as finite elements, which have nodes defined on the element boundaries, or within the element.

Step 2: Primary Variable Approximation

Primary variables such as displacements, stresses, etc., must be selected. The rules with regard to how these variables have to vary over a finite element are established. Nodal values are used to express the variations. Displacements are usually adopted as a primary variable in geotechnical.

Step 3 Element Equation

The elemental equations below are derived using an appropriate variation principle (the minimum potential energy).

$$[K]_e = \int [B]^T [D][B] dv \qquad \textbf{(3-1)}$$

Where, K is element stiffness matrix, D is material property (the elastic material matrix according to Hooke's law) is in terms of poison ration and young modulus and B is strain interpolation matrix.

Step 4 Global Stiffness Matrix

The element equation is combined to form the global equation or global stiffness matrix.

Step 5 Boundary Condition

Global equations are modified by formulating boundary conditions, loading like point loads, distributed loads, line loads it affects displacement.

$$\{\varepsilon\} = [B]_f \{\delta\} \qquad \textbf{(3-2)}$$

Where δ is the nodal displacement vector is strain and B is strain interpolation function

Step 6 Solve Global Equations

The displacement at all nodes can be obtained by solving the global equations, these Nodal displacements are used to evaluate the stress and strains

3.3 Boundary conditions

The boundary should be located sufficiently far from the piles, so that the stress transferred from the laterally loaded pile to the soil should not reach the boundary. For this paper 80m×100m (x, z) is taken, hence it is large group pile gets sufficient confinement from both directions.

At the bottom level of the model, all movements were restrained, whereas, at the lateral sides, lateral movements perpendicular to the boundary were prohibited (Younggyun Choi, 2018). To ensure that the stress zone around the pile group is not affected by the boundaries, they should be far enough from the piles. Sensitivity analyses were carried out to determine appropriate dimensions of the continuum model.

PLAXIS automatically imposes a set of general fixities to the boundaries of the geometry model. These conditions are generated according to the following rules:

- Vertical boundaries with their normal in x-direction (i.e. parallel to the y-z plane) are fixed in x-direction ($U_x = 0$) and free in y- and z-direction.
- Vertical boundaries with their normal in z-direction (i.e. parallel to the x-y plane) are fixed in z-direction ($U_z = 0$) and free in x- and y-direction.
- Vertical boundaries with their normal neither in x- nor in z-direction
- Boundary lines in a work plane) are fixed in x- and z-direction ($U_x = U_z = 0$) and free in y-direction.
- The bottom boundary is fixed in all directions ($U_x = U_y = U_z = 0$)

3.4 Interface modeling

Interfaces will be required to simulate the finite frictional resistance between the structure such as pile and adjacent soil and also pile to pile interaction, pile to raft interaction and raft to soil interaction.

In addition, it is assumed that no pile cap resistance is present on the applied load (i.e. only distributing the loads to the pile head). The raft is used to connect the pile group together and assume the same rows of the group piles are deformed equally, it allows relative displacement and separation between the structure and soil mass. When using 6-node elements for soil, the corresponding interface elements are defined by three pairs of nodes, whereas for 15-node soil elements the corresponding interface elements are defined by five pairs of nodes. Interfaces are modeled as 16-node interface elements and elements consist of eight pairs of nodes, compatible with the eight-nodded quadrilateral side of a soil element.

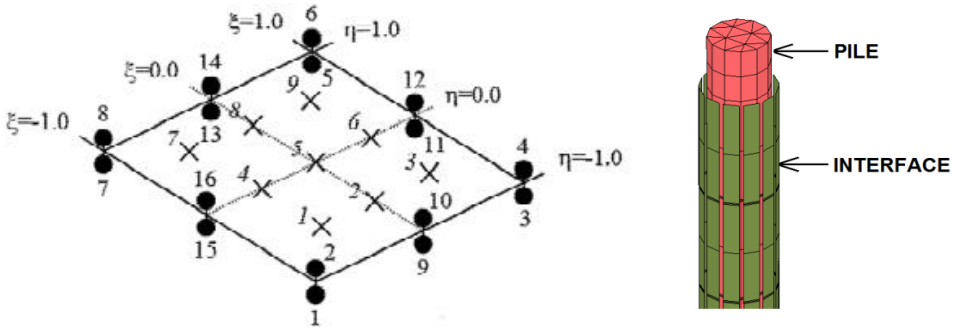

Figure 3-1 the adopted 3D interface element in the numerical modeling

The basic property of an interface element is the associated material data set for soil and interfaces. When interface element models the interaction between a pile and the soil, which is intermediate between smooth and fully rough. The roughness of the interaction is modeled by choosing a suitable value for the strength reduction factor in the interface (R-inter). This factor relates the interface strength (structure surface friction and adhesion) to the soil strength (friction angle and cohesion). Elastic-plastic model is used to describe the behavior of interfaces for the modeling of soil-structure interaction. The Coulomb criterion is used to distinguish between elastic behavior, where small displacements can occur within the interface, and plastic interface behavior when permanent slip may occur.

3.5 Material modeling

The parameters in study, soil is obtained from previous thesis on local soil properties (Emmanuel EJ**,** Addis Ababa University, 2016). The site of soil parameter is new head quarter of Commercial Bank of Ethiopia.

3.5.1 Soil modeling and soil properties of the study Area

The preliminary surface investigation was performed by Design and Share Company Limited under a contract with the China State Engineering Corporation Limited. The totals of 10 sampling borings were taken and the laboratory testing was done. The Standard Penetration Test (SPT) was useful in profiling, identification and assessing Engineering parameters of the soils during boring.

Characterization of the soil to determine the input parameters are used for modeling obtained from geotechnical investigation report conducted by Design Company, see table below , material properties are from the catalog of the manufacturer were used to determine the composite properties of materials by combining the Young's modulus, shear modulus and Poisson's ratio using Halpin-Tsai Equations. For further information refer geotechnical report of the site.

Soil is modeled as a cylindrical with outer diameter larger than 30 times diameter of pile. For each analysis, the mesh with 15 nodded elements is considered to be sufficient. The study is focused on the lateral displacement and soil reaction,

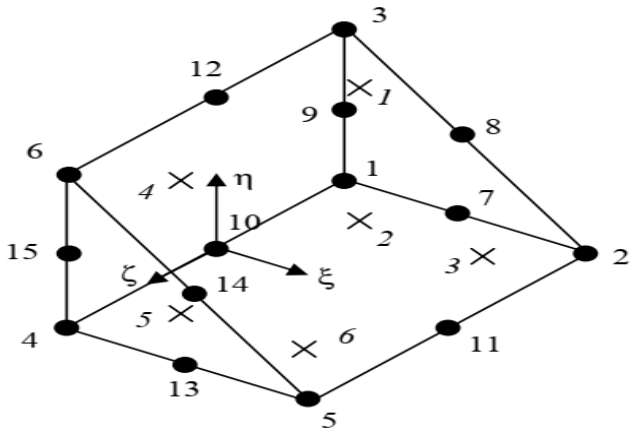

Figure 3-2 distribution of Nodes and Stress points in a 15-noded Wedge Element (Plaxis 3D Foundation Manual, 2004)

The soil parameters considered for this study were modeled by using Mohr coulomb (MC) constitutive relation. This analysis considered a layered soil profile. Therefore, the soil was divided into strata according to the thicknesses found from the field test results and as listed in the following table. Each stratum was assigned the properties as found from test results.

The Detailed Soil Properties which are taken as input for Plaxis- 3D software is presented in the table below.

Source: (Emmanuel EJ**,** Addis Ababa University, school of technology, journal of architectural Engineering, 2016)

Table 3-1 soil parameters used for analysis

Soil Description	Elv.	E50	E_{oed}	E_{ur}	γ_{uns}	γ_{sat}	C^{ref}	ϕ°	ν	R_{int}
	(m)	MPa			kN/m^3		kN/m^2		-	-
Soft organic Silty Clay	-4	4	4	12	12	14.7	0.015	13	0.3	1
Silty Clay	-6.6	4	4	12	14	15.3	0.02	17	0.3	0.95
Highly Weathered Basalt	-8.8	2770	2770	8310	23	32.7	7.8	33	0.27	0.95
Medium strong, to Fragment Moderately Weathered Basalt	-15	20630	20630	61890	24	35	18	34	0.26	0.8
Silty Clay	-18.2	4	4	12	12	14.2	0.02	17	0.3	0.95
Stiff, Sandy Clayey Silt	-21	4	4	12	14	16.7	0	28	0.3	0.9
Highly Weathered Scoriaceous weathered basalt	-25.5	630	630	1890	22	32.9	13.6	32	0.27	0.95
Moderately Weathered Basalt	-39	20630	20630	61890	24	34.5	26	36	0.27	0.8
swelling Clayey silt	-45	4	4	12	15	17.4	0.015	22	0.2	0.95
Moderately Weathered Basalt	-52	20630	20630	61890	24	35	26	35	0.27	0.8
Strong fractured, fresh to faintly weathered Basalt	-61	46510	46510	139530	26	36.8	29	38	0.3	0.6
Moderately Weathered Basalt	-75	20630	20630	61890	24	35	25	34	0.26	0.8
Strong fractured, fresh to faintly weathered Basalt.	-83	46510	46510	139530	26	37	29	38	0.19	0.6

3.5.2 Pile properties and modeling

The piles were modeled as cylindrical massive circular piles with different geometry, in active working space. Pile is generated by replacing the soil element by the pile with the adjusted strength and stiffness parameter. Between the pile element and the soil element, an interface is established to model the soil-pile interaction, the system is brought to equilibrium. The combinations of lateral loads are applied in each stage. The pile properties used for the inputs of Plaxis 3D Foundation are in the following table.

Table 3-2 Structural materials

Name	Material	Modeling type	Unit weight	Young's modulus	Poison ratio	Rint	Drainage type
Pile	Steel, massive circular pile	Linear	25kN/m^3	E=30GPa	v=0.2	1	Non-porous
Pile cap	Concrete	Linear	25kN/m^3	E=30GPa	v=0.2	1	

Pile number: the large group pile is containing four or more rows (McVay, e.tal.1998).The independent parameters are Loads, these stepping loads are 100kN/m, 200kN/m, 500kN/m, 1000kN/m 1500kN/m, 2000kN/m because of large group piles and the pile diameter is taken to be fixed as 65cm throughout this paper. Generally, the model parameters used to study in this paper are summarized in the table below.

Table 3-3 Pile group geometry and combination of parameters in the study

No	Pile number/rows	Pile depth	Spacing	
1	6× 6 (6 rows)	10m	3D	5D
		20m	3D	5D
		30m	3D	5D
2	4× 4 (4 rows)	10m	3D	5D
		20m	3D	5D
		30m	3D	5D
3	7× 3 (7 rows)	10	3D	5D
		20m	3D	5D
		30m	3D	5D

The combinations of the above pile parameters are used in modeling. Numerically Pile modeling by Plaxis 3-D Foundation has its own procedure, as can be referred in Plaxis 3D Foundation manual. Before starting the basic construction, stages fixing the dimensions and defining the working plane should be done. Basically, in case of this paper the construction stage has five stages. Initial phase, piling phase, excavation phase, pile cap phase and the Loading phases.

The first is the initial stage, in this stage if there is water table nearest to the foundation or pile layer, ignore it because of the water table is considered as the undrained condition, it is dissipated in the long time throughout the construction period. The next stage is the

installation of the piles. In this stage a group of piles are installed, in Plaxis 3D Foundation. Piles are installed according to the pile depth defined in the material cluster. The successive phase is the excavation stage and the pile cap. Pile cap are used to fix the head of the piles. The last construction stage is the loading stage, this stage takes a time up to performing the whole iteration and converge the whole iteration together and generate the output.

The figure below shows that the stage of excavation stage from construction stages. It is clearly seen that the white color indicates that the materials, soil and water were removed from it and the next is continued according to the models.

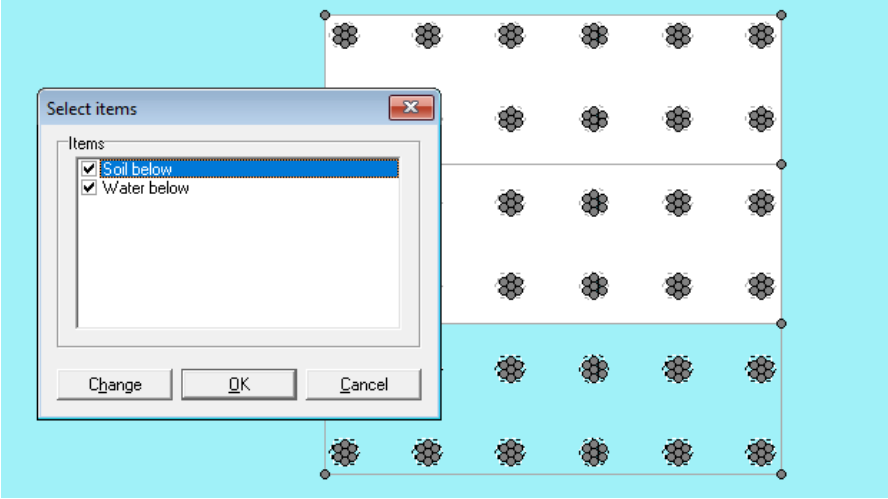

Figure 3-3 Geometric Parameters of Plaxis 3D Model excavation stage

3.5.3 Modeling Loads

The loading was displacement controlled, and this displacement was applied over the surface of the pile cap, with zero allowance of pile cap rotation. The large group pile is normally designed to carry the vertical load, lateral load and bending moment. But in this analysis only the static translational lateral load is considered. For the development of the soil resistance-pile displacement curves, the loads are applied in steps.

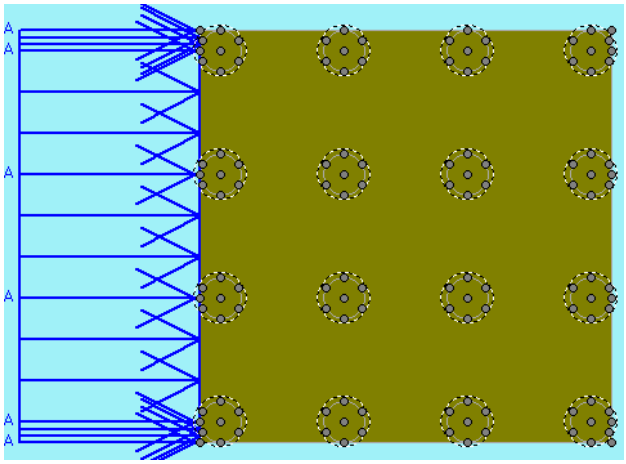

Figure 3-4 Plaxis 3-D Foundation of 4×4 pile arrangement during loading

3.6 Constitutive Model and Input Parameters

3.6.1 Mohr - Coulomb model

The Mohr-Coulomb plasticity model was obtained from extension of Coulomb frictional materials. The yield criterion is expressed in terms of shear stress, normal stress and frictional angle acting on a plane. The model suggests that the yielding begins as long as the shear stress and normal stress satisfy the following equation, $\tau = c + \delta \tan \phi'$ which is stated in equation (2-17) where, c is the cohesion and ϕ is the friction angle. It is based on plotting of Mohr's circle for state of stress at failure in the plane of maximum and minimum principal stresses. The failure line is the tangential line to the Mohr's circle. Basically for Plaxis 3D Foundation Mohr- coulomb model gives yield surface when all the yield functions give zero which means acting plasticity. Refer literature equation (2-18) and figure (2- 18).

Based on the data from geotechnical report of new head quarter CBE site, the parameters are not elastic in behavior it has inelastic property too. Their inelastic behavior under static loading can be described by elastic-plastic constitutive models. According to the constitutive model options available in Plaxis, Mohr-Coulomb's soil model was used for static analysis. Due to its simplicity, it is highly popular and gives reasonable results. The model involves five parameters, i.e. Young's modulus, E, Poisson's ratio, ν, cohesion, c, internal friction angle, ϕ, and dilatancy angle, ψ

3.6.2 Input parameters

When prescribing soil's stiffness Plaxis recommend using E_{50} as stiffness when modelling initial loading and E_{ur} when modelling unloading and reloading problems as excavations. Where E_{50} is the Young's modulus at 50% of the maximum stress-level occurred in a triaxial test and E_{ur} is the Young's module for soil when unloading and reloading. The latter is normally higher than for initial loading since the soil stiffens due to increased stress-level. When v is unknown Plaxis recommends using values in the range 0.3 to 0.4 and 0.15 to 0.25 for loading scenarios and reloading scenarios, respectively. When modelling sand without cohesive strength Plaxis will not perform well numerical. The cohesion should be prescribed to a small value, in the order of magnitude $c < 0.2kPa$. According to (Brinkgreve, 2008) the dilatancy angle for sand with high friction angle is roughly $\psi = \varphi - 30$. For sand with less friction angle less than 30˚and for clay the dilatancy is close to zero.

In addition to the five input parameters mentioned above three advanced parameters can be set; increase of stiffness, increase of cohesion and tension cut-off. Increase of stiffness involves soil's stress-dependency by introducing $E_{increment}$ and y_{ref}, i.e. increase of stiffness per meter and the depth where the increase starts, respectively. In an analogous way the cohesion could be increased with depth in "increase of cohesion".

Tension cut-off indicates prescribing soil's tensile-capacity to zero. The basic Mohr-Coulomb model has this option by default. Tension cut-off is suitable for most soils, such as sand and gravel which are cohesion less soils with no tensile strength. However, in clay it could be adequate to account for tensile strength and tension cut-off could then be deactivated.

3.7 Types of Calculations performed by Plaxis 3-D

The first parameter to be set when defining a calculation phase is the type of calculation. This was found at the upper right-hand side of the General tab sheet. Distinction is made between four basic types of calculations: Plastic calculation, Consolidation analysis, Gravity loading and K0 procedure. The latter two types are only available for the initial phases.

3.7.1 Plastic calculations

A Plastic calculation is used to carry out an elastic-plastic deformation analysis according to small deformation theory. The stiffness matrix in a plastic calculation is based on the original un-deformed geometry. This type of calculation is appropriate in most practical geotechnical applications. In general, a plastic calculation does not take time effects into account, except when the Soft Soil Creep model is used (see Material Models Manual).

Considering the quick loading of water-saturated clay-type soils, a Plastic calculation may be used for the limiting case of fully undrained behavior using the Un-drained option in the material data sets. On the other hand, performing a fully drained analysis can assess the settlements on the long term. This will give a reasonably accurate prediction of the final situation, although the precise loading history is not followed and the process of consolidation is not dealt with explicitly.

3.7.2 Gravity loading

Gravity loading is a type of Plastic calculation, in which initial stresses are generated based on the volumetric weight of the soil. All options that are available for a Plastic calculation are available. In a Gravity loading analysis the relative proportion of weight is raised from 0 to 1. In all phases after the initial phase, the full soil weight remains activated. If Gravity loading is adopted, then the initial stresses are set up by applying the soil self-weight in the first calculation phase. In this case, when using an elastic perfectly-plastic soil model such as the Mohr-Coulomb model, the ratio of horizontal effective stress over vertical effective stress, K_0, depends strongly on the assumed values of Poisson's ratio. It is important to choose values of Poisson's ratio that give realistic values of K_0. If necessary, separate material data sets may be used with Poisson's ratio adjusted to provide the proper K_0-value during gravity loading.

3.7.3 K_0- procedure

The K_0 procedure is only available for the initial calculation phase. It is a special calculation method available in PLAXIS 3D FOUNDATION which can be used to define the initial stresses for the model, taking into account the loading history of the soil. Two K_0 values can be specified, one for the x-direction and one for the z-direction

$$K_{o,x} = \frac{\delta_{xx}}{\delta_{yy}} \quad \textbf{(3-3)}$$

$$K_{o,z} = \frac{\delta_{zz}}{\delta_{yy}} \quad \textbf{(3-4)}$$

In practice, the value of K_0 for a normally consolidated soil is often assumed to be related to the friction angle by Jacky's empirical expression in an over-consolidated soil, K_0 would be expected to be larger than the value given by this expression**.**

$$K_o = 1 - \sin\phi' \quad \textbf{(3-5)}$$

3.8 Mesh size and properties

In using a finite element method to solve a problem, first the domain of the problem must be discretized. Selecting a proper mesh size is very important because it considerably affects the accuracy of the results. It is important to have a high-density mesh in regions of high stress or strain gradients. Sizing the mesh for accurate results, but with a reasonable number of zones, can be complicated. Mesh size significantly affects the analysis time. For selecting proper mesh size, these factors should be considered:

- Finer mesh leads to more accurate results because it provides a better representation of high stress gradients.
- Accuracy increases as zone aspect ratios approaches unity.
- If different zone sizes are depending on the expected stress concentrations, the results are more reliable.

The p-y method is widely used for design of laterally loaded piles. This method replaces the soil reaction with a series of independent nonlinear springs. The p-y curves represent the non-linear behavior of the soil by relating the soil reaction and pile deflection at points along the pile length.

Figure below shows the 3D mesh generation of 6 by 6 pile group

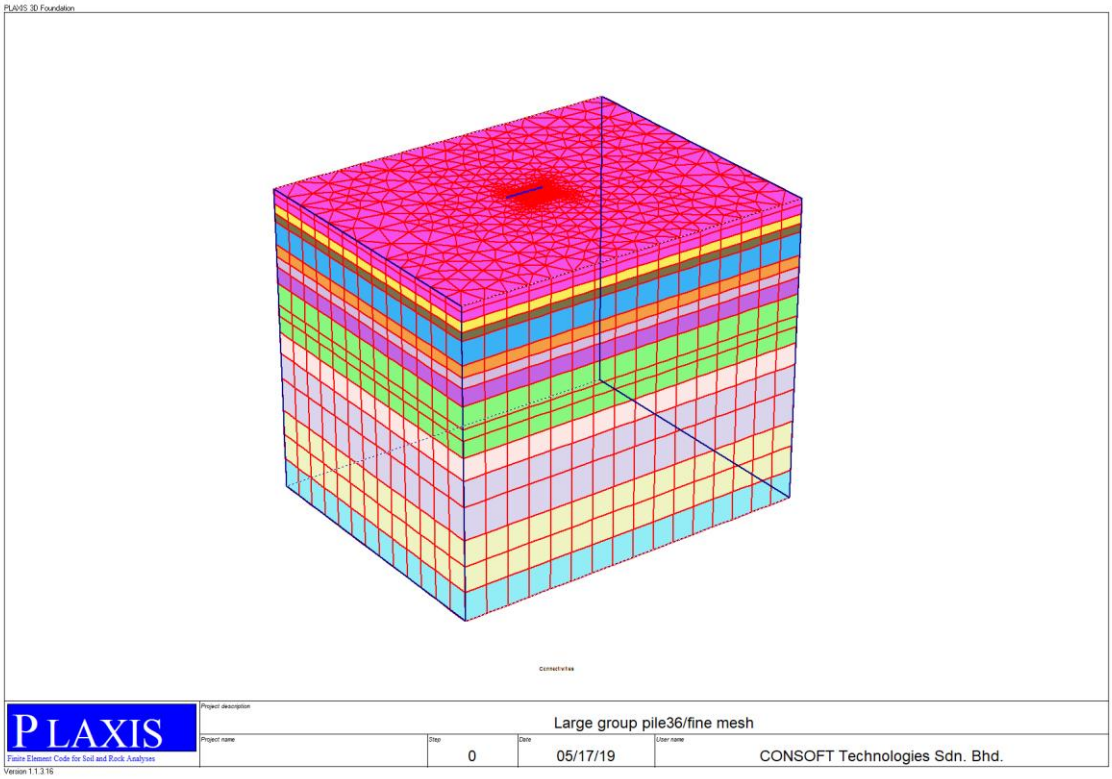

Figure 3-5 3D mesh generated of six by six group of pile

3.8.1 Evaluation of Mesh dependence

To perform finite element calculation, the model geometry has to be divided in to elements. In PLAXIS, the mesh coarseness is considered to have a significant effect influence on the calculation results. Furthermore, the mesh can be fine enough to get the accurate results in order to evaluate the mesh dependence, PLAXIS implemented with five types of mesh coarseness (very coarse, coarse, medium, fine, and very fine meshes) which indeed results in different number of the generated mesh elements. In this paper, in all model's finer mesh type is used. The following table shows how mesh types affects the number of elements and node number.

3.8.2 Sensitivity analysis

Sensitivity analysis in Plaxis 3D Foundation, is finding the results of pile movement by all meshing types. The more accurate displacement of element is the fine meshing types. But while doing with numerical cost and time should be considered., in case of this study sensitivity analysis were done on 4×4 model types, as it can be seen from table 3-5 ,18420 number of element's and 52517 node numbers have meshed by fine mesh types. Since while it compared with the very finer meshing types, maximum deformation was very

close to each other. Therefore, the whole model in this study were considered the finer mesh types.

Table 3-4 Mesh types and number of nodes with number of elements

Model type	Mesh type	Number of elements	Number of nodes	Average element size
4×4	Very coarse	6812	21179	$6.56*10^{\varphi}$m
	Coarse	7670	23620	$6.18*10^{\varphi}$m
	Medium	10660	31842	$5.24*10^{\varphi}$m
	Fine	18420	52517	$3.99*10^{\varphi}$m
	Very fine	36560	100865	$2.83*10^{\varphi}$m
6×6	Very coarse	6942	20276	$6.49*10^{\varphi}$m
	Coarse	8983	23710	$6.02*10^{\varphi}$m
	Medium	18503	49067	$5.78*10^{\varphi}$m
	Fine	24616	68816	$5.19*10^{\varphi}$m
	Very fine	53016	124340	$3.2*10^{\varphi}$m
3×7	Very coarse	8476	24817	$5.88*10^{\varphi}$m
	Coarse	10400	30087	$5.31*10^{\varphi}$m
	Medium	13244	37841	$4.7*10^{\varphi}$m
	Fine	20032	55903	$3.82*10^{\varphi}$m
	Very fine	42440	114751	$2.63*10^{\varphi}$m

Table 3-5 Maximum deformation of 4×4 pile model by different meshing types

4×4	number of elements	number of nodes	average element size	avg. deformation (mm)
very coarse	6812	21179	6.56*10m	45.9
coarse	7670	23620	6.18*10m	52
medium	10660	31842	5.24*10m	56.31
fine	18420	52517	3.99*10m	59.5
very fine	36560	100865	2.83*10m	59.87

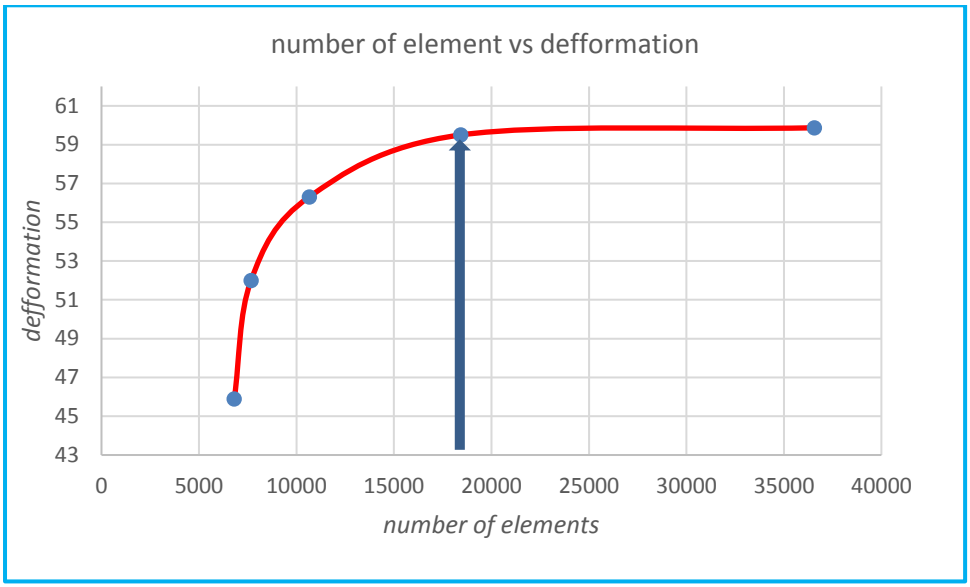

Figure 3-6 Deformation versus number of elements

3.9 Boreholes and ground water table condition

Bore holes are used to define the soil stratigraphy and ground surface level. Soil layers and ground surface may be non-horizontal by using several bore holes at different locations. Moreover, bore holes are used to define the pore pressure distribution in the sub-soil. In case of this paper, the case of New head quarter of commercial Bank of Ethiopia Building, it has 13 soil layers and totally 10 bore holes are excavated, 83 meter below Natural ground level and maximum depth of excavation is 90m (geotechnical report document of new CBE, 2016). The geological location is Located around FLOWWUHA, natural ground water table is found there and the geological formation of the location is within the Rift valley fault, in case of the ground water table are found at 6m and 5.5m below natural ground level with in different bore holes, but in case of this modeling the location of GWT is taken at 5.5m averagely.

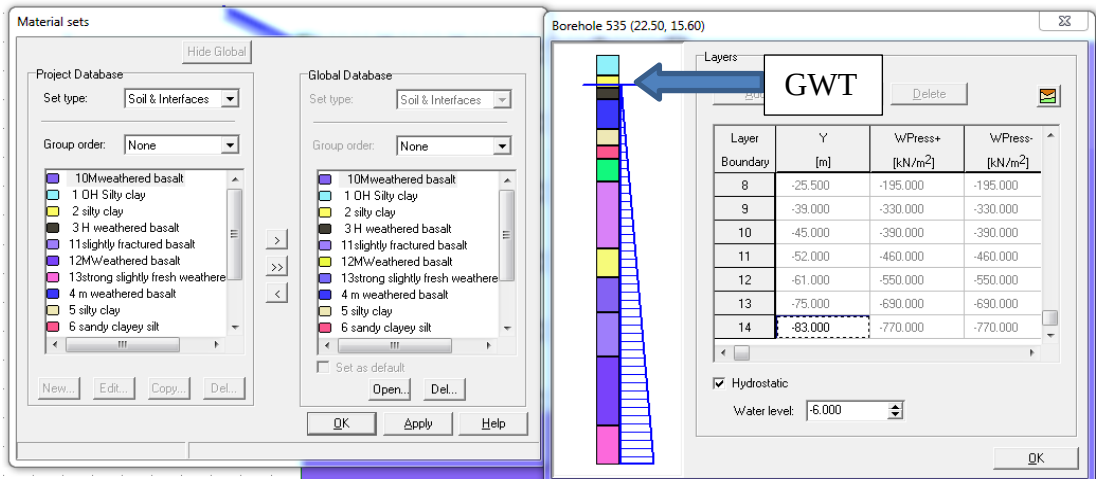

Figure 3-7 Soil stratigraphy of the Plaxis 3-D Foundation bore hole

3.10 Plaxis 3-D Foundation validation with the field test result

The validation is used to confirm the ability of Plaxis 3D Foundation finite element software to predict the load–displacement relationships for pile groups with various configurations. It is the procedure of determining the degree to which a model is an accurate representation of the real world from the perspective of the intended uses of the model (Oberkampf et al., 2002, Roy et al., 2015). Quantifying the confidence in the capability of the model in predicting the response by comparison with experimental data is the goal of validation.

3.10.1 Validation case-1

Pile load test on laterally loaded pile**:** A pile load test conducted by Ismael et al. (1998) has been modeled and studied. The pile was 0.3 m in diameter and had a length of 5 m situated in Kuwait. The surface soil was found to a depth of 5 m and was characterized as having both component of shear strength, c and ϕ. The soil profile consisted of a medium dense cemented silty sand layer to a depth 3 m. This was underlain by medium dense to very dense silty sand with cemented lumps to the bottom of the borehole. All properties of soil are listed in Table Below.

Table 3-6 Geotechnical properties of the soil layers and the pile

Parameter	symbol	Silty sandy, cemented	Very dense silty sand cemented	Pile	Unit
Unsaturated unit weight	γ_{unsat}	18	19	25	kN/m^3
Saturated unit weight	γ_{sat}	18	19	……..	kN/m^3
Young's modulus	E	13000	13000	2.*E10^9	kN/m^2
Poison ratio	ν	0.3	0.3	0.15	------
Cohesion	C'	20	1		kN/m^2
Friction angle	φ'	35	15	----	°

3.10.2 Validation result, case 1

The following 3D-block diagram indicates that the output of the validation result of 80kN load result. Generally, over all the load used by Ismael at the field test is starting from 20kN up to 180kN. In this research too, to validate with the test result the same stepping load is used and the output is shown below graphically as well as by tabular form.

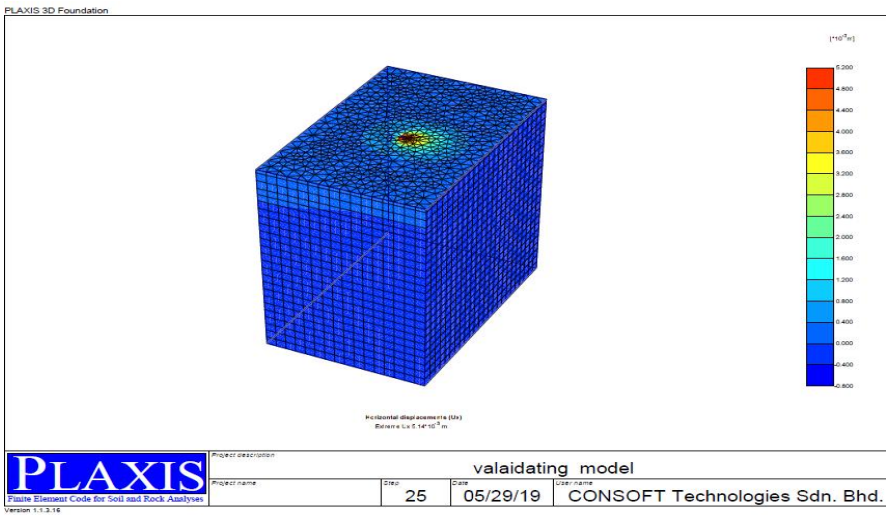

Figure 3-8 Plaxis 3-D Foundation output of from the field data

Table 3-7 Comparison of finite element results with field test data (ISMAEL, 1998)

Load (kN)	Field test result (Ismael,2010) (m)	Plaxis3D-FOUNDATION output(m)	Difference (%)
20	1.32E-03	1.44E-03	3.33
40	3.00E-03	3.45E-03	4.9
60	4.21E-03	4.32E-03	2.55
80	6.62E-03	6.65E-03	0.4
100	8.99E-03	9.50E-03	5.233
120	1.40E-02	1.46E-02	4.11
160	1.89E-02	1.95E-02	3.005
180	2.07E-02	2.09E-02	0.912

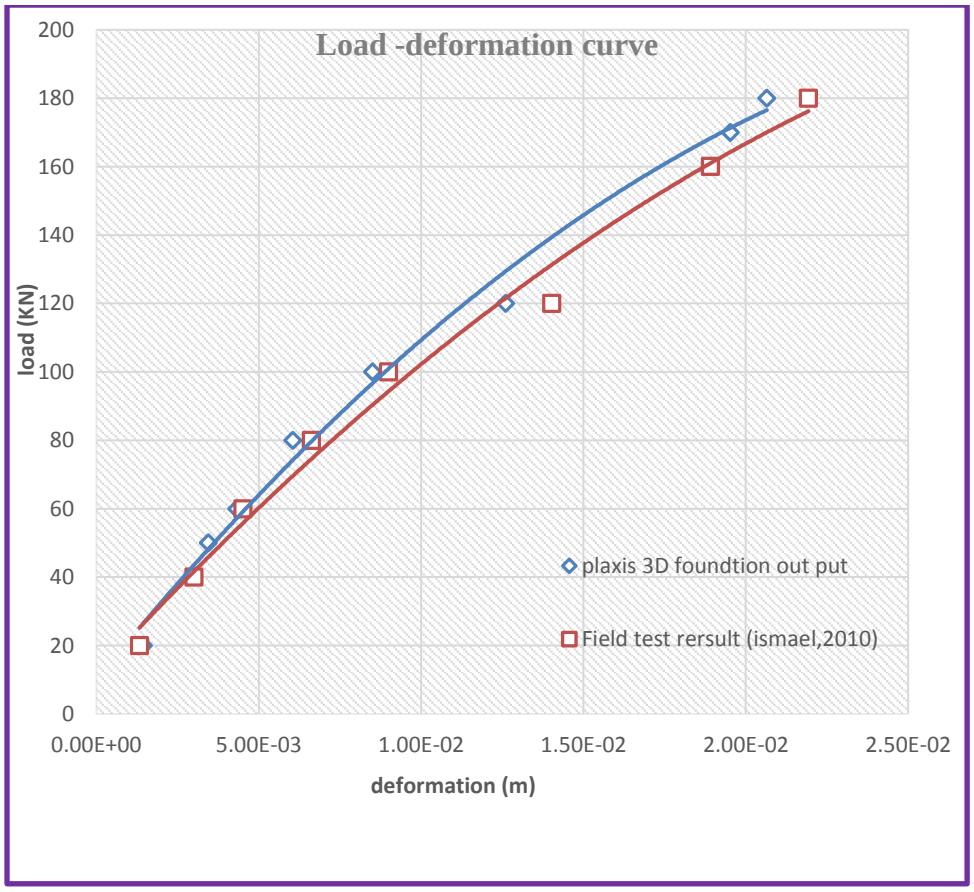

Figure 3-9: Validation result of the full -scale field test graphically (P-y) curve with Plaxis 3D

The above p-y curve and the table shows that both results are very close to each other therefore Plaxis 3-d foundation FEM is validated correctly**.**

3.10.3 Validation case -2 Field test of laterally loaded pile

The bored cast-in situ pile considered in this study is a diameter (D) of 1000 mm, length 17m and of C35 grade concrete. The site soil is composed of layers of sandy clay and soft-weathered rock. Table 3.8 lists the parameters of the soil stratums at the test site and Table 3.9 lists the parameters of the concrete pile. The same parameters have been used for the numerical simulations. A hydraulic jack, fixed horizontally between an immovable wall and the top of the pile, was used to apply lateral loads (Hu), in stages, up to 120kN (B.P. Naveen et.al, 2014)

Table 3-8 Field soil data parameters (B.P. Naveen, 2014.et.al)

		Layer 1	Layer 2
Material Model		Sandy clay Mohr-coulomb	Soft weathered rock Mohr- coulomb
Unit weight, ɤ	kN/m^3	18.00	21
Young's Modulus, E_{ref}	kN/m^2	55000	65000
Poisons ratio, v		0.330	0.330
Cohesion, $C_{ref,}$	kN/m^2	15.00	42.00
Friction angle, ϕ	°	42.00	65.00

Table 3-9 Pile data set parameters

Material	Normal stiffness, EA [kN/m]	Flexural rigidity, EI [kN/m^2
Pile	2.11E07	1.32E06

Therefore, the validated result is as follows. The soil layer is partially removed to indicate the pile deformation.

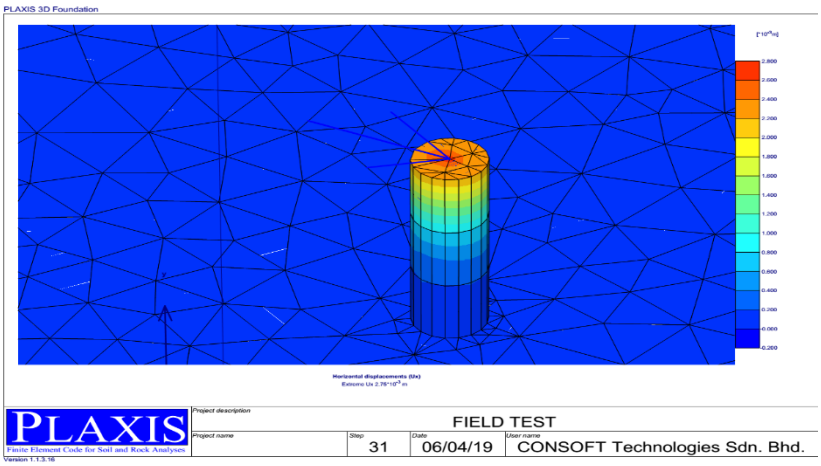

Figure 3-10 Plaxis 3d validation of meshed pile case 2

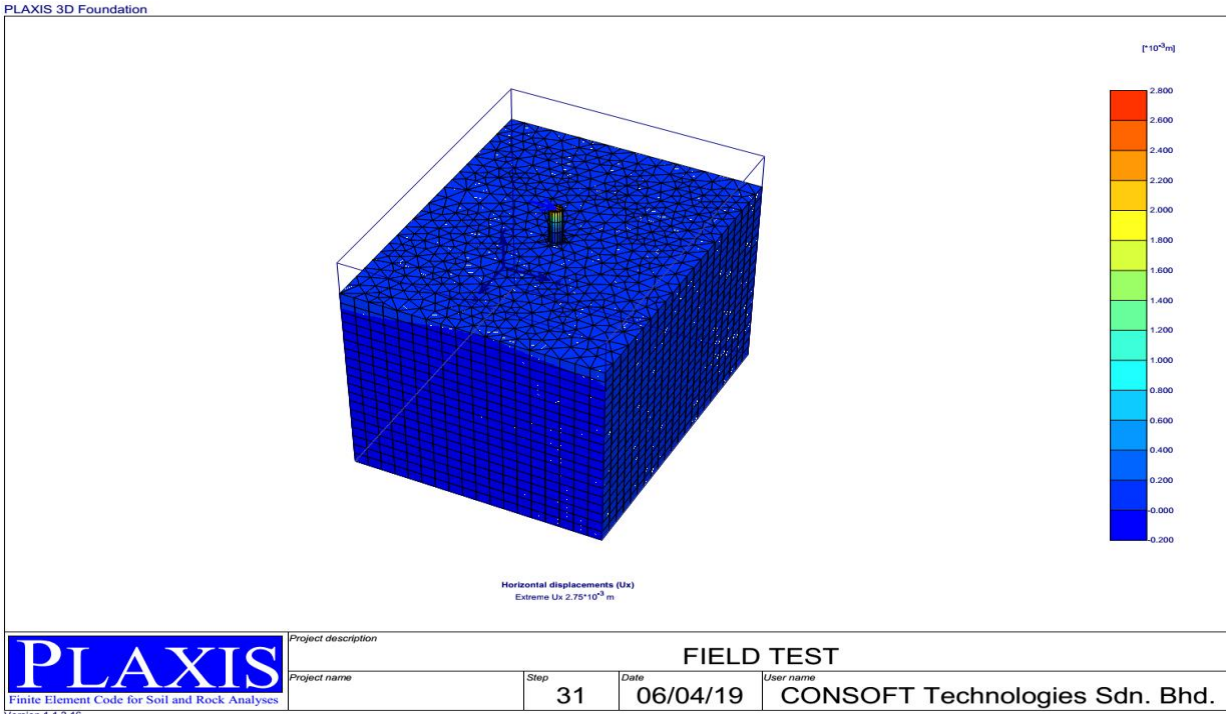

Figure 3-11 Plaxis 3d Foundation output with the soil block diagram model

The above figure clearly shows that the deformation of the field test and the Plaxis is very small due to small amount of applied load. Generally, by this applied load test the ultimate capacity of the pile was not satisfied, because of to reach the maximum ultimate capacity, the pile has deformed 0.1B (Terzaghi, 1995). The following table indicates the difference between field test and computational out puts.

Table 3-10 Comparison of Plaxis output with field test

Force(kN)	Plaxis 3d foundation (mm)	field test(mm)
20	0.345	0.5
40	0.8	1
60	1.35	1.78
80	1.74	2.14
100	2.56	3.6
120	2.812	4.1

Therefor the average deference of the field and the Plaxis 3-d foundation software is 4.74%, hence it is acceptable the difference is due to the following reasons.

3.10.4 Comparison of field test and numerical analysis

The prediction of the adopted method is reasonably close to the field test results. Hence the applied load at the field is only until 120kN and deformation of 4.1mm is attained. Even though this is the field test, it is nearly close with the results of FEM analysis. Since the soil layer of this field site is also close to the site where this research parameter of soil is taken, because both of them have weathered rock layer and sandy clay.

The little difference in deformations may come from, the ultimate load is not applied at the field, as seen from the original document of the field test data it is recommended that; non-availability of jacks and supports of adequate capacity might be the reason. This become more common due to large diameter piles.

CHAPTER 4 PARAMETRIC STUDIES

As mentioned in the previous chapter the study is focused mainly on the load - displacement of laterally loaded large group piles, mainly Load displacement curves of different models. Below there are out puts of Plaxis 3-D Foundation for different models and discussion of parameters mentioned in the objective.

4.1 Laterally loading piles versus deflection for each models

4.1.1 6×6 group pile arrangement

a) at 30m depth and 3d spacing center to center

Load displacement curve for each pile length is gathered and shown in figure below. Deformation of rows has been shown in figure 4.2 below. It indicates that the first leading rows which resist more loads than the other rows, because of the overlapping shear zone of the behind piles and they are stiffer than the trail rows, and it is more susceptible to lateral resistance, as a result leading rows deforms less than the trailing and intermediate rows.

Figure 4.1 is the output of Plaxis 3-D Foundation when 1000kN/m load is applied on 6 ×6 pile geometry and deformed laterally 22.7mm. Deformation which is shown on 3-D Plaxis output is total horizontal deformation of the body.

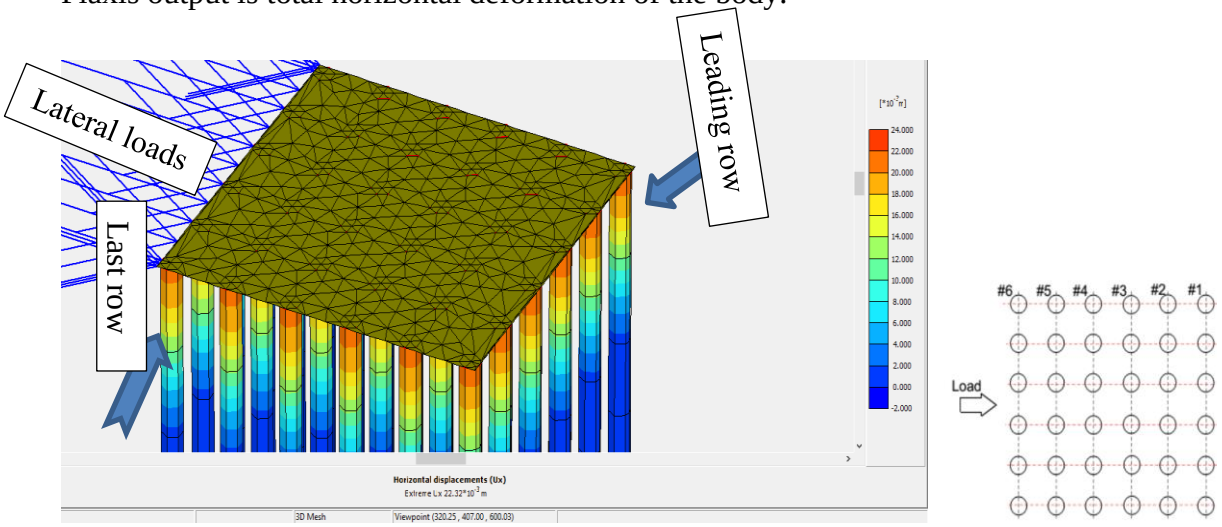

Figure 4-1 Plaxis 3-D foundation output of 6×6 pile groups at 3d spacing of 30m depth

The following graph indicates that the deformation of each rows.

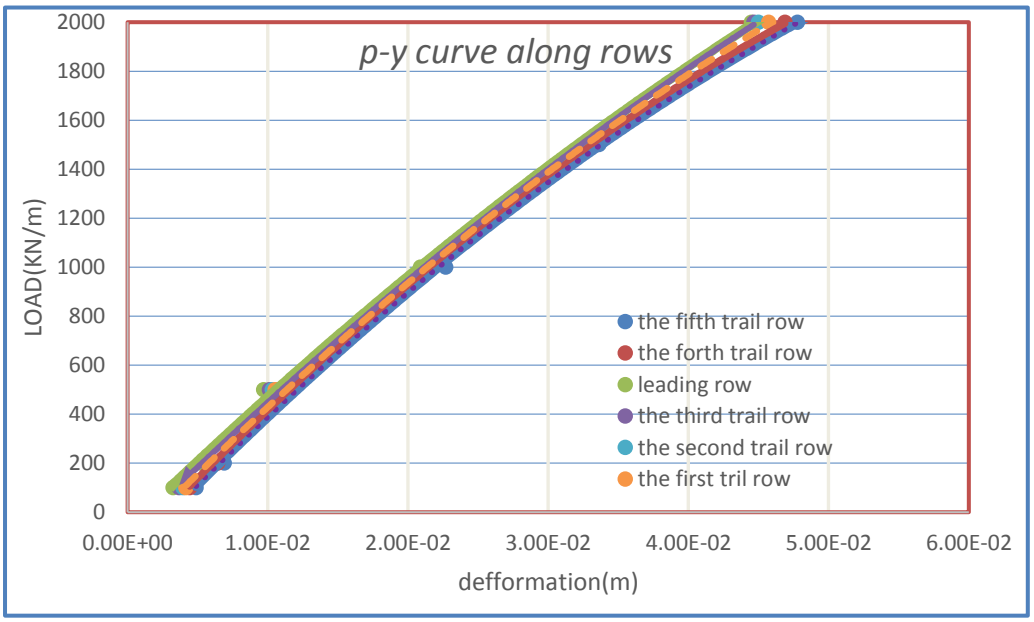

Figure 4-2 *p-y* curve for each row of 6×6 pile arrangement

Due to pile to pile interaction a group of piles tend to deform more than a proportionally loaded single piles. The simultaneous presences of piles with in the soil mass has an effect on stiffening soil continuum.

b) at 30m and 5d center to center spacing

Figure below indicates that, Plaxis-3D FOUNDATION result of total deformation of 6 ×6 pile arrangements at 30m depth. The legend indicates that by the last loading step of 2000kN/m, the lateral deformation of the last trail row is 47.8mm. But every row has successively descending deformation values. In this model the other parameter is the spacing of the pile.

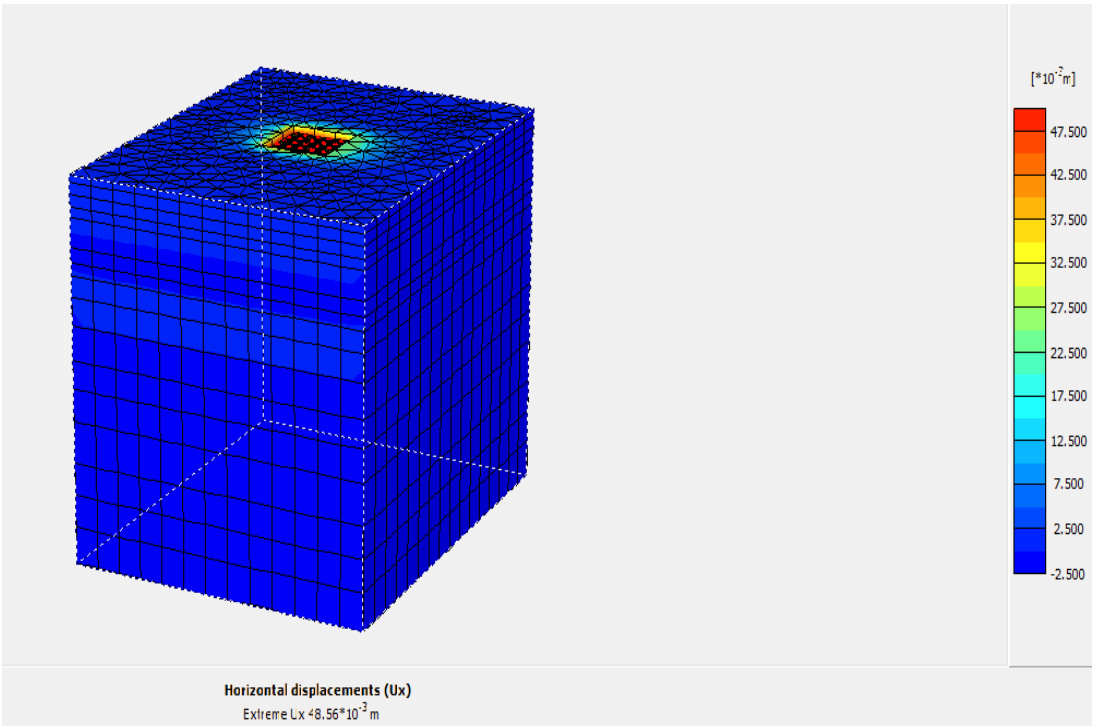

Figure 4-3 3-D deformed mesh of 6×6 at 5d spacing

Figure below indicates that, the difference of displacements of leading row with the other intermediate and trailing rows. For example, at load 1500kN the leading piles are deformed 25.23mm, while the last trailing row has been deformed 30.9mm, this is significant difference of 5.67mm it is about 19.35% decrement. This shows that the leading rows are the piles which deforms less than the other intermediate and trailing rows.

Figure 4.4 is the load-displacement curve of 6×6 pile model for each row, which is created by applying the stepping load from 100kN up to 2000kN in the Plaxis 3D Foundation.

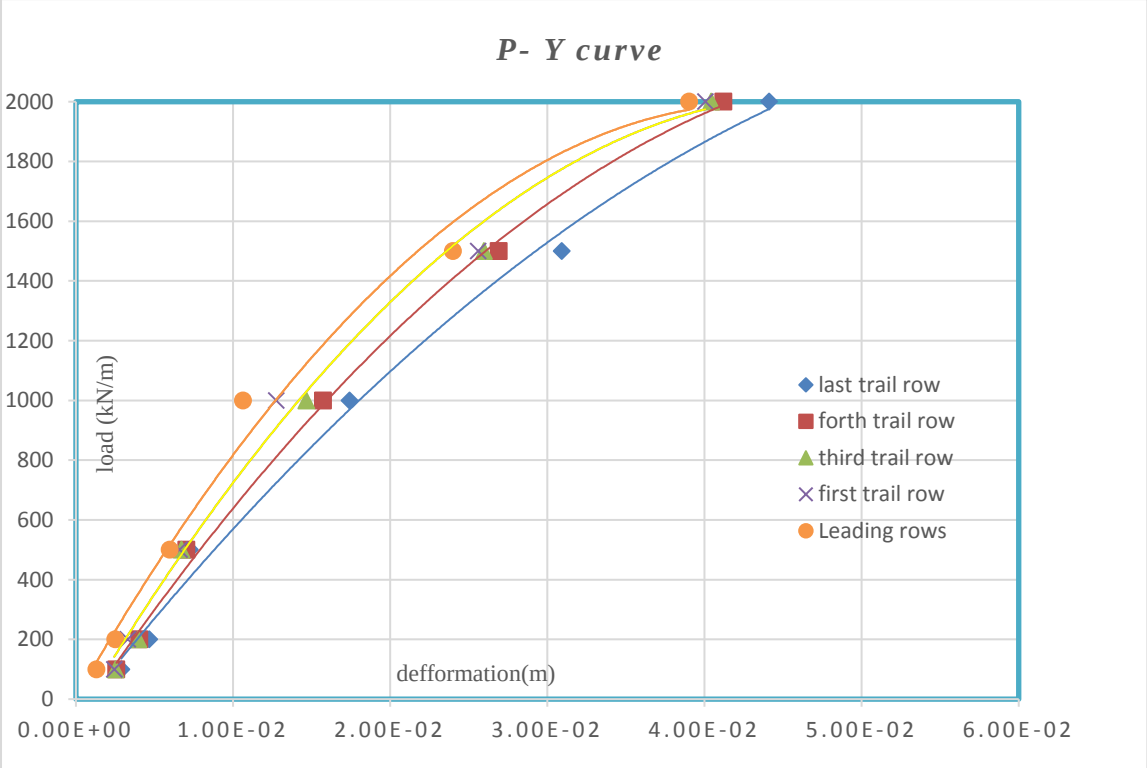

Figure 4-4 . P-y curve for every row in the 6×6 pile arrangements of 5d spacing

This graph shows that, the spacing of pile and deformation have opposite proportions, while spacing increasing, the piles get more confinement and shadowing effect decreases relative to 3d spacing at the same depth. Even though, some scholars mentioned that (McVay, 1995, et.al) after certain spacing, 6d the effect of stress overlapping is greatly decreased or totally neglected, piles may act like single pile. Actually, in this paper the whole model of large group pile laterally loaded were fixed head which is restrained, the deflection of the pile is takes place just below the pile cap.

c) At 20m pile length and 3d spacing center to center

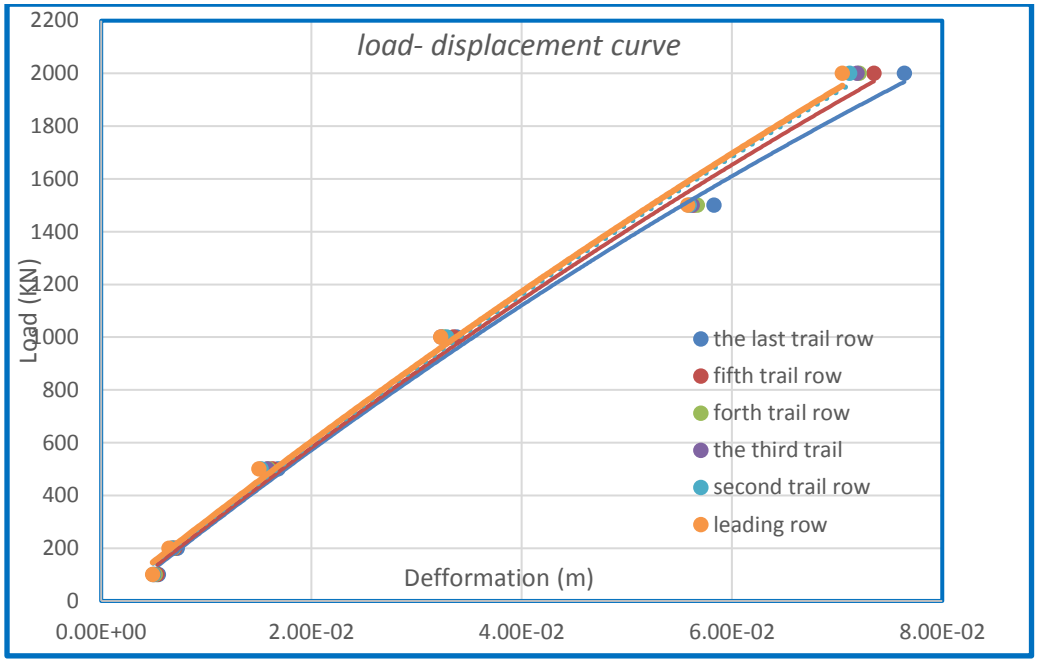

Figure 4-5 P-Y curve of 6×6 pile arrangement at 20m pile length at 3d center to center

The behavior of a pile within a pile group may differ substantially from that of a pile alone. Also, the behavior of a pile within the group varies depending on its group position. At 20m depth from the ground level the piles are more displaced than at 30m because of as the depth increases, stiffness of the soil increases .Therefore, depth and deformation are inversely proportional to each other while the application of load is at the ground level.

d) At 20m pile length 5d spacing center to center

The diameter of the pile is 65cm, 5×0.65m is 3.25m, and pile cap size of 17.8 × 17.8m. The following figure shows that partial view of deformed mesh of Plaxis 3D Foundation output for horizontal displacement.

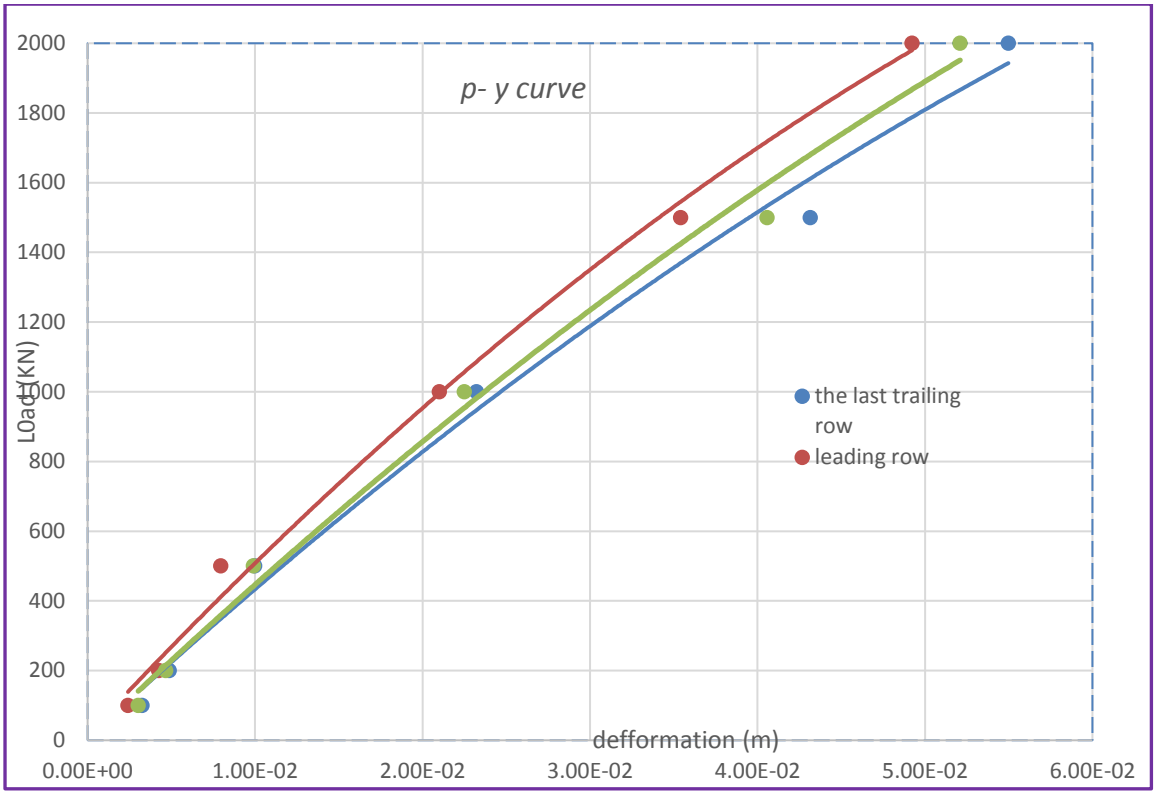

Figure 4-6 p-y curve of 6×6 pile arrangement of 20m pile length and 5d center to center

This indicates that as spacing increases from 3d to 5d Deformation decreases, here the graph try to show how the deformation is vary from leading rows, the first trailing row and the last trailing rows. The other intermediate rows also have descending order of deformation with their respective of their rows. For example, take the above model by the last stepping load of 2000kN the leading piles movement is 49.2mm while the last trailing row is 55.12mm hence the difference is very significant.

e) At 10m pile depth and 3d center to center spacing

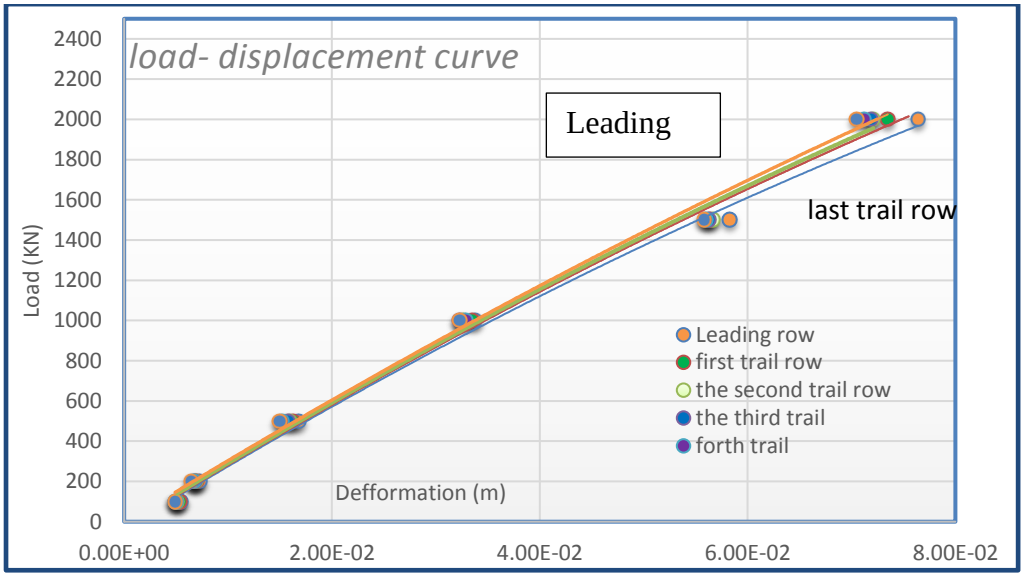

Figure 4-7 load-deflection curve of 6×6 pile and 3d center to center spacing

NB: The results obtained from the present analysis are quite comparable with result obtained by other researchers. The 15-Pile test was performed on five different days between July 29 and August 10, 2004 (J Walsh, 2004) Target deflections were selected as 6, 13, 19, 25, 38, 51, 64 and 89 mm. The system was loaded until the specific target deflection was reached for a predetermined string potentiometer. Because all piles deflected slightly different amounts, this string potentiometer was not necessarily equal to the average deflection of the group as a whole. Therefore, compare the figure 4.7 with the field-test result with figure 4.8. It is nearly close to each other. The result by 2000kN is 75mm and 76mm, almost close to each other.

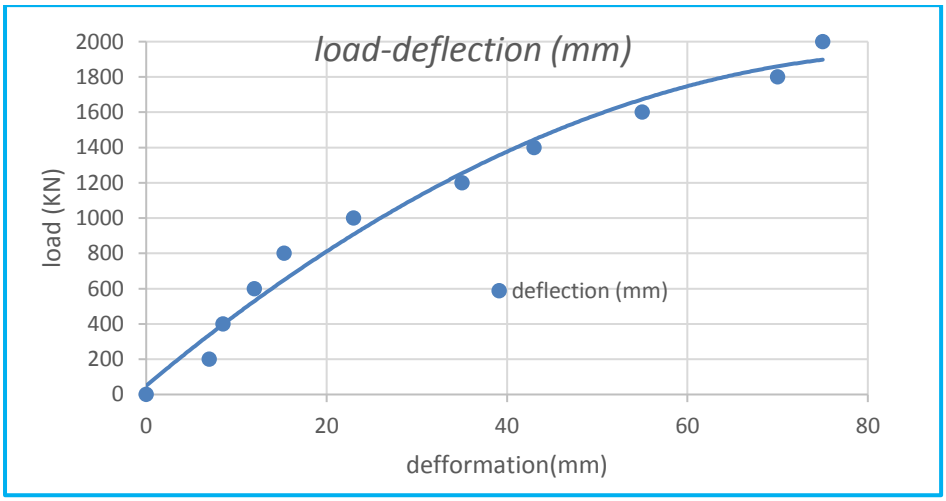

Figure 4-8 Load- deflection curve of loading test (J Walsh, 2005)

f) At 10m pile depth and 5d center to center spacing

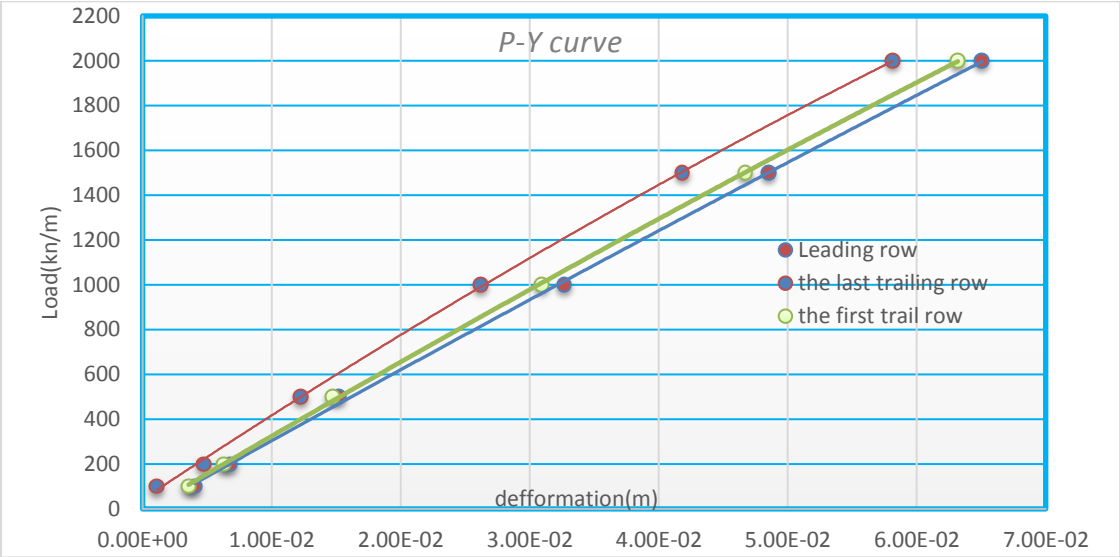

Figure 4-9 6×6 pile arrangement of laterally loaded large group pile at 10m pile depth and 5d center to center spacing

Leading row and trailing rows are outlined based on the direction of loading as shown in Figure 4.9. Group impact reduces the lateral resistance of every individual pile within the pile group compared to single pile. This indicate that the leading row of the piles in the group will carry higher loads than the piles in the trailing rows at the same deflection. Group effect is expected to become less significant as the spacing between piles increases because there is less overlap between adjacent zones of influence.

Table 4-1 Summary of 6×6 model by last stepping load (2000kN/m)

Pile arrangement	6×6		Deformation(mm)		
		Depth/pile length	The last trail row	Leading row	Difference (mm/%)
spacing	3d	10	76	70.5	5.5=7.23%
		20	66.4	62.5	3.9 = 5.87%
		30	47.8	44.5	3.3 =6.90%
	5d	10	65.12	58.2	6.8 =10.44%
		20	55	49.2	5.8 = 10.54%
		30	44.1	39	5.1 =11.56%

4.1.2 4×4 laterally loaded group of pile

a) At 10m pile length and 3d center to center spacing

Below, there are 4×4 pile models Plaxis 3D Foundation output with respect to spacing and depth of piles. Figure 4.11 shows that the leading rows have more resistant to the loading and the trail rows have less than the leadings, as a result the trail rows have higher displacement than the leading rows. There is summary of difference by percentage in the table 4.2 below.

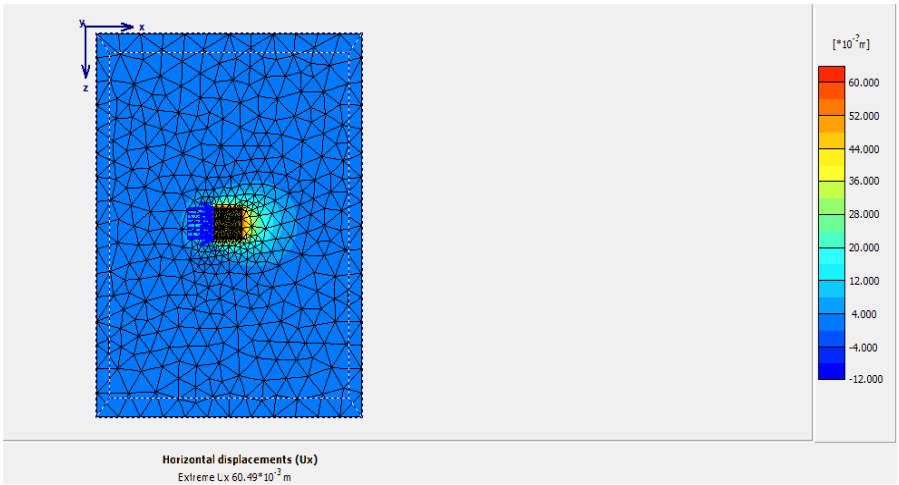

Figure 4-10 **Plaxis 3D-Foundation output of 4×4 pile arrangement top view**

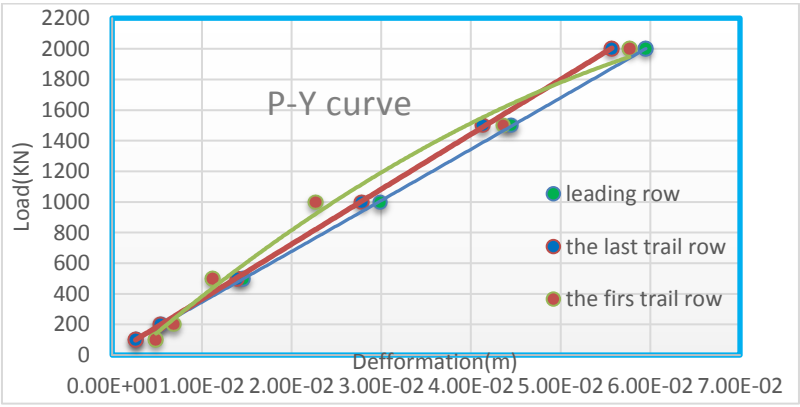

Figure 4-11. 4×4 laterally loaded group of pile at 10m pile length and 3d center to center

b) **At 10m pile length and 5d center to center spacing**.

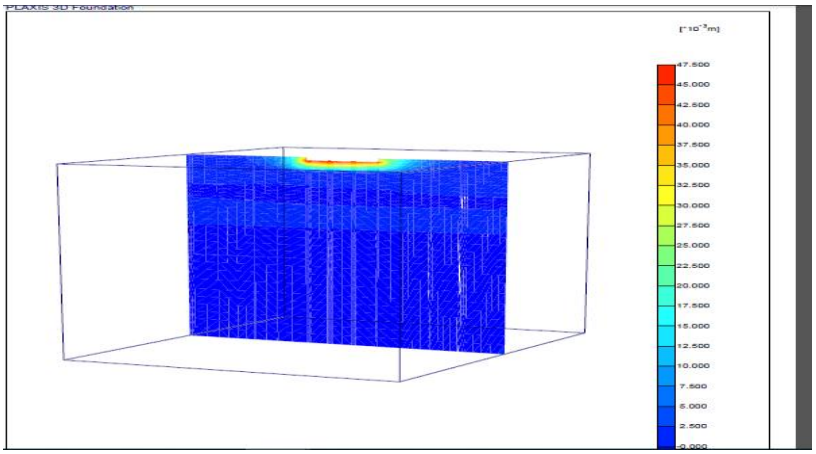

Figure 4-10 Plaxis 3-d foundation output of 4×4 arrangement section view of laterally deformed mesh

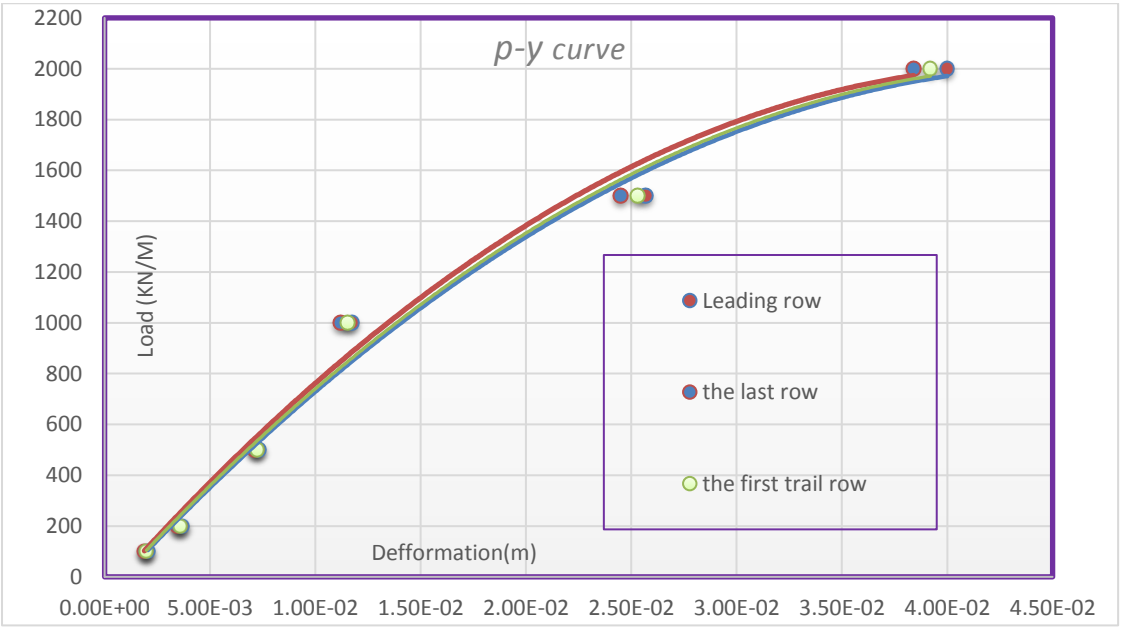

Figure 4-11 the result of p-y curve for each row graphically of 4×4 arrangements

c) At 20m pile length and 3d center to center spacing

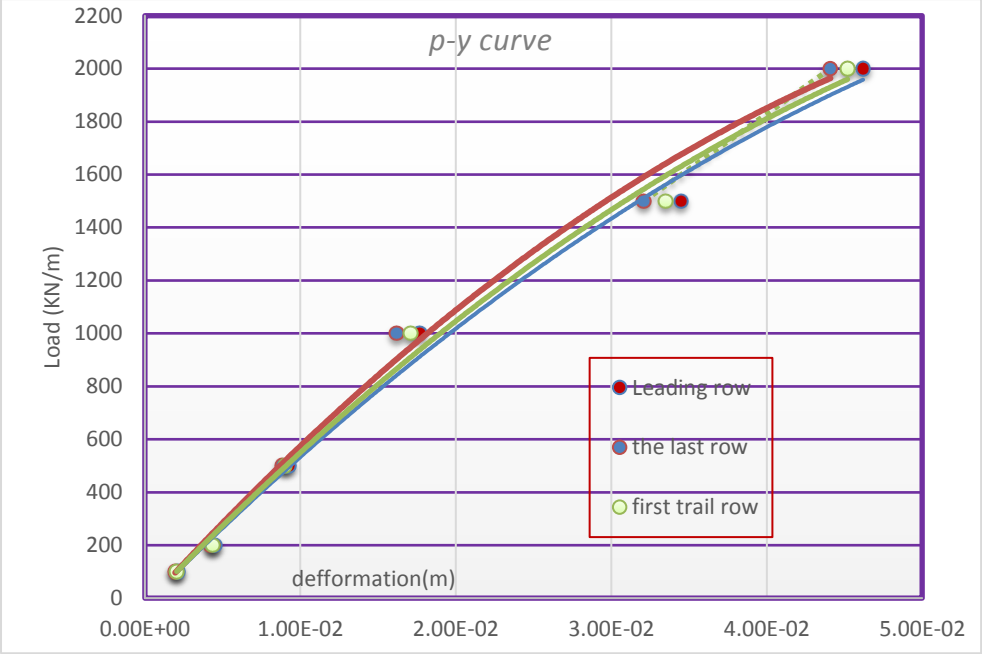

Figure 4-12 4×4 laterally loaded group of pile at 20m pile length and 3d center to center spacing

The shadowing effect, or decrease between the lead to the trail rows within a group, appears to be a function of pile spacing. Look figure 4-13 and compare it with above graph while the spacing was 3d that is why it is a function of spacing.

d) At 20m pile length and 5d spacing

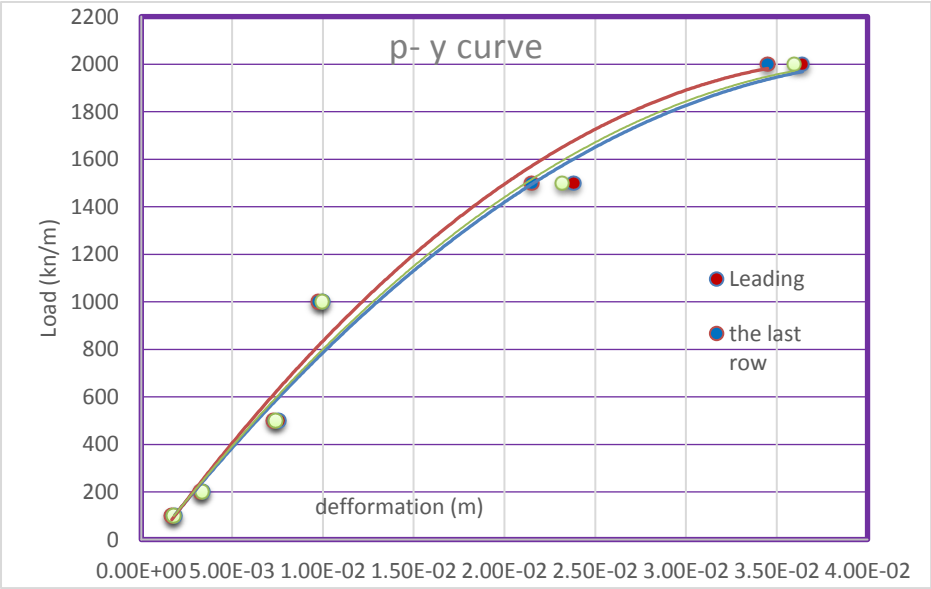

Figure 4-13 P-y curve of 4×4 pile arrangement at 5d spacing

Stiffness of the pile group decreases as the spacing of the piles in a pile group decreases. At the closer spacing, block failure mechanism is developed with full pile-soil slip being developed only along the outer face of the outer piles while widespread plastic zones form beneath the entire group. As the pile spacing increases, the amount of pile-soil slip along the inner piles increases and the region below the piles in which plasticity develops diminishes.as a result the displacement at 3d spacing is greater than at 5d spacing. From the figure 4-13 the last trailing rows has been deformed by 36.4mm while the leadings were 34.25mm. This is a significant difference.

e) At 30m pile length and 3d center to center spacing

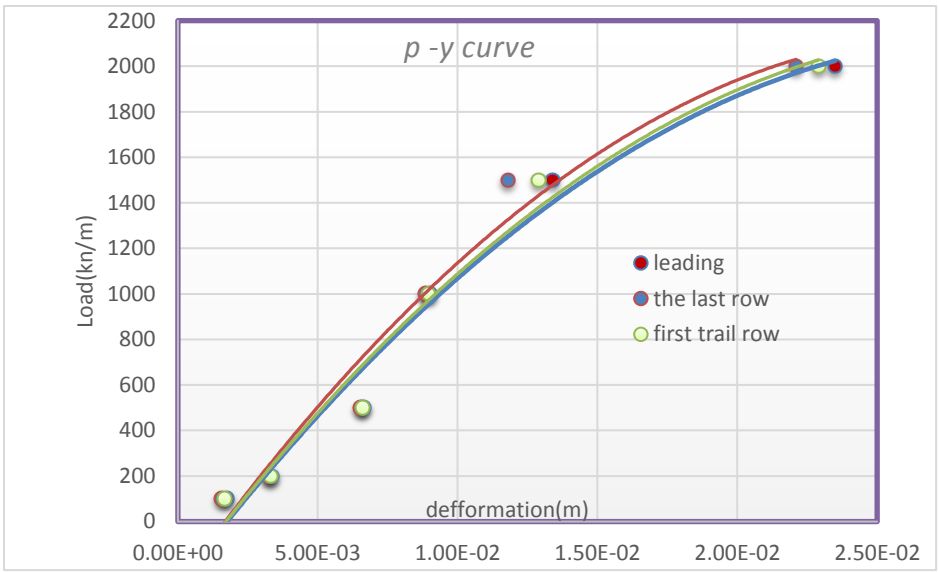

Figure 4-14 p-y curve of 4×4 pile arrangements at 30m pile length

e) At 30m pile length and 5d spacing

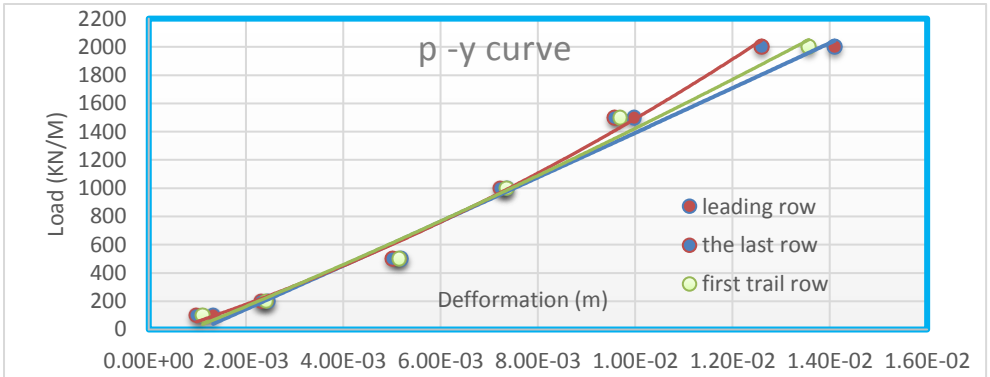

Figure 4-15 p-y curve of model 4×4 at 5d center to center

Table 4-2 Summary of 4×4 pile arrangement for deformations difference of leading and the last trailing row

Pile arrangement	4×4		Deformation(mm)		
		Depth/pile length	The last trail row	Leading row	Differences mm/%
spacing	3d	10	59.5	55.7	4.20 =7.05%
		20	46.2	44.1	2.1 = 4.54%
		30	23.5	22.1	1.4 = 5.9%
	5d	10	40	38.4	1.6 = 4.16%
		20	36.4	34.5	1.9 = 5.21%
		30	14.1	12.6	1.5 = 10.61%

N.B: The intermediate rows have between these values refer the movement curves and appendix.

4.1.3 7×3 Laterally Loaded Group of Pile

a) At 10m pile length and 3d spacing

Figure 4.16 represent the response of a 'representative pile' in each row in terms of load-displacement curve

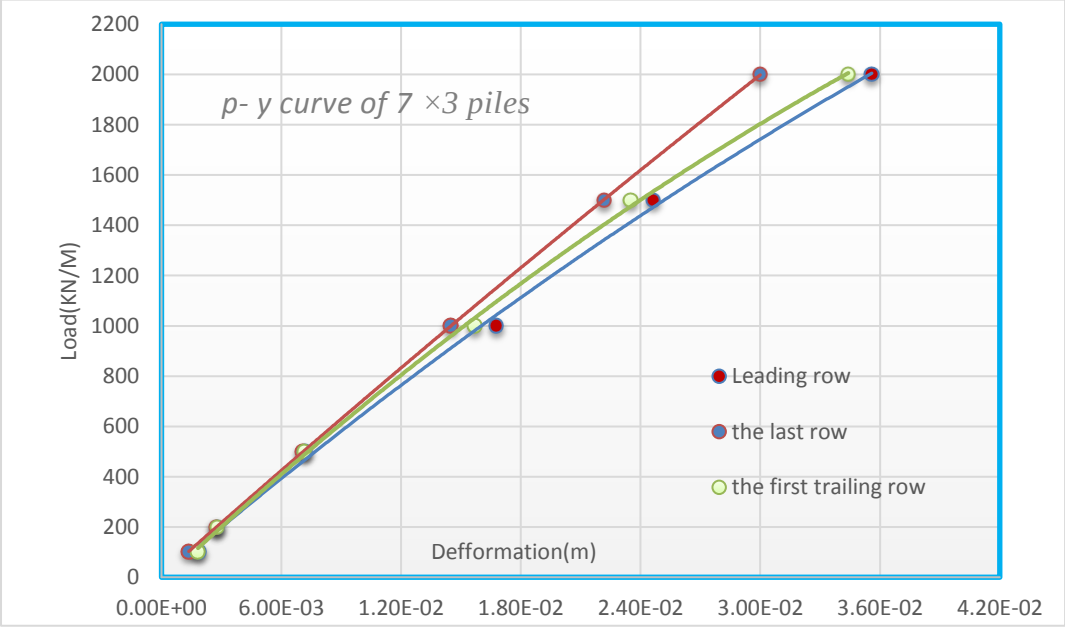

Figure 4-16 p-y curve of 3×7 pile arrangements

b) **At 20m pile length and 3d spacing**

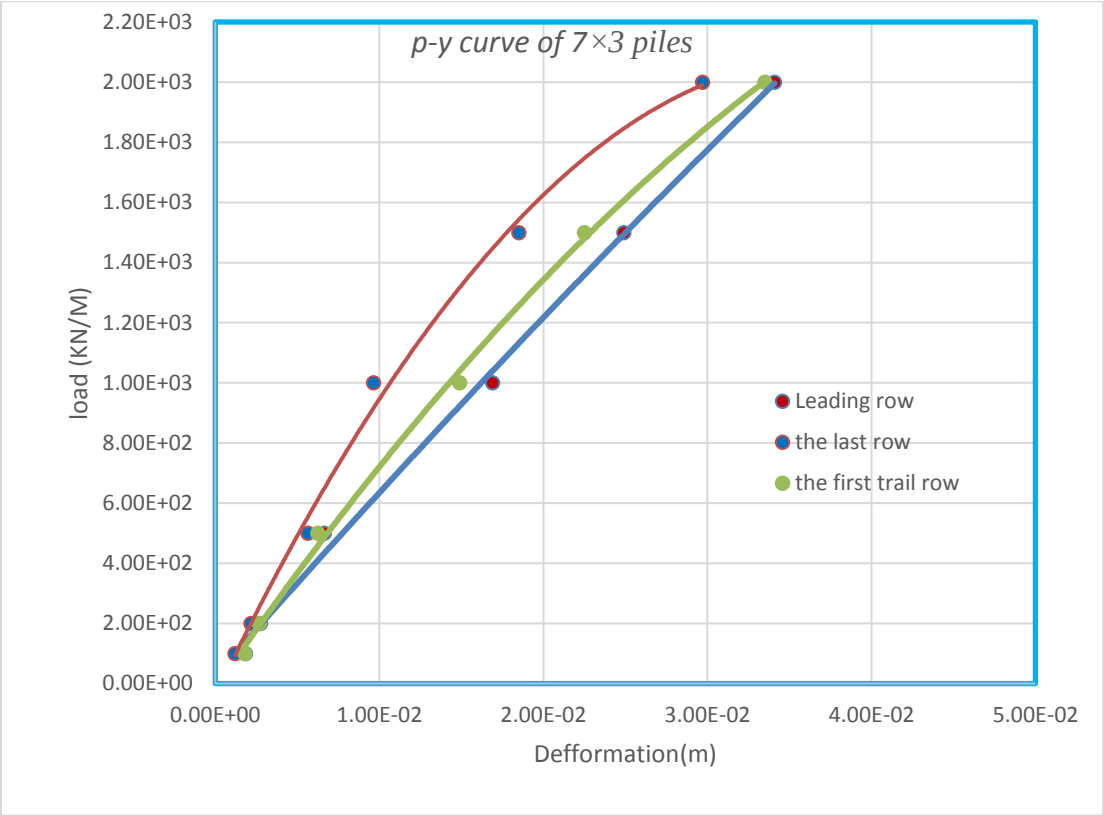

Figure 4-17 p-y curve of Model 7×3 at 20m depth of 3d center to center

d) At 10m pile length and 5d spacing center to center

The following model indicates that it is the 3-D section model of deformation of 21 piles, while 100kN/m load is applied on it, it shows that how it deform laterally while laterally load is applied on it in the direction of the applied load, and the magnitude of deformation is large in the direction of trail rows.

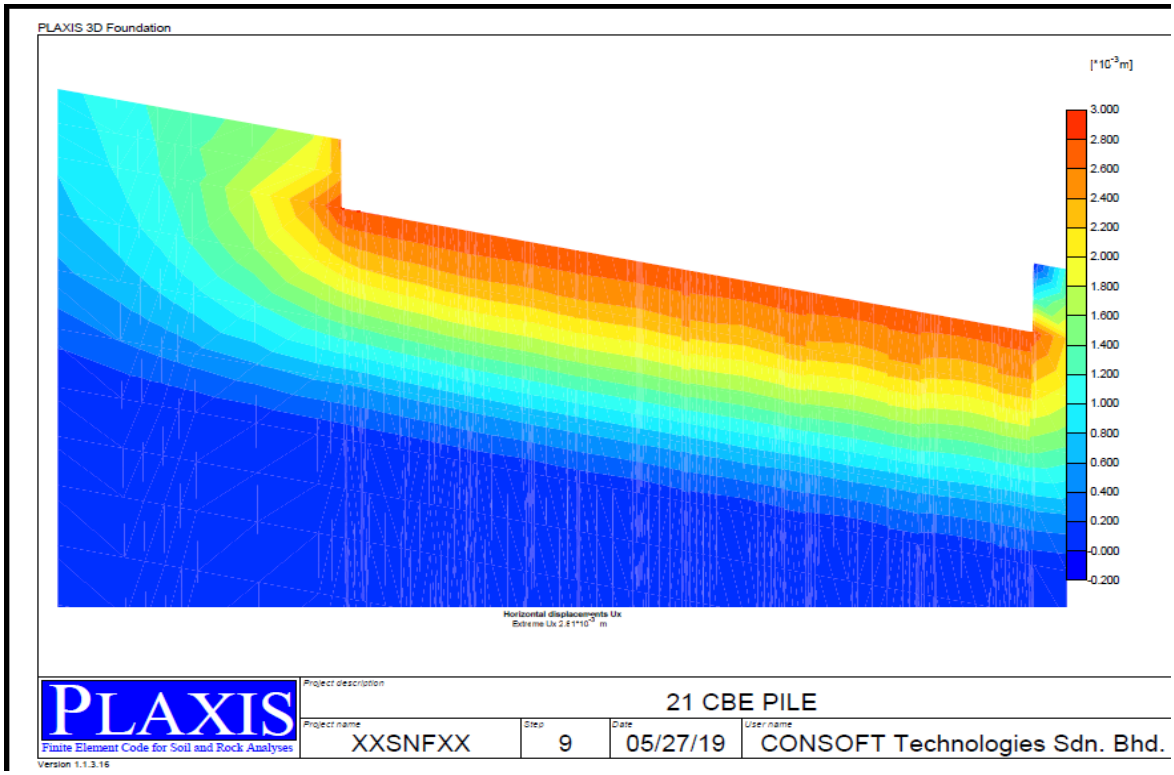

Figure 4-18 3-D section of Plaxis output for 7×3 at 3d center to center and 10m depth

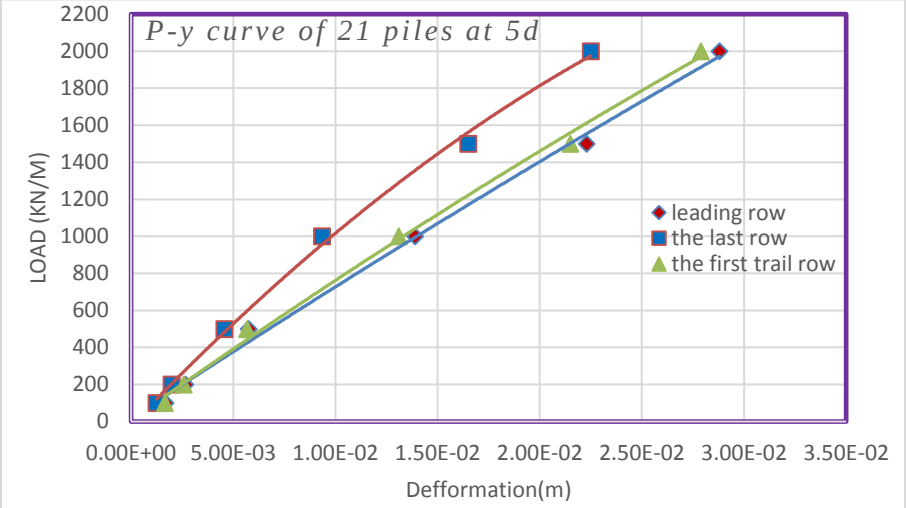

Figure 4-19 load-displacement curve of 7×3 and its Plaxis 3-D output

e) At 30m pile length and 3d center to center spacing

The load-displacement curves related to subsequent rows, instead, are significantly more flexible. In fact, the movements of the front piles induce a reduction in the stress state of the soil between the two rows of piles. The following rows, therefore, are in contact with a soil conditioned by the presence of the other piles.

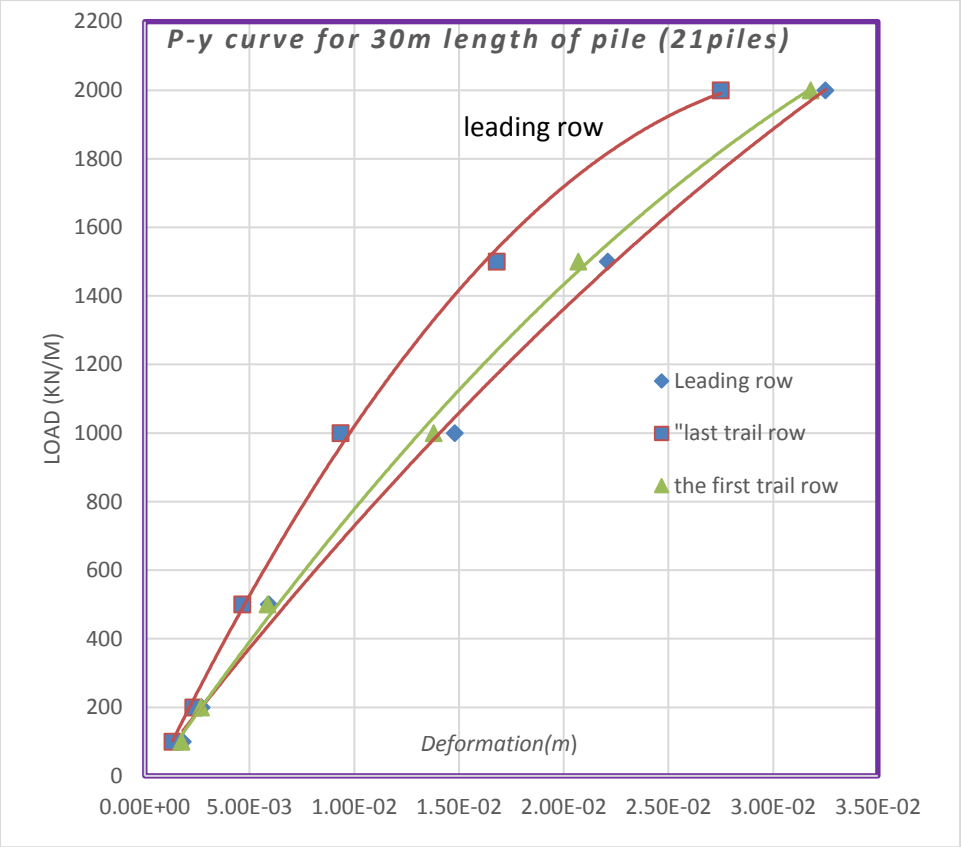

Figure 4-20 p-y curve of 30m pile length and 3d center to center spacing

The leading row is the first row on the right, where the lateral load acts from left to right. The rows following the leading row are labeled as 1st trailing row, 2nd trailing row, and so on. The spacing between two adjacent piles in a group is commonly described by the center to center spacing, measured either parallel or perpendicular to the direction of applied load. Pile spacing's are often normalized by the pile diameter, D. Thus, a spacing identified as 3D indicates the center to center spacing in a group is three times the pile diameter. Inside of the group a loss of efficiency of the piles occurred. The cause of this loss is related to the "shadowing phenomenon", which in terms of soil resistance means that the loss of soil resistance in the trailing rows is smaller than in the leading row.

Table 4-3 Summary for 7×3 pile arrangement for 2000kN load

Pile arrangement	7×3		Deformation(mm)		
		Depth/pile length	The last trail row	Leading row	Differences (mm/%)
spacing	3D	10	35.6	30	5.6 = 15.73%
		20	34.1	29.5	4.6 = 13.48%
		30	32.5	27.5	5.0 = 15.38%
	5D	10	28.8	22.5	6.3 = 21.87%
		20	23.37	19.12	4.25 = 18.18%
		30	17.25	14.12	3.13 = 18.14%

4.1.4 Pile length vs normalized deformation

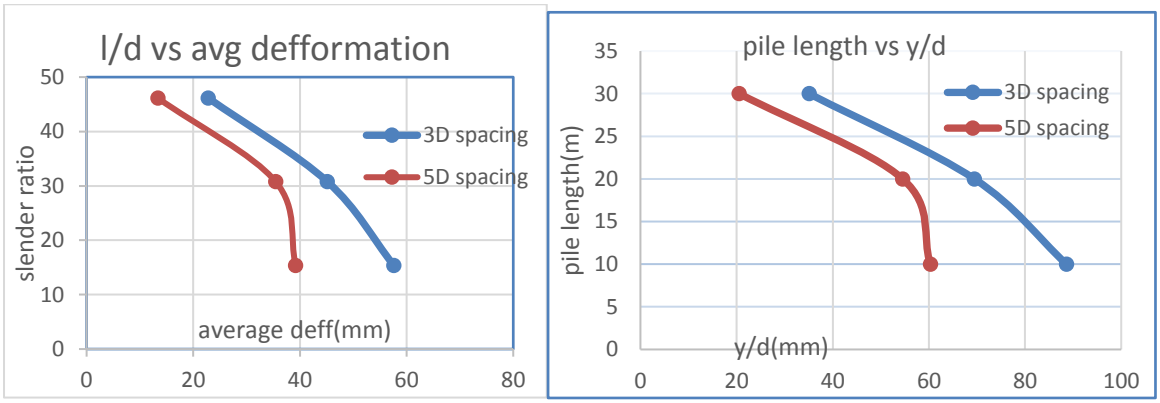

Figure 4-21 Pile length vs normalized deformation

Normalizing deformation at 5D spacing is also as shown in the figure below. It can be concluded that as the piles length increases the ultimate deformation decreases due to the increase in the lateral surface area of friction, and hence the ultimate deformation is attained below the pile cap.

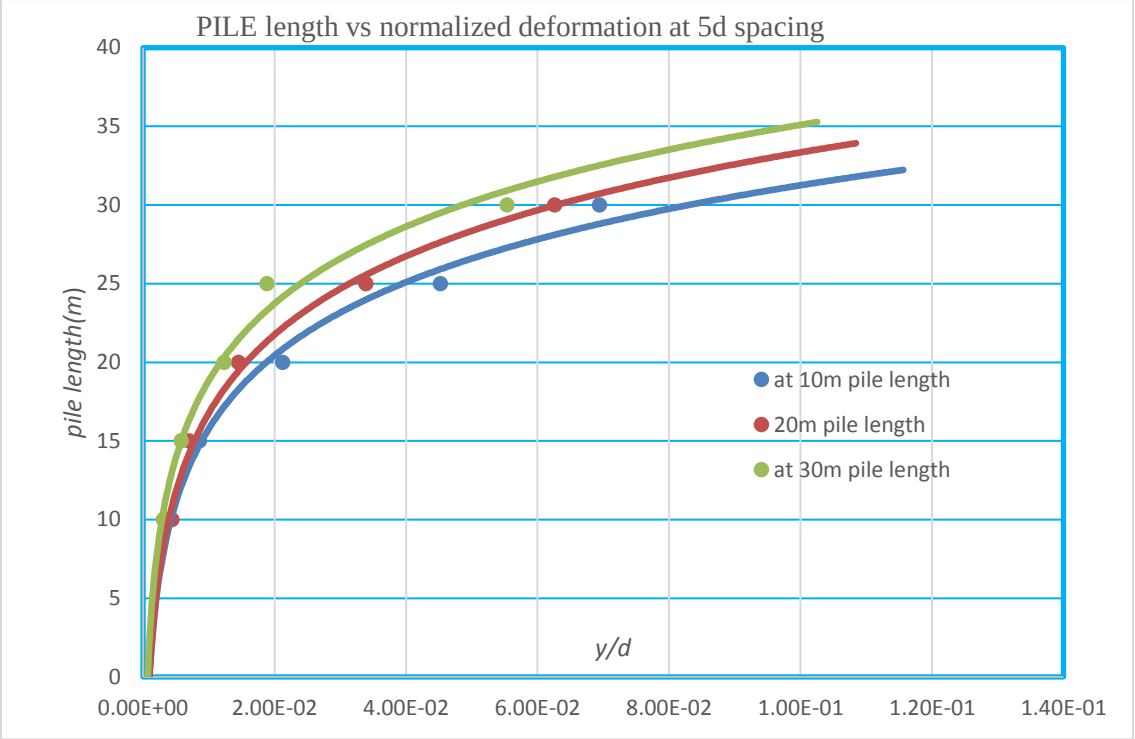

Figure 4-22 Normalizing deformation at 5D spacing

As expected, the soil resistance increases with depth. The figure also shows that p–y curves are non-linear .This indicates that as the pile length increase in to ground the deformation is decreased, as a result the deformation is high at the point of applications lateral load .it is clearly shown that on the model nearly on the ground, below the pile cap. This result is true for the rest of four by four and three by seven pile groups in this paper.

Generally Reese (1986) discussed that, the dependence of lateral behavior on pile length, short piles can deflect a large amount at the ground line given movement of the pile tip, but with increasing depth of penetration the soil resistance at the pile tip increases until a point is reached at which ground line deflection reaches a limiting value**.**

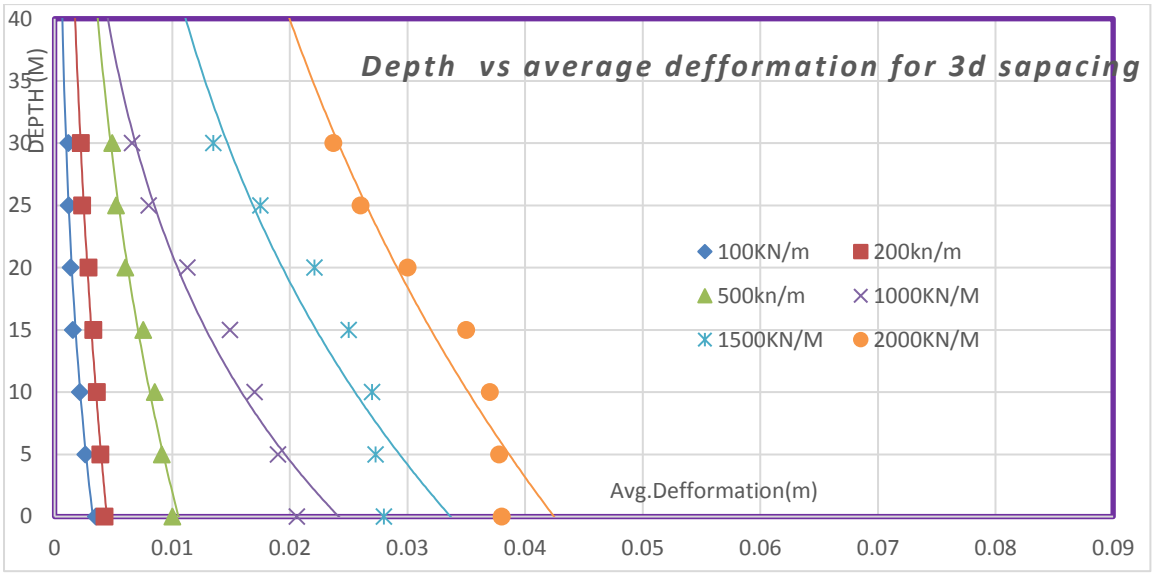

Figure 4-23 depth vs average deformation of 6×6 pile groups at 3D spacing

The above figure shows that as depth increases the deformation decreases the soil is became stiffer than the above layer due to overburden pressure. In addition, the stiffer behavior of the soil near the bedrock is likely due to the higher strength and stiffness of the bedrock; (Contribution of the bedrock stiffness becomes greater as the obtained *p-y* curves gets closer to the bedrock. (Soil resistance did not reach the ultimate value).

The following figure shows that soil lateral resistance of 16 piles with the average deformation of all rows at 3d spacing .it is unfortunately the leading rows can carry more loads than the other rows. This is true for the other group of piles in this research. It is on the back of appendix B.

Figure 4-24 Soil resistance (kN/m^2) vs average deformation for each row

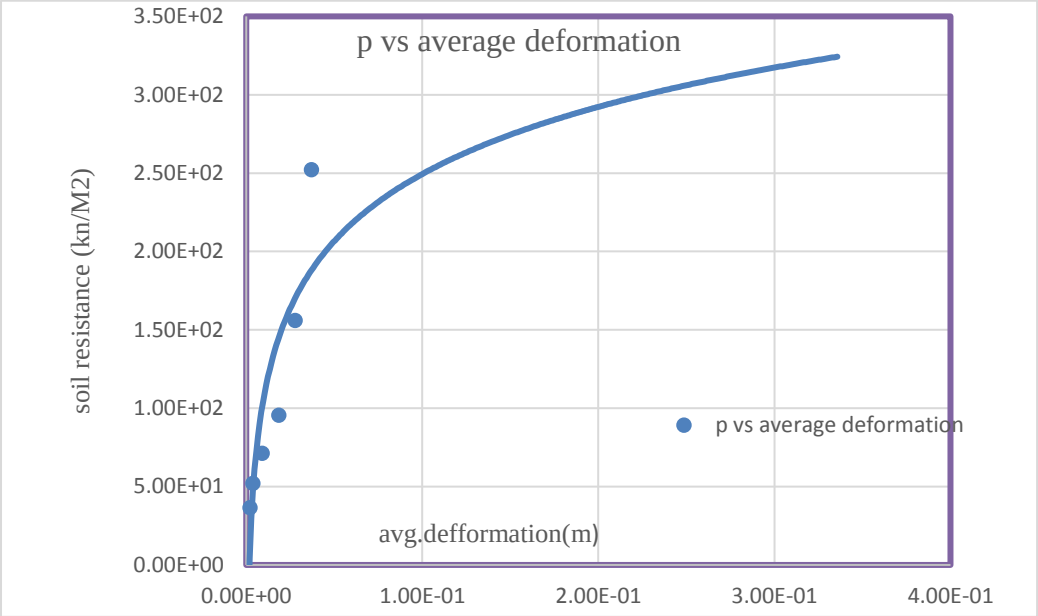

Figure 4-25 Soil resistance vs total average deformation of the rows for 6×6

4.1.5 Effects of stiffness on piles for 4×4 and 7×3 pile Arrangements

The stiffness of the interface element (*E*i) simulating the pile-soil interaction was determined by the stiffness of the surrounding soils (*E*s). Figure below illustrates the effect of the stiffness of the interface element on the lateral response of the pile. Stiffness of the pile group decreases as the spacing of the piles in a pile group decreases.

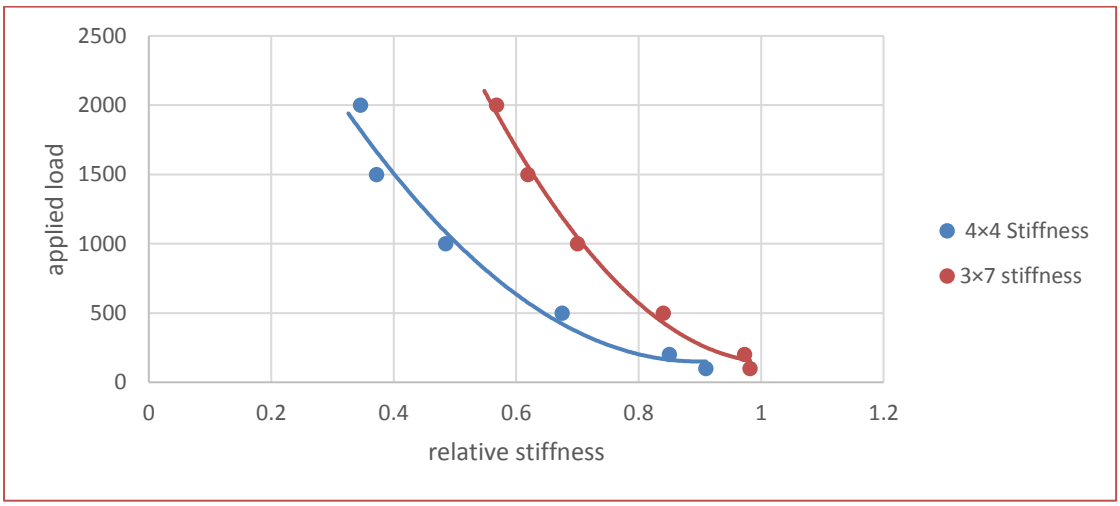

Figure 4-26 Soil stiffness vs applied load

In real soils, the stiffness depends significantly on the stress level, which means that the stiffness generally increases with depth (Plaxis manual, scientific,)

By changing lateral load values, soil reaction and pile deflection will be changed. Therefore, according to Eq. (2.6), the subgrade reaction modulus definitely will be changed. Figure 4.27 applied load vs stiffness curve for some values of lateral loads for long pile. By comparing curves, it can be seen that with increasing lateral loads, the horizontal subgrade reaction modulus is reduced.

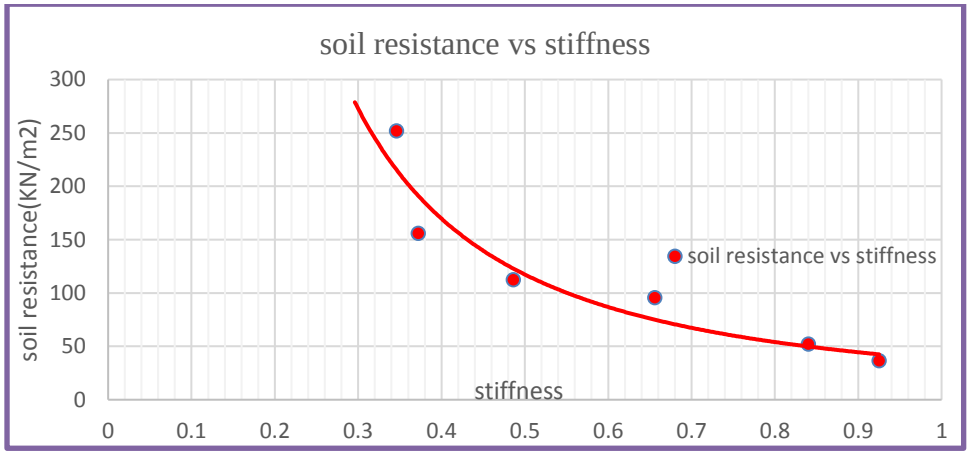

Figure 4-27 Soil reaction vs stiffness

Stiffness of the interface element (**E**i) simulating the pile-soil interaction was determined by the stiffness of the surrounding soils (**E**s). By changing lateral load values, soil reaction and pile deflection will be change. Therefore, the subgrade reaction modulus definitely will change. Figure 4-28 shows subgrade reaction-depth curve for some values of lateral loads for long pile. By comparison the curves, it can be seen that with increasing lateral loads, the horizontal subgrade reaction modulus is reduced.

(7×3) pile arrangement deformed mesh out put

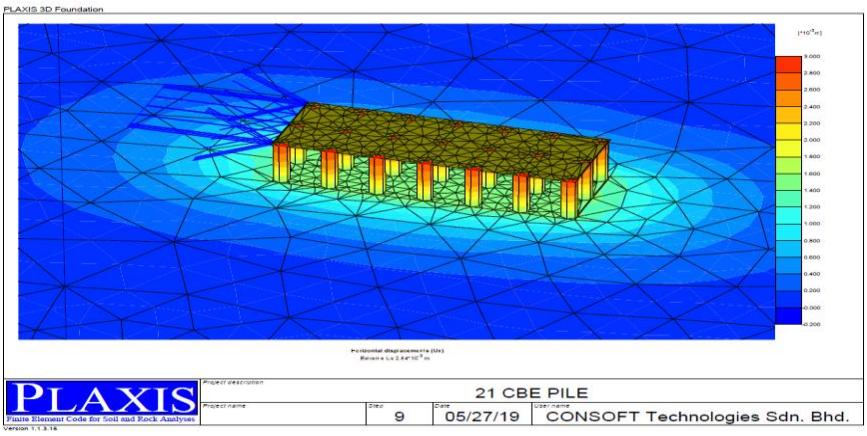

Figure 4-28 - 21 piles (7×3) pile arrangement deformed mesh out put

4.1.6 Slender ratio against row deformation of 6×6 pile arrangements

The influence of pile slenderness ratio is an important parameter to be considered in pile design. The influence of the pile slenderness ratio **(**L/D) under the effect of laterally loaded employed by Plaxis 3D Foundation at different pile depth is shown in figure 4-30. The analysis was carried out by 100kN, 200kN, 500kN, 1000kN, 1500 and 2000kN of applied load. The Result indicates from the following graph were as the slender ratio increases the deformation decreases and vice versa.

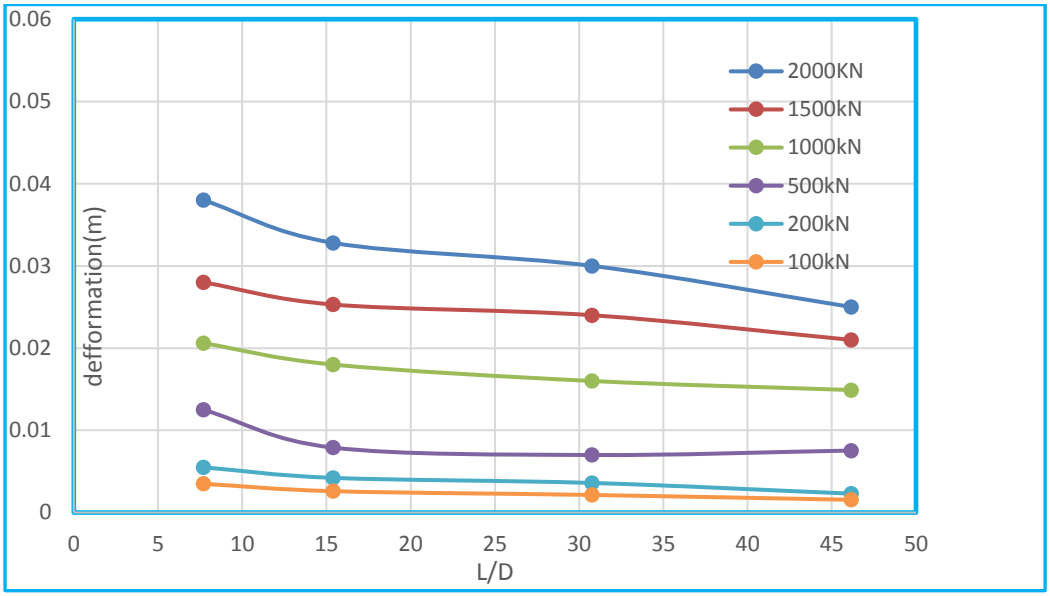

Figure 4-29 Average deformation vs slender ratio

The soil stratigraphy near the top of the pile is the most important when studying laterally loaded piles (Duncan, et al., 1994). Typically, the significant lateral deflections of piles occur within the upper 10 to 15 meters.

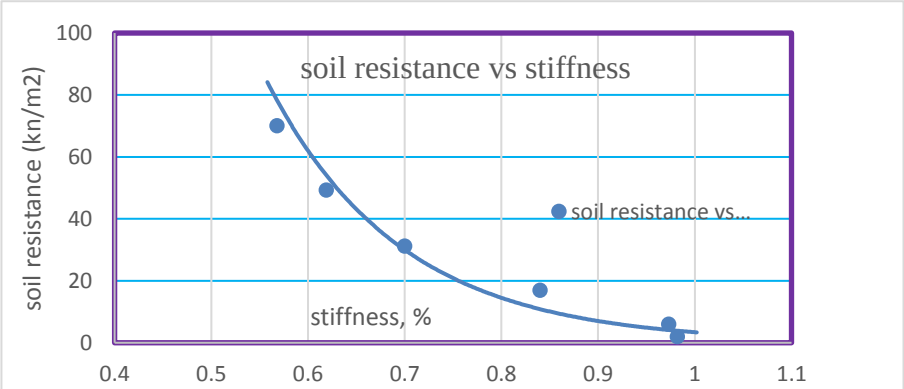

Figure 4-30 Soil reaction vs stiffness

It can be observed that in figure 4.31, lateral pile displacement occurred when there is a decrease in pile flexural rigidity EI or stiffness. It can also be observed that the pile with low amount of stiffness behave as a most flexible element, whilst, the pile with high amount of EI tend to behave as rigid element or more stiff

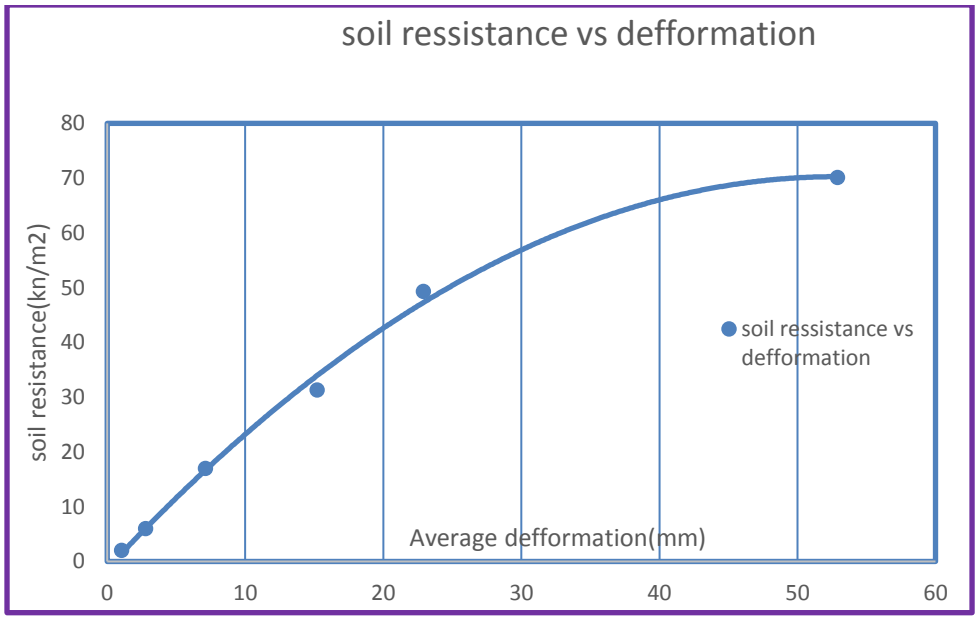

Figure 4-31 Soil reaction vs average deformation for 36 piles

Pile-soil-pile interaction causes a decrease of the stiffness of the overall system. In general, for an equal average load at each pile, the displacement of a pile group is greater than the displacement of a single isolated pile**.**

4.2 Result interpretations and discussion

The lateral displacement behavior of group of pile was depended on several factors such as number of piles, pile length, and pile spacing.

4.2.1 Assessments of Lateral pile displacement

The influence of group interaction on the three Large pile groups (i.e. 6 × 6, 4 × 4 and 3 × 7) on the lateral pile displacement at two different pile spacing (i.e. s = 3D and 5D) were shown in Figs. Above. For the same magnitude of lateral load Group interaction obtained showed an increase in lateral pile displacement. This conclusion was also supported by Brown et al. [1998], and Rollins et al. [2005]. Generally, even in the same pile group arrangements the lateral displacement of the Leading piles and the trailing piles are not equal. The leading piles are the one which resist more Loads and deflects less. There are also a difference of the displacement with intermediate rows but it is not significant as leading and the last trailing rows. It has been shown graphically in the previous section and tabular form in the chapter 7of Appendixes.

4.2.2 Effects of spacing in the large group pile

Several analyses were shown that from the above model, first, the lateral resistance of the piles within the group was a function of row location. All the piles within a row carried the same amount of load. Additionally, the front row piles carried more load than the trailing row piles with the second row carrying the next highest load followed by third row. However, the fourth and fifth rows carried approximately the same load as the third with the back row carrying a slightly higher load than the preceding row.

Spacing affected the lateral resistance of the pile groups. The group spaced at 5D showed very little reduction on lateral resistance. However, lateral resistance consistently decreased with closer spacing as a result it can show that the lateral resistance of the group piles of 3d spacing is less than the 5d.

4.2.3 Effects of depth

In case of this research three slenderness ratio were taken to analyze L/d i.e.15.4, 30.76 and 46.15 by keeping the cross-section of the pile constant through the study to 65cm diameter and varying the length of the piles 10m, 20m and 30m. Lateral deflections were obtained along the longitudinal for the three cases considered are shown in the above

summary table for each group arrangements. Different lateral loads are 100 kN/m, 200kN/m, 500kN/m 1000kN/m, 1500kN/m and 2000kN/m (Briaud, 1997, Walsh, 2005) takes the same loading step for field test, are applied at the center of the pile cap, It is observed that as the slender ratio of the pile increases, corresponding there is a decrease in deflection of the pile.

4.2.4 Effect of pile head fixation

In this study, the fixity of the pile head affects its load–displacement under lateral loading. Typically, in the large group piles the cap is used to restrain the pile head and equally distributed the applied load to all of the piles in the rows(Duncan,1998, 2001), therefore in this case the load is only static translational loads and the fixed head is preventing the rotation and torsion of the pile head.

A pile cap that remains in contact with the ground provides additional lateral restraint to the group. However, scour of the soil around the piles may reduce or eliminate the cap-soil contact and thereby reduce the lateral restraint provided by the cap. For this reason, the resistance of the cap to lateral loads is usually neglected (duncan, 1994).

4.2.5 Effect of interfaces

The contact between the piles and soil is modelled by an interface element, characterized by the parameter $R_{int,}$ which allows the relative displacement between pile and soil. When interface element models the interaction between a pile and the soil, which is intermediate between smooth and fully rough. The roughness of the interaction is modeled by choosing a suitable value for the strength reduction factor in the interface (R_{inter}).

The value of interface R_{int} is different for every layer, refer chapter 3 table3.1 the values were between 0.6 and 1. For the interface to remain elastic, the shear stress, $|\tau| < \sigma_n \tan \Phi i + ci$**,** where Φi and ci are the friction angle and cohesion (adhesion) of the interface respectively and σn, the effective normal stress.

CHAPTER 5 CONCLUSIONS AND RECOMENDATIONS

5.1 Conclusions

Based on the analysis using Plaxis 3D Foundation, it is summarized that the spacing and number of piles, in addition the soil stiffness and pile depth have an appreciable effects to the lateral displacement for the large group pile, the greater the pile spacing between rows the greater the reduction of deformation, this is due to the reaction area of the soil behind pile.

In the large group piles, the shadowing effect, is successively decreasing from the last trailing row to the leading row, this causes directly minimizing the pile movement through the rows. Increasing the pile spacing from 3D to 5D within a group shows, Groups of large spaced piles; and groups of closely spaced piles. Group of large spaced piles were analyzed by distributing the lateral loads equally among all piles within the group, and considering the behavior of anyone pile in isolation. In group of closely spaced piles, the response of one pile affects the close piles by influencing deflection of the soil between them.

For pile groups with fixed head, the leading row in the group carries the highest load, middle and backrow piles carry smaller loads for a given active loading, since intermediate rows carry more loads than the last rows without considering the edge effect. The over-lapping zones of influence of each pile not only transfer load to neighboring piles but also cause a reduction in the soil stiffness between the piles.

Increasing the number of piles within the group lead to decrease lateral deformation but it decreases the efficiency. The lateral soil pressure and stiffness under lateral loads in group piles changed with pile depth due to stiffness is stress dependent.

Finally based on the parameter analysis the difference of row displacement of leading, intermediate and trailing row were from 4% up to 8%, 9% up to 14%, 15 up to 20% respectively of total pile movements. Depending on the other parameters like depth of pile, spacing, number of rows and applied loads.

5.2 Recommendations

- Full-scale tests are generally believed to provide for the most accurate results but are rare because of large costs required to successfully perform a test for group piles.
- Usually the unloading modulus is determined by performing unloading and reloading test in the Odometer laboratory test. For this simulation the results used were not obtained from the Odometer test but default value as suggested by Plaxis from tangent modulus, this is not accurate as the laboratory result.
- For future analysis it is better while modeling laterally loaded group of piles, to consider both linear and non- linear combination properties of the soil, because the soil property nearest to the shaft of the pile may act like the linear and the away have non- linear property.

CHAPTER 6 REFERENCES

American Petroleum Institute (API), (1991), "Recommended Practice for Planning, Designing and Constructing of Fixed Offshore Platforms –RP2A-LRFD, 19th Edition, Washington.

Ashour M, Norris G (2000) Modelling Lateral Soil-Pile Response Based on Soil-Pile Interaction, Journal of Geotechnical and Geoenvironmental Engineering, 126(5), 420-428

Banerjee, P. K., and Davies, T. G. (1979). "Analysis of some reported case histories of laterally loaded pile groups." *Institution of Civil Engineers (ICE). Numerical Methods in Offshore Piling*, London, 83-90.

Broms, B. (1964). *Lateral resistance of piles in cohesive soils*. Journal of Soil Mechanics and Foundation Engineering, ASCE, 90(2).

Brown, D. A., and Shie, C. F. (1991). "Modification of p-y curves to account for group effects on laterally loaded piles." Geotechnical Engineering Congress, (G.S.P. No.27),

Coduto C.P. (1999): Geotechnical Engineering - Principles and Practices, Prentice-Hall, United States of America

Duncan, J.M. and Ooi, P.S.K. (1994). *Lateral load analysis of single piles and drilled shafts.* Journal of Geotechnical Engineering, ASCE, 120(5), pp. 1018-1033.

Duncan, J.M., & Chang, C.Y., (1970) "Nonlinear Analysis of Stress and Strain in Soil". ASCE Journal of the Soil Mechanics and Foundation Division, Vol. 96, pp. 1629-1653.

Feagin, L. B. 1935. Lateral pile loading tests. Transactions of ASCE 102:

Gouw, T.L. and Hidayat, I., 2015, "Effects of Pile Cap Thickness and Magnitudes of Lateral Movement on Laterally Loaded Group Piles", Electronic Journal of Geotechnical Engineering, 2015 Vol. 27

Holloway, D. M., Moriwaki, Y., Stevens, J. B., and Perez, J.-Y. (1981). "Response of a pile group to combined altial and lateral loading." Proc., 10th Int. Con! on Soil Mech. and Found. Engrg., Vol. 2, Boulimia Publishers, Stockholm, Sweden, 731-734.

Ismael N. F. (1998) "Lateral loading tests on bored piles in cemented sands". Proceedings of the 3rd International Geotechnical Seminar on Deep Foundation on Bored and Auger PilesGhentBelgium

Karthigeyan, S., Ramakrishna, V. V. G. S. T. & Rajagopal K. (2006) Influence of vertical load on the lateral response of piles in sand. Computer and Geotechnics, Vol.33, 121-131.

McVay, M., Casper, R., and Shang, T., (1995). ‘‘Lateral response of three row groups in loose to dense sands at 3D and 5D pile spacing.’’ *J. Geotech. Eng.*, 121(5), 436–441.

McVay, M., Shang, T., and Casper, R., (1996) ‘‘Centrifuge testing of fixed head laterally loaded battered and plumb pile groups in sand.’’ *Geotech. Test. J.*, 19(10) 41–50.

McVay, M., Zhang, L., Molnit, T., and Lai, P… (1998). ‘‘Centrifuge testing of large laterally loaded pile groups in sands.’’ *J. Geotech. Geoenviron. Eng.*, 124(10)1019 1026.

McVay, M., Zhang, L., Molnit, T., and Lai, P. [1998]. “Centrifuge testing of large laterally loaded pile groups in sands,” *Journal of Geotechnical and Geoenvironmental Engineering*, Vol. 124, No. 10, October 1998, pp. 1016-1026

Mokwa, R. L. (1999). Investigation of the resistance of pile caps to lateral loading. Ph.D. Dissertation, Virginia Polytechnic Institute and State University, Civil and Environmental Engineering Department.

O’Neill, M.W., and Raines, R.D., (1991), “Load Transfer for Pipe Piles in Highly Pressured Dense Sand”, Journal of Geotechnical Engineering, ASCE, Vol.117, No. 8

PLAXIS 3D Foundation version 1.6, *Material Model manual*, Delft University of Technology & PLAXIS B.V, 2004.

Poulos, H.G. dan Davis, E.H. (1980). *Pile Foundation Analysis and Design*. New York: John Wiley & sons

Poulos, H.G. & Davis, E.H. (1980) Pile Foundation Analysis and Design. John Wiley & Sons, Inc, United States.

Randolph, M. F., May, M., Leong, E.C., and Houlsby, G. T. (1991), “One-Dimensional Analysis of Soil Plug in Pipe Piles”, Geotechnique Vol. 41, No. 4

Rollins, K. M., Peterson, K. T., and Weaver, T. J. _1998_. “Lateral load behavior of full-scale pile group in clay.” *J. Geotech. Geoenviron. Eng.*, 124_6_, 468–478.

Rollins, K. M., and Sparks, A. _2002_. “Lateral resistance of full-scale pile cap with gravel backfill.” *J. Geotech. Geoenviron. Eng.*, 128_9_,

Ruesta, P. F., and Townsend, F. C. _1997_. “Evaluation of laterally loaded pile group at Roosevelt Bridge.” *J. Geotech. Geoenviron. Eng.*, 123_12_, 1153–161.

Reese Lymon C., William M. Isenhower, Shin-Tower Wang (2006), “Shallow and Deep Foundations,” John Wiley & Sons, ISBN 0-471-43159-1,

Reese, L.C. and Wang, S.T., Isenhower, W.M., and Arrellaga, J.A. (2000), “Computer program LPILE plus version 4.0 technical manual,” Ensoft, Inc., Austin, Texas

Reese, L.C., Cox, W. R., and Koch, F.D. (1974), "Analysis of Laterally Loaded Piles in Sand," Proceedings, Offshore Technology Conference, Houston, TX, Vol. II,

S. Prakash, Behavior of pile groups subjected to lateral loads (Ph.D. dissertation), University of Illinois at Urbana, IL, USA, 1962.

Terzaghi. K., (1955), "Evaluation of coefficients of subgrade reaction," Geotechnique, Vol. 5

Truty A. Hardening Soil Model with Small Strain Stiffness, ZACE Services, 2008

CHAPTER 7 APPENDIXES

APENDIX A Plaxis 3-D Manual

Basic Equations of Continuum Deformation

The static equilibrium of a continuum can be formulated as:

$$\underline{\underline{L}}^T \underline{\sigma} + \underline{p} = \underline{0}$$

This equation relates the spatial derivatives of the six stress components, assembled in vector σ, to the three components of the body forces, assembled in vector *p*. *LT* is the transpose of a differential operator, defined as :

$$\underline{\underline{L}}^T = \begin{bmatrix} \frac{\partial}{\partial x} & 0 & 0 & \frac{\partial}{\partial y} & 0 & \frac{\partial}{\partial z} \\ 0 & \frac{\partial}{\partial y} & 0 & \frac{\partial}{\partial x} & \frac{\partial}{\partial z} & 0 \\ 0 & 0 & \frac{\partial}{\partial z} & 0 & \frac{\partial}{\partial y} & \frac{\partial}{\partial x} \end{bmatrix} \qquad \underline{\varepsilon} = \underline{\underline{L}}\, \underline{u}$$

, $\dot{\underline{\sigma}} = \underline{\underline{M}}\, \dot{\underline{\varepsilon}}$, $\int \delta \underline{u}^T \left(\underline{L}^T \underline{\sigma} + p \right) dV = 0$,

$$\int \delta \underline{\varepsilon}^T \underline{\sigma}\, dV = \int \delta \underline{u}^T \underline{p}\, dV + \int \delta \underline{u}^T \underline{t}\, dS$$

$$\int \delta \underline{\varepsilon}^T \Delta \underline{\sigma}\, dV = \int \delta \underline{u}^T \underline{p}^i\, dV + \int \delta \underline{u}^T \underline{t}^i\, dS - \int \delta \underline{\varepsilon}^T \underline{\sigma}^{i-1} dV$$

Discretization of elements,

$\underline{u} = \underline{\underline{N}}\,\underline{v}$, $\underline{\varepsilon} = \underline{\underline{L}}\,\underline{\underline{N}}\,\underline{v} = \underline{\underline{B}}\,\underline{v}$ then the above equation is rewrite as

$$\int (\underline{\underline{B}}\,\delta\underline{v})^T \Delta\underline{\sigma}\, dV = \int (\underline{\underline{N}}\,\delta\underline{v})^T\, \underline{p}^i\, dV + \int (\underline{\underline{N}}\,\delta\underline{v})^T\, \underline{t}^i\, dS - \int (\underline{\underline{B}}\,\delta\underline{v})^T\, \underline{\sigma}^{i-1}\, dV$$

Finally,

Discretized equation in equilibrium is

$$\int \underline{\underline{B}}^T\, \Delta\underline{\sigma}\; dV = \int \underline{\underline{N}}^T\, \underline{p}^i\, dV + \int \underline{\underline{N}}^T\, \underline{t}^i\, dS - \int \underline{\underline{B}}^T\, \underline{\sigma}^{i-1}\, dV$$

Global iterative procedure:

Substitution of the relationship between increments of stress and increments of strain,

$\Delta\sigma = M\,\Delta\varepsilon$, into the equilibrium equation above

$\underline{\underline{K}}^i\, \Delta\underline{v}^i = \underline{f}_{ex}^{\,i} - \underline{f}_{in}^{\,i-1}$ While K is the stiffness matrix and v is the incremental displacement f*ex* is the external force vector and f*in* is the internal vector reaction

APENDIX B TABLES

1. Plaxis 3-DFOUNDATION output for deformations at different loading step of 6×6 or 36 piles with 6 rows .at 3D center to center pile spacing and 30m.

Force kN	Row A (leading row)	Row B	Row C	Row D	Row E	F (the last trail row)	Avg. Deformation	y/d
	(m)	(m)	(m)	(m)	(x)	(m)	(m)	y/d
100	3.23E-03	3.68E-03	3.94E-03	4.16E-03	4.43E-03	4.89E-03	4.06E-03	6.24E-03
200	5.23E-03	5.68E-03	5.94E-03	6.16E-03	6.43E-03	6.89E-03	6.06E-03	9.32E-03
500	9.70E-03	1.01E-02	1.03E-02	1.05E-02	1.08E-02	1.12E-02	1.04E-02	1.61E-02
1000	2.09E-02	2.12E-02	2.14E-02	2.15E-02	2.17E-02	2.27E-02	2.16E-02	3.32E-02
1500	3.26E-02	3.28E-02	3.29E-02	3.30E-02	3.32E-02	3.36E-02	3.30E-02	5.08E-02
2000	4.45E-02	4.47E-02	4.47E-02	4.47E-02	4.49E-02	4.53E-02	4.48E-02	6.89E-02

2. Table: **out puts at 10m depth for 3D spacing 6×6 large group pile

Load(force) kN/m	Row a m	Row b m	Row c m	Row d m	Row e m	Row f m	Avg.deform m	y/d
100	4.90E-03	4.96E-03	4.99E-03	5.12E-03	5.32E-03	5.45E-03	5.12E-03	7.88E-03
200	6.45E-03	6.68E-03	6.79E-03	6.86E-03	6.99E-03	7.25E-03	6.84E-03	1.05E-02
500	1.50E-02	1.52E-02	1.58E-02	1.60E-02	1.63E-02	1.68E-02	1.58E-02	2.44E-02
1000	3.23E-02	3.29E-02	3.23E-02	3.26E-02	3.35E-02	3.38E-02	3.29E-02	5.06E-02
1500	5.58E-02	5.60E-02	5.62E-02	5.67E-02	5.74E-02	5.83E-02	5.67E-02	8.73E-02
2000	6.15E-02	6.17E-02	6.19E-02	6.21E-02	6.23E-02	6.24E-02	6.20E-02	9.54E-02

3. Plaxis 3D foundation output at 10m 5D spacing of 6×6 piles at 30m depth

Force	Row a	Row b	Row c	Row d	Row e	Row f	Avg.deform	y/d
100kN	1.09E-03	1.88E-03	2.06E-03	3.17E-03	3.56E-03	4.05E-03	2.64E-03	4.06E-03
200kN	4.72E-03	4.82E-03	4.90E-03	5.91E-03	6.30E-03	6.79E-03	5.57E-03	8.57E-03
500kN	1.23E-02	1.31E-02	1.32E-02	1.43E-02	1.47E-02	1.52E-02	1.38E-02	2.12E-02
1000kN	2.62E-02	2.79E-02	2.89E-02	2.98E-02	3.09E-02	3.27E-02	2.94E-02	4.52E-02
1500kN	4.18E-02	4.36E-02	4.46E-02	4.55E-02	4.67E-02	4.85E-02	4.51E-02	6.94E-02
2000kN	5.82E-02	5.99E-02	6.09E-02	6.19E-02	6.32E-02	6.51E-02	6.15E-02	9.47E-02

4: 6×6 piles at 5D center to center pile spacing.

FORCE	Row a	Row b	Row c	Row d	Row e	Row f	Avg.deform.	y/d
100kN	1.30E-04	1.40E-03	2.44E-03	2.52E-03	2.57E-03	2.88E-03	1.99E-03	3.06E-03
200kN	2.50E-03	3.18E-03	3.29E-03	3.98E-03	4.02E-03	5.66E-03	3.77E-03	5.80E-03
500kN	6.97E-03	7.30E-03	7.60E-03	8.26E-03	8.59E-03	9.26E-03	7.99E-03	1.23E-02
1000kN	1.06E-03	1.08E-02	1.37E-02	1.47E-02	1.57E-02	1.74E-02	1.22E-02	1.88E-02
1500kN	3.40E-02	3.46E-02	3.56E-02	3.60E-02	3.69E-02	3.89E-02	3.60E-02	5.54E-02
2000kN	4.51E-02	4.62E-02	4.75E-02	4.85E-02	4.98E-02	5.02E-02	4.79E-02	7.37E-02
All deformations are by meters *** ****For all above: ROW-F last trailing row Row e-first trail row ,Row –d-second trail row, Row c-third trailing row, row B forth trailing row and Row -A the leading row								

5: out puts of Plaxis 3d-Foundation for 16 or 4×4 pile arrangement at 10m depth and 3D center to center

Force(kN)	Deformation (m)					
	Row a	Row b	Row c	Row d	Avg	Y/d
100	2.62E-03	2.65E-03	4.89E-03	2.69E-03	2.14E-03	3.29E-03
200	5.35E-03	5.37E-03	6.89E-03	5.43E-03	3.84E-03	5.91E-03
500	1.39E-02	1.42E-02	1.12E-02	1.46E-02	9.00E-03	1.39E-02
1000	2.89E-02	2.94E-02	2.27E-02	2.99E-02	1.85E-02	2.84E-02
1500	4.43E-02	4.43E-02	3.36E-02	4.45E-02	2.78E-02	4.28E-02
2000	5.87E-02	5.87E-02	4.53E-02	5.90E-02	3.70E-02	5.69E-02

6. Table: Plaxis 3D-Foundation output at 20m depth and 3d center to center for 4×4 pile

Force(kN)	deformation(m)					
	Row a	Row b	Row c	Row d	Average deformation (m)	y/d
100	1.95E-03	1.99E-03	2.05E-03	2.13E-03	1.35E-03	2.08E-03
200	4.21E-03	4.26E-03	4.35E-03	4.47E-03	2.88E-03	4.43E-03
500	8.85E-03	8.95E-03	9.02E-03	9.25E-03	6.01E-03	9.25E-03
1000	1.62E-02	1.65E-02	1.71E-02	1.77E-02	1.13E-02	1.73E-02
1500	3.21E-02	3.25E-02	3.35E-02	3.45E-02	2.21E-02	3.40E-02
2000	4.41E-02	4.46E-02	4.52E-02	4.62E-02	3.00E-02	4.62E-02

7. Plaxis 3D-Foundation output at 10m depth and 5D center to center for 4×4

Force(kN)	Deformation(m)					
	Row a	Row b	Row c	Row d	Avg.def	y/d
100	1.89E-03	1.95E-03	1.99E-03	2.05E-03	1.31E-03	2.02E-03
200	3.45E-03	3.53E-03	3.59E-03	3.68E-03	2.37E-03	3.65E-03
500	7.12E-03	7.16E-03	7.25E-03	7.32E-03	4.81E-03	7.40E-03
1000	1.12E-02	1.14E-02	1.16E-02	1.18E-02	7.65E-03	1.18E-02
1500	2.45E-02	2.49E-02	2.53E-02	2.57E-02	1.67E-02	2.57E-02
2000	3.84E-02	3.87E-02	3.92E-02	3.96E-02	2.60E-02	4.00E-02

8. Plaxis 3D-Foundation output at 20m depth and 5D center to center for 4×4

Force(kN)	Deformation(m)				
	Row a	Row b	Row c	Row d	y/d
100	1.58E-03	1.64E-03	1.67E-03	1.77E-03	1.71E-03
200	3.23E-03	3.28E-03	3.33E-03	3.36E-03	3.38E-03
500	6.54E-03	6.58E-03	6.61E-03	6.65E-03	6.76E-03
1000	8.85E-03	8.89E-03	8.96E-03	9.01E-03	9.16E-03
1500	1.18E-02	1.25E-02	1.29E-02	1.34E-02	1.30E-02
2000	2.21E-02	2.25E-02	2.29E-02	2.35E-02	2.33E-02

NB: row, d = the last trail row, row, c= second trail row, Row, b =first trail row. Row, a= leading row

9. Plaxis 3-D foundation output of 7×3 pile arrangement, deformation of rows, average deformation, normalized deformation and soil reaction at 10m of pile length.

Force (kN/m)	Deformation(m)									Soil. Reac(kN/m^2)
	Row a	Row b	Row c	Row d	Row e	Row f	Row g	Avg.deform.	y/d	
100	1.37E-03	1.37E-03	1.47E-03	1.67E-03	1.78E-03	1.83E-03	1.90E-03	1.67E-03	2.57E-03	1.63E+01
200	2.75E-03	2.75E-03	2.76E-03	2.76E-03	2.77E-03	2.79E-03	2.81E-03	2.77E-03	4.27E-03	1.62E+01
500	7.06E-03	7.06E-03	7.08E-03	7.10E-03	7.13E-03	7.16E-03	7.20E-03	7.12E-03	1.10E-02	1.70E+01
1000	1.45E-02	1.45E-02	1.45E-02	1.46E-02	1.49E-02	1.57E-02	1.68E-02	1.52E-02	2.33E-02	-3.13E+01
1500	2.22E-02	2.22E-02	2.23E-02	2.23E-02	2.24E-02	2.35E-02	2.46E-02	2.29E-02	3.52E-02	-4.93E+01
2000	3.00E-02	3.00E-02	3.12E-02	3.32E-02	3.33E-02	3.44E-02	3.56E-02	3.29E-02	5.07E-02	-7.01E+01

10. Table: 7×3 pile arrangement at 20m depth and 3D center to center spacing

Force(kN)	Deformations (m)								
	Row a	Row b	Row c	Row d	Row e	Row f	Row g	Avg.	y/d
1.00E+02	1.20E-03	1.41E-03	1.52E-03	1.65E-03	1.75E-03	1.80E-03	1.85E-03	1.86E-03	2.87E-03
2.00E+02	2.18E-03	2.25E-03	2.38E-03	2.45E-03	2.61E-03	2.69E-03	2.75E-03	2.89E-03	4.44E-03
5.00E+02	5.65E-03	5.71E-03	5.85E-03	5.96E-03	6.05E-03	6.25E-03	6.65E-03	7.02E-03	1.08E-02
1.00E+03	9.65E-03	1.01E-02	1.33E-02	1.44E-02	1.56E-02	1.59E-02	1.69E-03	1.34E-02	2.07E-02
1.50E+03	1.85E-02	1.90E-02	1.95E-02	2.05E-02	2.15E-02	2.25E-02	2.29E-02	2.41E-02	3.70E-02
2.00E+03	2.97E-02	3.05E-02	3.25E-02	3.27E-02	3.31E-02	3.35E-02	3.41E-02	3.77E-02	5.80E-02

11. 7×3 pile arrangement at 10m pile depth and 5D center to center spacing

Force(kN/m)	Deformation(m)								
	Row a	Row b	Row c	Row d	Row e	Row f	Row g	Avg deformation;	y/d
100	1.25E-03	1.29E-03	1.39E-03	1.42E-03	1.52E-03	1.65E-03	1.68E-03	4.45E-03	6.85E-03
200	1.98E-03	2.09E-03	2.32E-03	2.41E-03	2.48E-03	2.58E-03	2.65E-03	8.78E-03	1.35E-02
500	4.56E-03	4.68E-03	4.85E-03	5.01E-03	5.64E-03	5.68E-03	5.76E-03	1.95E-02	3.01E-02
1000	9.35E-03	9.89E-03	1.12E-02	1.15E-02	1.21E-02	1.31E-02	1.39E-02	3.58E-02	5.51E-02
1500	1.65E-02	1.69E-02	1.78E-02	1.89E-02	1.99E-02	2.15E-02	2.23E-02	5.24E-02	8.06E-02
2000	2.25E-02	2.39E-02	2.48E-02	2.58E-02	2.69E-02	2.79E-02	2.88E-02	3.01E-02	4.63E-02

12. Table 7×3 pile arrangement at 30m pile depth and 3D center to center spacing for the same load as above

Deformation(m)								
Row a	Row b	Row c	Row d	Row e	Row f	Row g	Avg.	y/d
1.32E-02	1.42E-03	1.49E-03	1.55E-03	1.69E-03	1.75E-03	1.82E-03	3.82E-03	5.88E-03
2.32E-03	2.39E-03	2.45E-03	2.52E-03	2.65E-03	2.69E-03	2.71E-03	2.96E-03	4.55E-03
4.65E-03	4.75E-03	4.79E-03	5.23E-03	5.69E-03	5.86E-03	5.92E-03	6.15E-03	9.46E-03
9.35E-03	9.65E-03	1.05E-02	1.15E-02	1.24E-02	1.38E-02	1.48E-02	1.37E-02	2.10E-02
1.68E-02	1.74E-02	1.79E-03	1.87E-02	1.99E-02	2.07E-02	2.21E-02	1.96E-02	3.01E-02
2.15E-02	2.37E-02	2.46E-02	3.02E-02	3.01E-02	3.08E-02	3.25E-02	3.22E-02	4.96E-02

APPENDIX C

OUT PUTS OF PLAXIS 3-D FOUNDATION

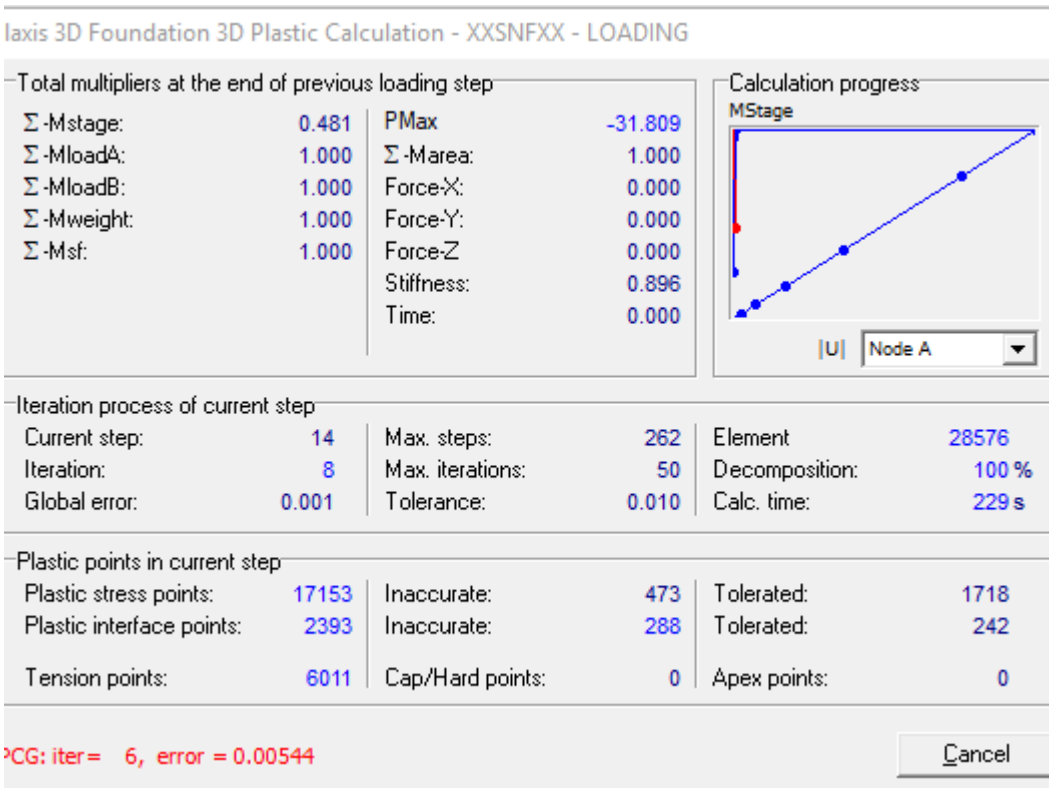

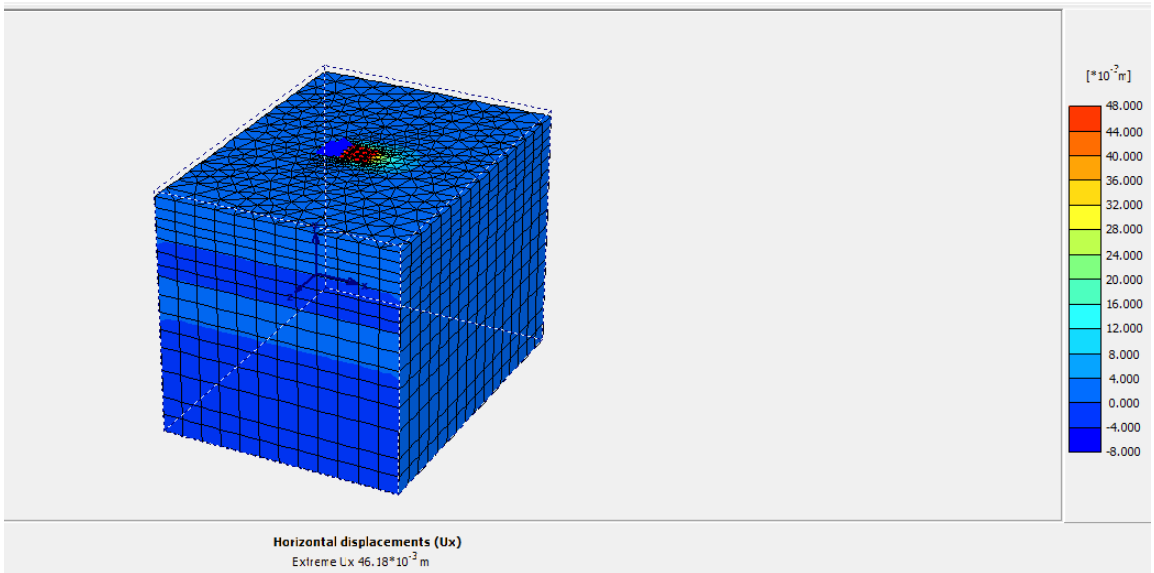

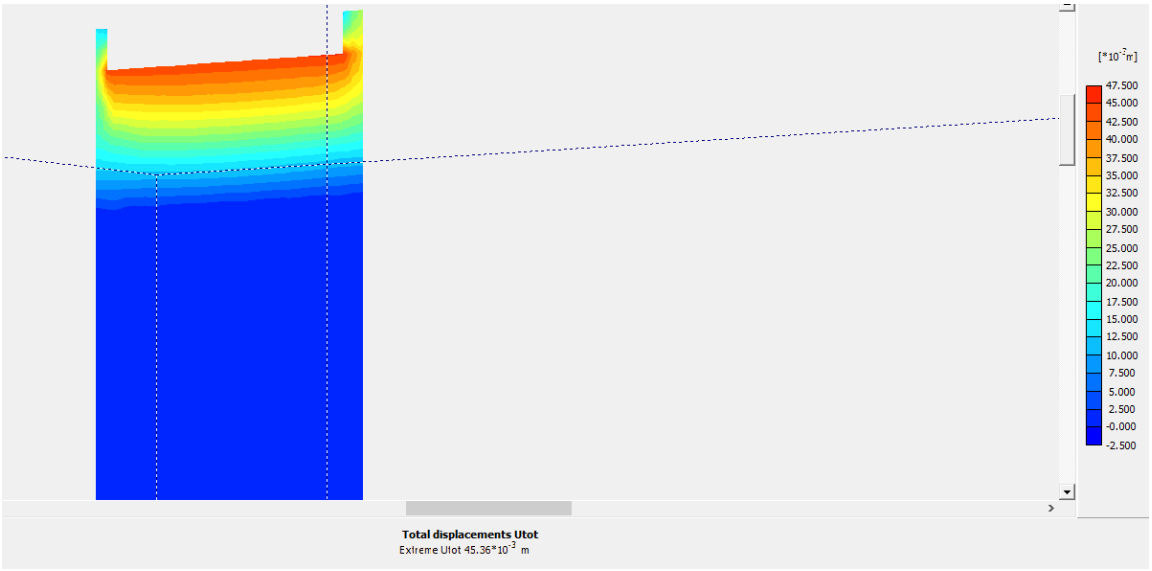

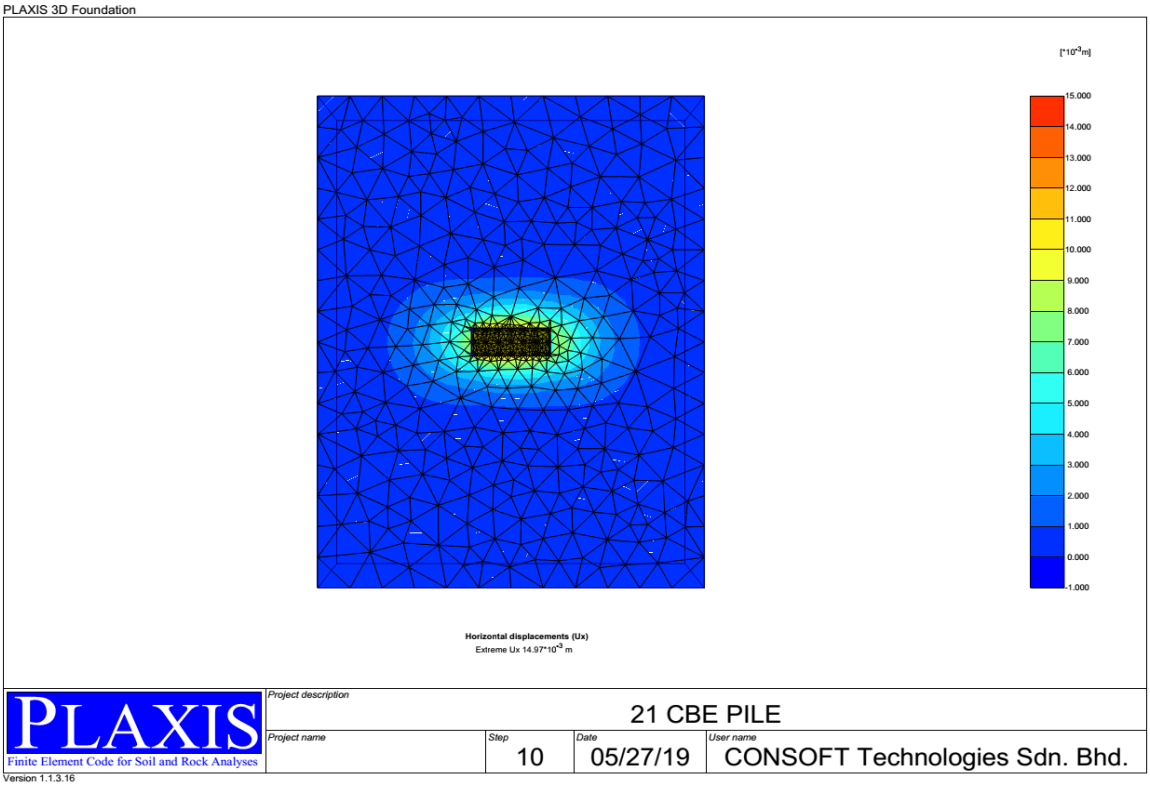

. Plaxis 3-D foundation output 6×6 pile arrangement with pile cap at 3d center to center spacing at 30m pile length by 1500kN

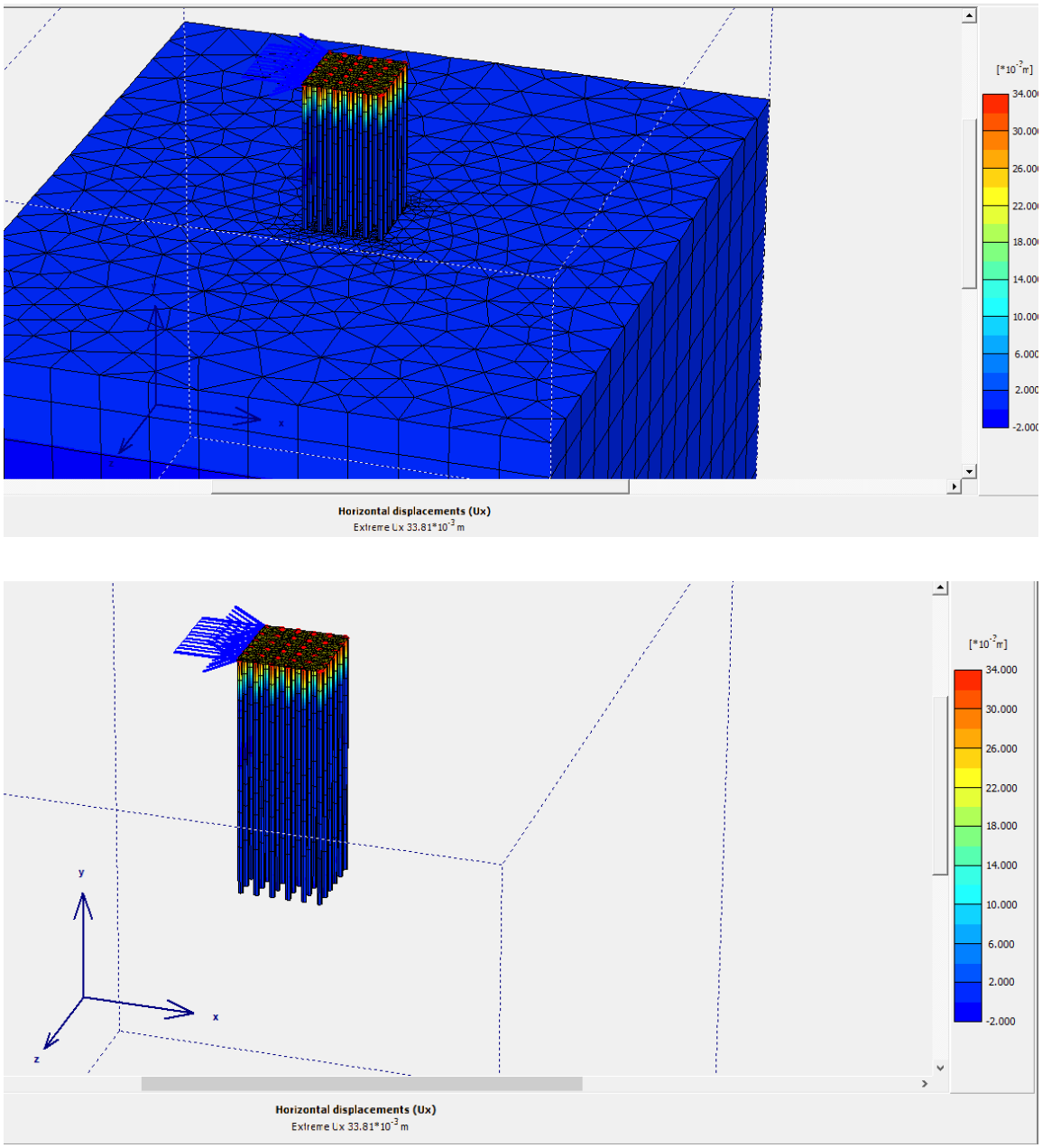

Plaxis 3-D FOUNDATION of 6×6 partial view of pile meshed deformation

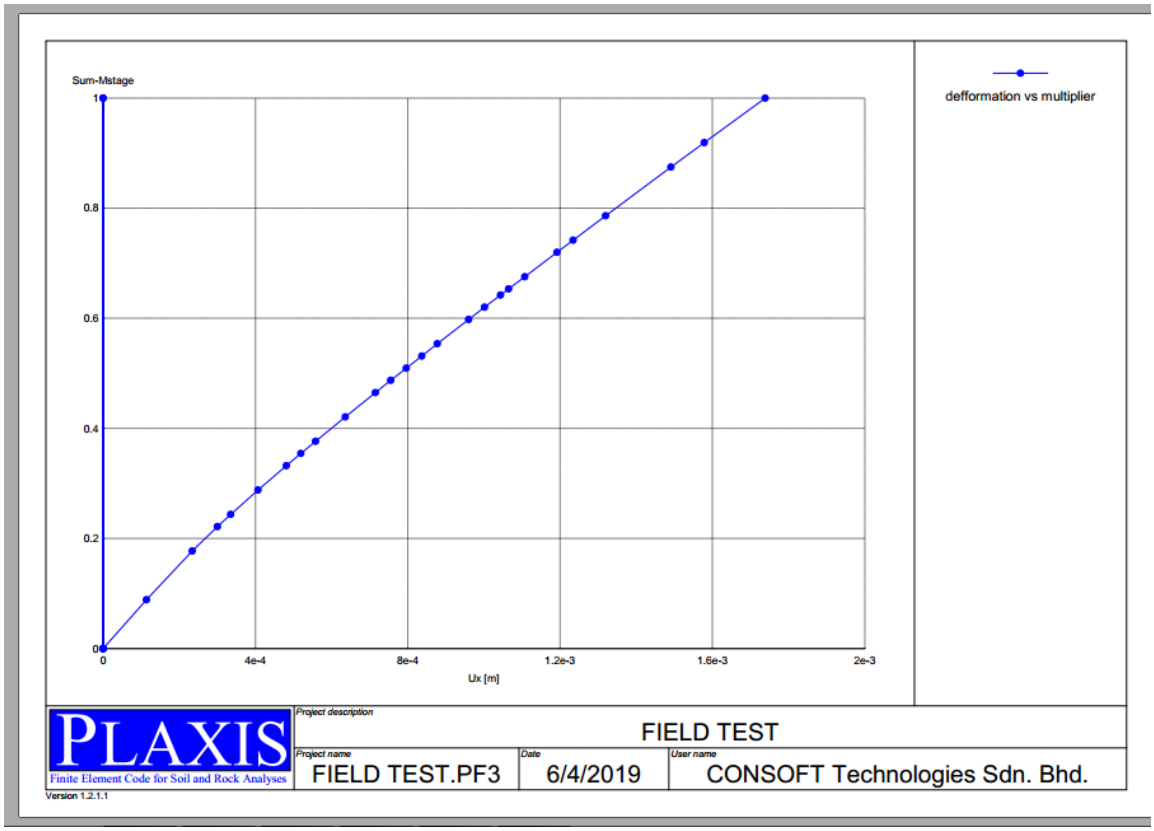
Sum-Mstage
1
0.8
0.6
0.4
0.2
0
0
4e-4
8e-4
1.2e-3
1.6e-3
2e-3
Ux [m]
defformation vs multiplier
PLAXIS
Finite Element Code for Soil and Rock Analyses
Version 1.2.1.1
Project description
FIELD TEST
Project name
FIELD TEST.PF3
Date
6/4/2019
User name
CONSOFT Technologies Sdn. Bhd.

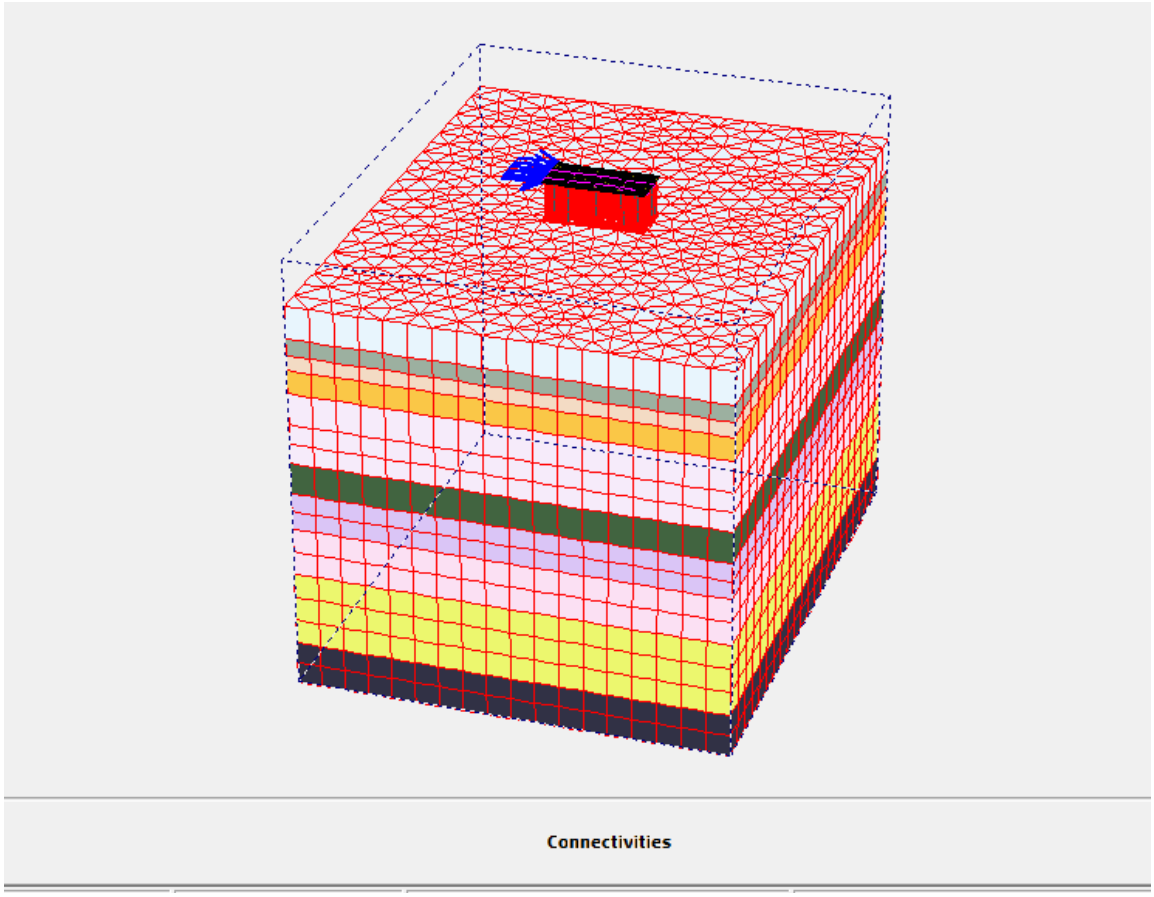
Connectivities